UNIVERSITY OF CALIFORNIA, SAN DIEGO

Synthesis of Caged *Garcinia* Xanthone Analogues

A thesis submitted in partial satisfaction of the requirements for the degree

Master of Science

in

Chemistry

by

Woo Cheal Cho

Committee in charge:

Professor Emmanuel A. Theodorakis, Chair
Professor Yoshihisa Kobayashi
Professor Douglas Magde

2009

The Thesis of Woo Cheal Cho is approved, and it is acceptable in quality and form for publication on microfilm and electronically:

Chair

University of California, San Diego

2009

Dedicated with love and respect to my parents Won Jung Cho and Kyoung Hea Song

and my soul mate Haruko Kunugida

TABLE OF CONTENTS

LIST OF SYMBOLS AND ABBREVIATIONS

Å	angstroms
ADR	adriamycin-resistant
$AlCl_3$	aluminum chloride
BBr_3	boron tribromide
Bu	*n*-butyl
calcd	calculated
ClCOCOCl	oxayl chloride
DCC	1,3-dicyclohexylcarbodiimide
DCM	dichloromethane
DIBAL-H	diisobutylaluminum hydride
DIPEA	*N*,*N*-diisopropylethylamine
DMAP	4-(*N*,*N*-dimethylamino)pyridine
DMF	*N*,*N*-dimethylformamide
EC_{50}	effect concentration 50 %
equiv.	equivalents
Et	ethyl

FAB	fast atom bombardment
FT	fourier transform
Δ	heat
h	hours
HATU	1-[bis(dimethylamino)methylene]-1H-1,2,3-triazolo[4,5-b]pyridinium 3-oxide hexafluorophosphate
HEL	human embryonic lung fibroblasts
HeLa	henrietta lacks cervical cancer
HRMS	high resolution mass spectra
IC_{50}	inhibition concentration 50 %
IR	infrared
Me	methyl
MeOH	methanol
Na_2CO_3	sodium carbonate
$NaClO_2$	sodium chlorite
OsO_4	osmium tetroxide
PCC	pyridinium chlorochromate

Pd	palladium
Ph	phenyl
R_f	retardation factor
rt	room temperature
SeO_2	selenium dioxide
t	tert
t-BuOOH	tert-butyl hydroperoxide
THF	tetrahydrofuran
TFA	trifluoroacetic acid
TFAA	trifluoroacetic anhydride
TLC	thin layer chromatography

LIST OF FIGURES

Chapter 1

Chapter 2

LIST OF SCHEMES

Chapter 1

Chapter 2

LIST OF TABLES

Chapter 2

LIST OF SPECTRA

Chapter 2

ACKNOWLEDGEMENTS

I would first like to thank Professor Emmanuel A. Theodorakis for the opportunity to work on his projects. Thank you for being a drill sergeant and a mentor at the same time. Next I thank all the lab members, past and present, for their support, insights, and contributions. I especially want to thank those that I had the pleasure to work with during the *Garcinia* xanthone project.

Thank you mom and dad for your love and support. Thank you my lovely dog, Choko for bringing luck and fortune to our family. Last but most importantly, I would like to thank Haruko Kunugida. Thank you for your love, companionship, understanding, patient, support, and above all, your belief in me. Without you by my side, all this would remain a distant dream. Thank you for fitting that missing piece of the puzzle in my life. I love you and I look forward to spending the rest of my life with you.

VITA

2006-2007	Laboratory Assistant, Tanabe Research Laboratories U.S.A., Inc.
2007	B.S. Biochemistry/Chemistry, University of California, San Diego
2008-2009	Teaching Assistant, Department of Biochemistry and Chemistry University of California, San Diego
2009	M.S. Chemistry, University of California, San Diego Advisor: Dr. Emmanuel A. Theodorakis.

ABSTRACT OF THE THESIS

Synthesis of Caged *Garcinia* Xanthone Analogues

by

Woo Cheal Cho

Master of Science in Chemistry

University of California, San Diego, 2009

Professor Emmanuel A. Theodorakis, Chair

A new synthetic strategy is developed toward the synthesis of the caged *Garcinia* xanthone analogues. The key to the strategy is a Pd-catalyzed reverse prenylation reaction. This new synthetic approach provides a rapid and efficient access to various caged analogues, including cluvenone which is known to induce apoptosis and exhibit significant cytotoxicity in various cancer cell lines. Evaluation of their growth inhibitory activities also leads to identification of the pharmacophoric motif of the caged *Garcinia* xanthones.

CHAPTER 1

BACKGROUND AND SIGNIFICANCE

Section 1.1 Background of the Caged Garcinia Xanthones

The tropical trees of the genus *Garcinia*, found in lowland rainforests of Southeast Asia, are widely known for their use in folk medicines.[1] Phytochemically, these trees are recognized as a rich source of xanthone and xanthonoid natural products that are considered to hold high pharmaceutical potential. For example, mangosteen, the fruit of *Garcinia mangostana* is highly praised for its medicinal value attributed to its content of xanthones and related products.[2,3] In fact, a mangosteen-based drink is currently sold to consumers for its tonic, immunostimulant, and antioxidant properties. On the other hand, gamboge, the commercially available exudates of *Garcinia hanburyi*, has been used in traditional Asian medicine for the treatment of indigestion, inflammation, and ulcers.[4]

Efforts to identify the bioactive ingredients from the *Garcinia* plants have yielded an ever growing family of natural products typified by a xanthone-based motif that has undergone a series of plant specific prenylations and/or oxidation reactions. Among them, morellin (**3**) (Figure 1),[5] produced by *Garcinia Morella*, became the first example of a structural motif in which a 4-oxa-tricyclo[4.3.1.$0^{3,7}$]dec-8-en-2-one scaffold was built into a xanthone backbone. This motif is further customized via substitutions on the aromatic residue and peripheral oxidations to produce a variety of structural subfamilies including the morellins (**1**-**4**),[6,7] forbesione (**5**),[8] desoxygambogenin (**6**),[9] desoxygaudichaudione (**7**),[10] gambogic acid (**8**),[11] the related gambogin (**9**),[12] and the bractatins (**10**-**12**).[13] An additional level of architectural complexity is found in the structure of lateriflorone (**13**)[14] in which the tricyclic caged motif is attached to an unprecedented spiroxalactone core (Figure 1).

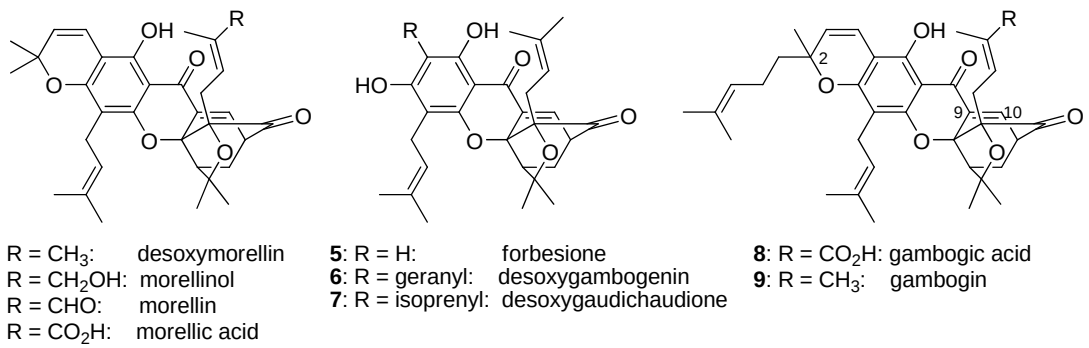

1: R = CH_3: desoxymorellin
2: R = CH_2OH: morellinol
3: R = CHO: morellin
4: R = CO_2H: morellic acid

5: R = H: forbesione
6: R = geranyl: desoxygambogenin
7: R = isoprenyl: desoxygaudichaudione

8: R = CO_2H: gambogic acid
9: R = CH_3: gambogin

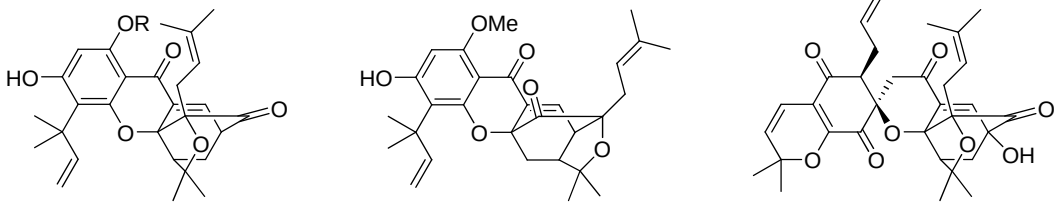

10: R = H: bractatin
11: R = Me: 1-*O*-methylbractatin

12: 1-*O*-methylneobractatin

13: lateriflorone

Figure 1. Representative examples of caged *Garcinia* xanthones

Biosynthetically, the *Garcinia* natural products are presumed to derive from a common benzophenone intermediate of a mixed shikimate-acetate pathyway.[15] Subsequent alkylations, rearrangements, and/or oxidation reactions are thought to give rise to the families of caged xanthonoids, representative members of which are shown in Figure 1.[16] Based on this scenario, forbesione (**5**) and related natural products could arise from 1,3,5,6-tetrahydroxyxanthone (**14**) (Scheme 1). A polyisoprenylation reaction by the electrophilic dimethylallyl diphosphate (DMAPP) could deliver three dimethylallyl groups at the C3, C5, and C6 phenolic oxygens forming compound **15**. Several hypotheses have been reported for the formation of the caged motif of the *Garcinia* natural products.[17] Among them, the most meritorious, proposed by Quillinan and Scheinamann in 1971, rests upon a tandem Claisen/Diels-Alder rearrangements.[18] In the specific case of forbesione (**5**), the C-ring (shikimate ring) could be formed by the

Claisen/Diels-Alder cascade, while the A ring (acetate-ring) could be formed by another Claisen rearrangement. We have explored this reaction cascade and used it as a cornersone for the development of a unified strategy to several caged *Garcinia* xanthones.

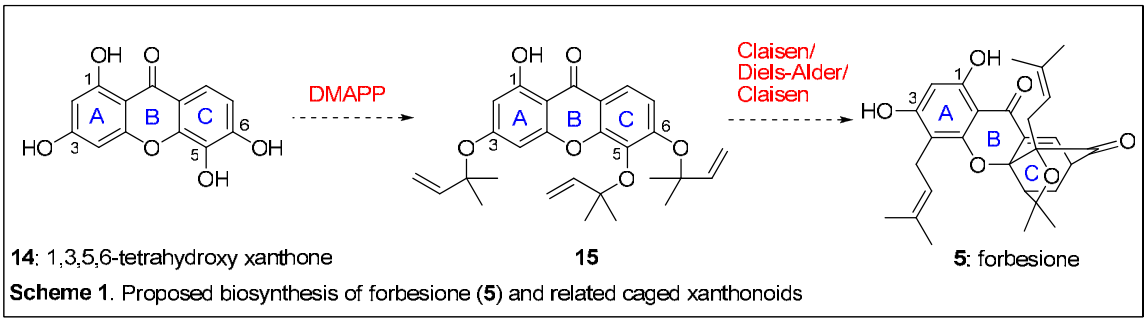

14: 1,3,5,6-tetrahydroxy xanthone **15** **5**: forbesione

Scheme 1. Proposed biosynthesis of forbesione (**5**) and related caged xanthonoids

Section 1.2 Significance of the Caged Garcinia Xanthones in Biology and Drug Discovery

Aside from their striking chemical structure and biosynthesis, the caged *Garcinia* natural products exhibit interesting bioactivities and have a documented value in traditional Eastern medicine. Studies from different laboratories have shown that selected members of the caged *Garcinia* xanthones possess several essential characteristics that highlight clearly their enormous potential in drug discovery. Specifically, it has been found that: (a) they exhibit potent cytotoxicity against a variety of tumor cells including multidrug-resistant cell lines; (b) they have a good therapeutic window for clinical applications as suggested by studies in animal models; (c) they kill cancer cells by inducing apoptosis; (d) they bind to the transferrin receptor (TfR), as suggested by studies with gambogic acid. A detailed presentation of these characteristics and their significance in drug discovery will be presented in the following sections.

Section 1.2.1 Inhibition of Tumor Cell Growth by the Caged Garcinia Xanthones

The ability of several caged *Garcinia* xanthones to inhibit tumor cell proliferation and exhibit potent cytotoxicity at low μM concentrations has been well documented. For instance, desoxymorellin (**1**) was cytotoxic against HEL (Human Embryonic Lung fibroblasts) and HeLa (Henrietta Lacks cervical cancer) cells with a minimum inhibitory concentration (IC_{50}) of 0.39 μg/mL.[12] The bractatins (**10**-**12**) were tested against the KB cell line (human Epidermoid Carcinoma) with 1-*O*-methylneobractatin (**12**) showing the lowest IC_{50} value of 0.20 μg/mL.[13] The gaudichaudiones have been tested against a panel of cell lines, such as P388 (mouse lymphocytic leukemia), WEH11640 (mouse fibrosarcoma), THP-1 (human monocytic leukemia), MOLT4 (human acute lymphoblastic leukemia), HePG2 (human heptocellular carcinoma), LL/2 (Lewis lung carcinoma, mouse), and found to be broadly cytotoxic with effective dose (ED_{50}) values between 0.50 and 8.0 μg/mL.[19] Similar data have been recorded with gambogic acid (**8**).[20] In addition, lateriflorone (**13**) was cytotoxic against the P388 cancer cell line with ED_{50} value of 5.4 μg/mL.[14]

More recently, gaudichaudione A was reported to display strong inhibitory activity against both parental murine leukemic P388 and P388/doxorubicin-resistant cell lines at low micromolar dosage, but was less toxic against normal human liver cells at these concentrations.[21] Similar results were obtained with gambogic acid.[22] Studies from our own laboratories have confirmed these findings.[23] Specifically, we have found that adriamycin-resistant HL-60 cells have similar sensitivity to the anti-proliferative effects of several caged *Garcinia* xanthones as the parental HL-60 cell line. These findings indicate that the caged *Garcinia* xanthones are not subjects of the multidrug-resistance

mechanisms, often associated with overexpression of P glycoprotein, which is typical of relapsed cancers, and thus they represent a pharmacologically promising chemical scaffold.[24, 25]

Section 1.2.2 Therapeutic Window of the Caged Garcinia Xanthones

Recent studies with gambogic acid (**8**) in animal models have documented its promising pharmacological profile. Notably, it was found that intravenous injection of gambogic acid at 6 mg/Kg (4 doses on alternate days) did not affect the body weight or white blood cells count of healthy rats, suggesting that this compound is non-toxic at the doses tested.[26] Related toxicological studies demonstrated that the LD_{50} of gambogic acid is 45-96 mg/Kg in experiments using mice. In addition, in experiments with dogs, the innocuous dose was established to be 4 mg/Kg after administration for a total of 13 weeks at a frequency of one injection every other day.[27] These results indicate that the therapeutic window of gambogic acid is adequate for clinical applications as an anticancer agent. In turn, this suggests that the caged *Garcinia* xanthones have a promising clinical potential.

Section 1.2.3 Induction of Apoptosis by the Caged Garcinia Xanthones

Studies from several laboratories, including our own work,[23] have shown that the caged *Garcinia* xanthones induce apoptotic cell death in a variety of cancer cell lines. For instance, the apoptotic effects of gaudicaudione A were shown by the collapse of the mitochondrial transmembrane potential, the activation caspase-3 and induction of internucleosomal DNA fragmentation.[21] Related studies with gambogic acid (**8**) have

shown that this compound induces apoptosis selectively in certain tumor cells *in vitro* in a dose-dependent manner. In T47D (breast cancer) cells, the EC_{50} value of gambogic acid was 0.78 μM.[20] In MGC-803 cells (human gastric carcinoma) the EC_{50} value after 48 hours of incubation was 0.96 μg/mL.[26,27] Similar EC_{50} values were recorded by our laboratory in a variety of solid and non-solid tumor cells.[23] In addition, immunohistochemical studies indicated that **8** regulates expression of Bax and Bcl-2 proteins that are known to play a crucial role during apoptosis.[26, 28]

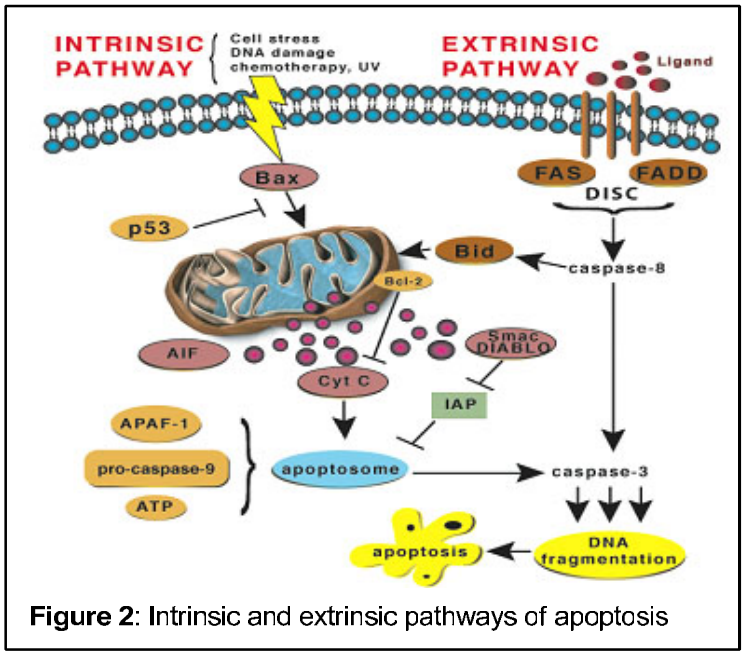

Figure 2: Intrinsic and extrinsic pathways of apoptosis

To better appreciate the significance of the above results it is important to introduce the process of apoptosis and its role in cancer.[29] Apoptosis, or programmed cell death, is a highly regulated process that allows a cell to self-degrade in order for the body to eliminate unwanted or dysfunctional cells. As such, it is essential to embryonic development and the maintenance of homeostasis in multicellular organisms. In humans, for example, the rate of cell growth and cell death is balanced to maintain the weight of

the body. It has been estimated that each day between 50-70 billion cells in the human body perish due to apoptosis.[30] This event is necessary to make room for the billions of new cells produced daily. In fact, within one year this flux of cells corresponds to a production and eradication of a mass equal to almost our entire body weight. Once triggered, the apoptotic event leads to cell deletion via a process that includes chromatin condensation, nuclear fragmentation, cell shrinkage, plasma membrane blebbing and other ultrastructural changes.[31] These changes lead ultimately to phagocytosis by the neighboring cells without inciting unnecessary inflammatory reactions or tissue scaring.

In general, apoptosis can be induced in two different ways, referred to as the intrinsic and extrinsic pathways (Figure 2).[32] The intrinsic pathway is activated by stress signals resulting from cellular damage sensors (e.g. p53) or developmental cues. Upon receiving the stress signal, pro-apoptotic members of the Bcl-2 family of proteins, such as Bax and Bid, bind to the outer membrane of the mitochondria to signal the release of cytochrome C.[33] Cytochrome C binds to ATP and Apaf-1 to form a large ternary protein complex, known as the apoptosome that recruits and activates caspase-9.[34] In turn, this activates caspase-3, the executioner of apoptosis that initiates DNA fragmentation. Besides the release of cytochrome C from the intramembrane space, the intramembrane content released also contains apoptosis inducing factor (AIF) to facilitate DNA fragmentation, and Smac/Diablo proteins to inhibit the inhibitor of apoptosis (IAP). On the other hand, the extrinsic pathway is initiated by binding of a small molecule to a death receptor, such as TNF-R1, Fas or DR4, which leads to receptor aggregation (usually homo-trimerization). The activated receptor then recruits the cytoplasmic proteins FADD (Fas-associated death domain protein) and procaspase-8 to form a

complex known as death-inducing signaling complex (DISC). In certain cells, such as lymphocytes, DISC formation leads directly to activation of caspase-3, to trigger apoptosis without involving mitochondria. In other cells, the formation of DISC can activate the mitochondrial apoptotic pathway through cleavage and activation of the Bid protein.[35]

There is compelling evidence that insufficient apoptosis can result in cancer or autoimmunity while accelerated cell death is evident in degenerative diseases, immunodeficiency and infertility. In fact, tumorigenesis is a multi-step process based on genetic alterations that drive the progressive transformation of normal cells into highly malignant derivatives. It has been suggested that the large diversity of human cancer cell genotypes is a manifestation of six essential alterations in cell physiology that collectively dictate malignant growth.[36] These alterations, also referred to as the hallmarks of cancer, involve: (a) self-sufficiency in growth signals; (b) insensitivity to growth inhibitory signals; (c) evasion of apoptosis; (d) limitless replicating ability; (e) sustained angiogenesis; and (f) tissue invasion and metastasis. These physiologic changes are shared by most, if not all, types of human cancer and represent points for therapeutic intervention. The third alteration from the above list refers to the ability of cancer cells to circumvent normal pathways leading to apoptosis, thus expanding their population in a non-controlled manner. Downregulation of pro-apoptotic proteins, such as Bax, overexpression of the anti-apoptotic protein Bcl-2, and/or mutations that destroy their function (e.g. p53 mutations), decrease the ability of the cell to undergo apoptosis leading ultimately to tumorigenesis.[37, 38]

It has also been shown that effectively all traditional anticancer drugs use apoptosis pathways to exert their cytotoxic actions.[31] Consequently, defects in the regulation of apoptosis can render cells intrinsically resistant to chemotherapy, not because the drugs or irradiation fails to induce damage to DNA, microtubules and other structures, but because tumor cells remain viable after suffering the damage and hence have opportunities to undergo repair and resume their proliferative activities.[39]

Section 1.2.4 Gambogic Acid Binds to the Transferrin Receptor-1 (TfR)

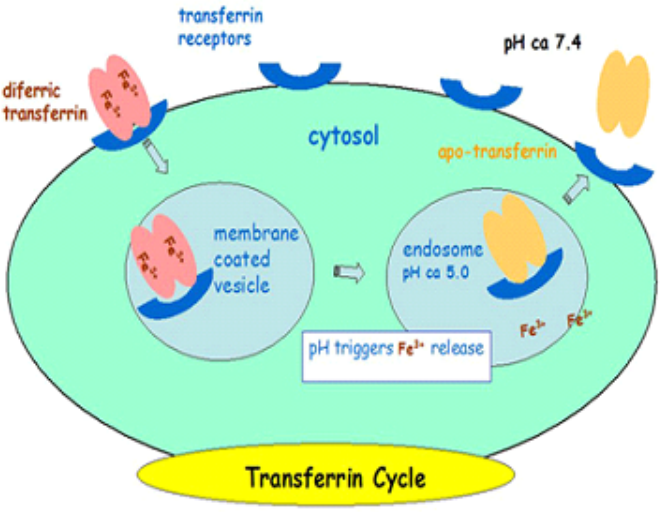

Figure 3. Function of the transferrin receptor-1 (TfR)

The recent finding that gambogic acid (**8**) induces apoptosis by binding to the transferrin receptor (TfR)[40] is of paramount significance for drug discovery studies for two main reasons: (a) it suggests that TfR is involved in regulation of apoptosis via an unknown mechanism that could be explored using the caged *Garcinia* xanthones as biological tools and (b) it suggests that identification of the binding site of this compound on TfR would lead to a methodical SAR study that, departing from the "privileged motif"

of **8**, would aim to enhance its binding efficiency and optimize its overall pharmacological properties.

Transferrin receptor-1 (TfR) is a homodimeric type II transmembrane protein with a molecular mass of 90 kDa per monomer.[41] Its physiological function involves iron uptake into vertebrate cells via a cycle of endo- and exocytosis of the iron transport protein transferrin (Tf).[42] As shown in Figure 3, TfR binds diferric transferrin at the cell surface and carries it to the endosome. There, upon acidification, the iron is released from Tf and the Tf-TfR complex returns to the cell surface. The apotransferrin is then replaced by diferric transferrin from serum, thus completing the catalytic cycle. This cycle has become one of the most widely used models for receptor-mediated endocytosis.

It has been reported that gambogic acid binds to TfR at a different site from that required for transferrin binding.[40] However, the biological and medicinal potential of this finding cannot be explored without obtaining structural information on this binding site. It would be very important to learn whether the binding of these compounds to TfR affects receptor endocytosis and how this receptor induces apoptotic signals. One possibility is such binding inhibits TfR internalization which suggests that these compounds induce apoptosis without entering the cytoplasm. Alternatively, if binding of the caged *Garcinia* xanthones to TfR does not affect TfR internalization, these molecules could enter the cell and be targeted to the endosomes. Either scenario could explain why these compounds are not affected by the P glycoprotein and thus circumvent the multidrug resistance mechanisms.[24,25] Moreover, if TfR internalization is not affected, one could use this binding site for cargo delivery inside the cytoplasm.

The clinical relevance of the TfR in cancer has been extensively documented.[43] Growing cells require iron to maintain the activity of ribonucleotide reductase, an enzyme involved in deoxynucleotide synthesis. Since the uptake of iron by cells is mediated by the TfR, several tumor cells display higher levels of this receptor on their surface compared to normal cells.[44, 45] Moreover, TfR overexpression was suggested to contribute to the pathogenesis of chronic anemia, often associated with advanced malignancy, due to the competition of bone marrow and the tumor for circulating transferrin-bound iron.[43] These findings have led to the notion that the TfR is a useful marker for malignancy[45, 46] and to the development of anti-TfR antibodies that inhibit the growth of human melanoma in nude mice.[47, 48] TfR overexpression has been detected in several malignant cells including promyelocytic leukemia,[49] pancreatic,[50] breast[46] and colon[51] cancers, as well as in esophageal adenocarcinoma.[52] In other cancer cells, accelerated TfR cycling, rather than increased TfR expression, was observed resulting in increased cell death via TfR targeting.[53] Thus, the TfR has been identified as a target for therapeutic intervention for cancer.[54, 55] Importantly, a most recent study reported that the chicken TfR represents a new cell-death receptor and further highlighted the significance of TfR as a therapeutic target in cancer.[56]

It is worth pointing out the use of both transferrin and transferrin receptors as carriers to direct toxins, diagnostic reagents or therapeutic molecules to cancer cells.[57] For example, a variety of conjugate molecules including those conjugated to Tf, such as Tf-nerve growth factor, have been successfully used to deliver therapeutic agents across epithelial barriers, including the blood brain barrier, via the TfR.[58, 59] Diagnostic reagents and small molecule cargos can also be delivered in this way, and might be particularly

effective if they can be unpackaged upon arrival.[60] For example, liposomes targeting TfR can efficiently deliver encapsulated doxorubicin in multidrug-resistant tumor cells and induce increased cytotoxicity (3.5-fold higher than free doxorubicin).[61] Together, these studies provide strong validation for the use of the TfR to transport diagnostic and therapeutic reagents into the brain. It is worth mentioning that the presence of the blood brain barrier is known to exclude >95% of all drugs in the circulation from entering the brain, and thus it poses a major obstacle in the development of drugs targeting components of the central nervous system.

Section 1.3 References

1. Kumar, P.; Baslas, R. K. Phytochemical and the biological studies of the plants of the genus *Garcinia*. *Herba Hungarica* **1980**, *19*, 81-91.

2. Nakatami, K.; Nakahata, N.; Arakawa, T.; Yasuda, H.; Ohizumi, Y. "Inhibition of cyclooxygenase and prostanglandin E2 synthesis by g-mangostin, a xanthone derivative in mangosteen, in C6 rat glioma cells. *Biochem. Pharmacol.* **2002**, *63*, 73-79.

3. Matsumoto, K.; Akao, Y.; Kobayashi, E.; Ohbuchi, K.; Ito, T.; Tanaka, T.; Iinuma, M.; Nozawa, Y. "Induction of apoptosis by xanthones from mangosteen in human leukemia cell lines" *J. Nat. Prod.* **2003**, *66*, 1124-1127.

4. Gruenwald, J.; Brendler, T.; and Jaenicke, C. Eds. PDR for Herbal Medicines, 2nd Ed, Medical Economics Co. Montvale, NJ, 2000, pp325-326.

5. Rao, B. S. "Morellin, a constituent of the seeds of *Garcinia morella"*. *J. Chem. Soc. C* **1937**, 853-855.

6. Karanjgaonkar, C. G.; Nair, P. M.; Venkataraman, K. "The coloring matters of *Garcinia morella*. VI. Morellic, isomorellic, and gambogic acids". *Tetrahedron Lett.* **1966**, 687-691.

7. Bhat, H. B.; Nair, P. M.; Venkataraman, K. "The coloring matters of *Garcinia morella*. V. Isolation of desoxymorellin and dihydroisomorellin". *Indian J. Chem.* **1964**, *2*, 405-410.

8. Leong, Y.-W.; Harrison, L. J.; Bennett, G. J.; Tan, H. T. W. "Forbesione, a modified xanthone from *Garcinia forbesii"*. *J. Chem. Res., Synop.* **1996**, 392-393.

9. Han, Q.-B.; Wang, Y.-L.; Yang, L.; Tso, T.-F.; Qiao, C.-F.; Song, J.-Z.; Xu, L.-J.; Chen, S.-L.; Yang, D.-J.; Xu, H.-X. "Cytotoxic polyprenylated xanthones from the resin of *Garcinia hanburyi" Chem. Pharm. Bull.* **2006**, *54*, 265-267.

10. Cao, S.-G.; Wu, X.-H.; Sim, K.-Y.; Tan, B. K. H.; Pereira, J. T.; Wong, W. H.; Hew, N. F.; Goh, S. H. "Cytotoxic caged tetraprenylated xanthonoids from *Garcinia gaudichaudii* (Guttiferae)". *Tetrahedron Lett.* **1998**, *39*, 3353-3356.

11. Weakley, T. J. R.; Cai, S.-X.; Zhang, H.-Z.; Keana, J. F. W. "Crystal structure of the pyridine salt of gambogic acid". *J. Chem. Crystallog.* **2001**, *31*, 501-505.

12. Asano, J.; Chiba, K.; Tada, M.; Yoshii, T. "Cytotoxic xanthones from *Garcinia hanburyi*". *Phytochemistry* **1996**, *41*, 815-820.

13. Thoison, O.; Fahy, J.; Dumontet, V.; Chiaroni, A.; Riche, C.; Tri, M. V.; Sevenet, T. "Cytotoxic prenylxanthones from *Garcinia bracteata*". *J. Nat. Prod.* **2000**, *63*, 441-446.

14. Kosela, S.; Cao, S.-G.; Wu, X.-H.; Vittal, J. J.; Sukri, T.; Masdianto; Goh, S.-H.; Sim, K.-Y. "Lateriflorone, a cytotoxic spiroxalactone with a novel skeleton, from *Garcinia lateriflora* Bl". *Tetrahedron Lett.* **1999**, *40*, 157-160.

15. Bennett, G. J.; Lee, H. H.; Das, N. "Biosynthesis of mangostin. Part 1. The origin of the xanthone skeleton". *J. Chem. Soc., Perkin Trans. 1* **1990**, 2671-2676.

16. Dewick, P. M. "The biosynthesis of shikimate metabolites". *Nat. Prod. Rep.* **1998**, *15*, 17-58.

17. Ollis, W. D.; Ramsay, M. V. J.; Sutherland, I. O.; Mongkolsuk, S. "Constitution of gambogic acid". *Tetrahedron* **1965**, *21*, 1453-1470.

18. Quillinan, A. J.; Scheinmann, F. "Application of the Claisen rearrangement to the synthesis of heterocyclic bicyclo[2,2,2]octenones: An approach to the morellins based on new biogenetic suggestions". *J. Chem. Soc., Chem. Commun.* **1971**, 966-967.

19. Cao, S.-G.; Sng, V. H. L.; Wu, X.-H.; Sim, K.-Y.; Tan, B. H. K.; Pereira, J. T.; Goh, S. H. "Novel cytotoxic polyprenylated xanthonoids from *Garcinia gaudichaudii* (Guttiferae)". *Tetrahedron* **1998**, *54*, 10915-10924.

20. Zhang, H.-Z.; Kasibhatla, S.; Wang, Y.; Herich, J.; Guastella, J.; Tseng, B.; Drewe, J.; Cai, S.-X. “Discovery, characterization and SAR of gambogic acid as a potent apoptosis inducer by a HTS assay”. *Bioorg. Med. Chem.* **2004**, *12*, 309-317.

21. Wu, X.; Cao, S.; Goh, S.; Hsu, A.; Tan, B. K. H. “Mitochondrial destabilization and caspase-3 activation are involved in the apoptosis of Jurkat cells induced by gaudichaudione A, a cytotoxic xanthone”. *Planta Med.* **2002**, *68*, 198-203.

22. Han, Q.; Yang, L.; Liu, Y.; Wang, Y.; Qiao, C.; Song, J.; Xu, L.; Yang, D.; Chen, S.; Xu, H. “Gambogic acid and epigambogic acid, C-2 epimers with novel anticancer effects from *Garcinia hanburyi*”. *Planta Med.* **2006**, *72*, 281-284.

23. Batova, A.; Lam, T., Waschol owski, V.; Yu, A. L.; Giannis, A.; Theodorakis, E. A. “Synthesis and Evaluation of Caged *Garcinia* Xanthones” *Org. & Biomol. Chem.* **2007**, *5*, 494-500.

24. La Porta, C. A. M. “Drug resistance in melanoma: New perspectives” *Curr. Med. Chem.* **2007**, *14*, 387-391.

25. Larsen, A. K.; Escargeuil, A. E.; Skladanowski, A. “Resistance mechanisms associated with intracellular distribution of anticancer agents” *Pharmacol. & Therapeutics* **2000**, *85*, 217-229.

26. Zhao, L.; Guo, Q.-L.; You, Q.-D.; Wu, Z.-Q.; Gu, H.-Y. “Gambogic acid induces apoptosis and regulates expressions of Bax and Bcl-2 protein in human gastric carcinoma MGC-803 cells”. *Biol. Pharm. Bull.* **2004**, *27*, 998-1003.

27. Guo, Q.; Qi, Q.; Gu, H.; Wu, Z. “Toxocological studies of gambogic acid and its potential targets in experimental animals” *Basic and Clin. Pharmacol. & Toxicol.* **2006**, *99*, 178-184.

28. Liu, W.; Guo, Q.-L.; You, Q.-D.; Zhao, L.; Gu, H.-Y.; Yuan, S.-T. “Anticancer effect and apoptosis induction of gambogic acid in human gastric carcinoma line BGC-823” *World J. Gastroenterol.* **2005**, *11*, 3655-3659.

29. Lowe, S. W.; Lin, A. W. “Apoptosis in cancer” *Carcinogenesis* **2000**, *21*, 485-495.

30. Reed, J. C.; Tomaselli, K. J. “Drug discovery opportunities from apoptosis research” *Curr. Opin. Biotechnol.* **2000**, *11*, 586-592.

31. Reed, J. C. “Dysregulaton of Apoptosis in Cancer” *J. Clin. Oncol.* **1999**, *17*, 2941-2953.

32. Wesche-Soldato, D. E.; Swan, R. Z.; Chung, C. S.; Ayala, A. “the apoptotic pathway as a therapeutic target in sepsis” *Curr. Drug Targets* **2007**, *8*, 493-500.

33. van Gurp, M.; Festjens, N.; van Loo, G.; Saelens, X.; Vandenabeele, P. “Mitochondrial intermembrane proteins in cell death” *Biochem. & Biophys. Res. Commun.* **2003**, *304*, 487-497.

34. Acehan, D.; Jiang, X.; Morgan, D. G.; Heuser, J. E.; Wang, X.; Akey, C. W. “Three-dimensional structure of the apoptosome: Implications for assembly, procaspase-9 binding, and activation” *Molec. Cell* **2002**, *9*, 423-432.

35. Beurel, E.; Jope, R. S. “The paradoxical pro- and anti-apoptotic actions of GSK3 in the intrinsic and extrinsic apoptosis signaling pathways” *Progress in Neurobiol.* **2006**, *79*, 173-189.

36. Hanahan, D.; Weinberg, R. A. “The Hallmarks of Cancer” *Cell* **2000**, *100*, 57-70.

37. Catz, S. D.; Johnson, J. L. “Bcl-2 in prostate cancer: A minireview**”** *Apoptosis* **2003**, *8*, 29-37.

38. Rapp, U. R.; Rennefahrt, U.; Troppmair, J. “Bcl-2 proteins: master switches at the intersection of death signaling and the survival control by Raf kinases” *Biochim. Biophys. Acta* **2004**, *1644*, 149-158.

39. Kim, R.; Tanabe, K.; Uchida, Y.; Emi, M.; Inoue, H.; Toge, T. “Current status of the molecular mechanisms of anticancer drug-induced apoptosis” *Cancer Chemother. Pharmacol.* **2002**, *50*, 343-352.

40. Kasibhatia, S.; Jessen, K. A.; Maliartchouk, S.; Wang, J. Y.; English, N. M.; Drewe, J.; Qiu, L.; Archer, S. P.; Ponce, A. E.; Sirisoma, N.; Jiang, S.; Zhang, H.; Gehisen, K. R.; Cai, S. X.; Green, D. R.; Tseng, B. "A role for transferring receptor in triggering apoptosis when targeted with gambogic acid" *PNAS* **2005**, *102*, 12095-12100.

41. Lawrence, C. M.; Ray, S.; Babyonyshev, M.; Galluser, R.; Borhani, D. W.; Harrison, S. C. "Crystal structure of the ectodomain of human transferrin receptor" *Science* **1999**, *286*, 779-782.

42. Trowbridge, I. S.; Newman, R. A.; Domingo, D. L.; Sauvage, C. "Transferrin receptors: structure and function" *Biochem. Pharmacol.* **1984**, *33*, 925-932. Aisen, P. "Transferrin receptor 1" *Int. J. Biochem. & Cell Biol.* **2004**, *36*, 2137-2143.

43. Gatter, K. C.; Brown, G.; Trowbridge, I. S.; Woolston, R. E.; Mason, D. Y. "Transferrin receptors in human tissues: their distribution and possible clinical relevance" *J. Clin. Pathol.* **1983**, *36*, 539-545.

44. Jones, D. T.; Trowbridge, I. S.; Harris, A. L. "Effects of transferrin receptor blockade on cancer cell proliferation and hypoxia-inducible factor function and their differential regulation by ascorbate" *Cancer Res.* **2006**, *66*, 2749-2756.

45. Niitsu, Y.; Kohgo, Y.; Nishisato, T.; Kondo, H.; Kato, J.; Urishizaki, Y.; Urishizaki, I. "Transferrin receptors in human cancerous tissues" *Tohoku J. Exp. Med.* **1987**, *153*, 239-243.

46. Shindleman, J. E.; Ortmeyer, A. E.; Sussman, H. H. "Demostration of the transferrin receptor in human breast cancer tissue. Potential marker for identifying dividing cells" *Int. J. Cancer* **1981**, *27*, 329-334.

47. Trowbridge, I. S.; Domingo, D. L. "Anti-transferrin receptor monoclonal antibody and toxin-antibody conjugates affect growth of human tumor cells" *Nature*, **1981**, *294*, 171-173.

48. Kemp, J. D. “Iron deprivation and cancer: a view beginning with studies of monoclonal antibodies against the transferring receptor” *Histol. & Pathol.* **1997**, *12*, 291-296.

49. Chitambar, C. R.; Massey, E. J.; Seligman, P. A. “Regulation of transferrin receptor expression on human leukemic cells during proliferation and induction of differentiation” *J. Clin. Investig.* **1983**, *72*, 1314-1325.

50. Ryschich, E.; Huszty, G.; Knaebel, H. P.; Hartel, M.; Buechler, M. W.; Schmidt, J. “Transferrin receptor is a marker of malignant phenotype in human pancreatic cancer and in neuroendocrine carcinoma of the pancreas” *Eur. J. Cancer* **2004**, *40*, 1418-1422.

51. Prutki, M.; Poljak-Blazi, M.; Jakopovic, M.; Tomas, D.; Stipancic, I.; Zarkovic, N. “Altered iron metabolism, transferrin receptor 1 and ferritin in patients with colon cancers” *Cancer Lett.* **2006**, *238*, 188-196.

52. Boult, J.; Roberts, K.; Brookes, M. J.; Hughes, S.; Bury, J. P.; Cross, S. S.; Anderson, G. J.; Spychal, R.; Iqbal, T.; Tselepis, C. “Overexpression of cellular iron transport proteins is associated with malignant progression of esophageal adenocarcinoma” *Clin. Cancer Res.* **2008**, *14*, 379-387.

53. Chitambar, C. R.; Werely, J. P.; Matsuyama, S. “Gallium-induced cell death in lymphoma: role of transferrin receptor cycling, involvement of Bax and the mitochondria and effects of proteasome inhibition” *Mol. Cancer Therap.* **2006**, *5*, 2834-2843.

54. White, C.; Taetle, R.; Seligman, P. A.; Rutherford, M.; Trwobridge, I. S. “Combinations of anti-transferrin receptor monoclonal antibodies inhibit human tumor cell growth *in vitro* and *in vivo*: Evidence for synergistic antiproliferative effects” *Cancer Res.* **1990**, *50*, 6295-6301. Sauvage, C. A.; Mendelson, J. C.; Lesley, J. F.; Trowbridge, I. S. “Effects of monoclonal antibodies that block transferring receptor function on the *in vivo* growth of a syngeneic murine leukemia” *Cancer Res.* **1987**, *47*, 747-753.

55. Taetle, R.; Rhyner, K.; Castagnola, J.; To, D.; Mendelsohn, J. “Role of transferrin Fe and transferrin receptors in myeloid leukemia cell growth” *J. Clin. Invest.* **1985**, *75*, 1061-1067. Szekeres, T.; Sedlak, J.; Novotny, L. “Benzamide riboside,

a recent inhibitor of inosine 5'-monophosphate dehydrogenase induces transferrin receptors in cancer cells" *Curr. Med. Chem.* **2002**, *9*, 759-764.

56. Ohno, Y.; Yagi, H.; Nakamura, M.; Masudo, K.; Hashimoto, Y.; Masuko, T. "Cell-death inducing monoclonal antibodies raised against DT40 tumor cells: Identification of chicken transferrin receptor as a novel cell-death receptor" *Cancer Sci* **2008** publication ahead of print.

57. Pardridge, W. M. "Molecular Trojan horses for blood-brain barrier drug delivery" *Curr. Opin. Pharmacol.* **2006**, *6*, 494-500.

58. Widera, A.; Kim, K. J.; Crandall, E. D.; Shen, W. C. "Transcytosis of GCSF-transferrin across rat alveolar epithelial cell monolayers" *Pharm. Res.* **2003**, *20*, 1231-1238. Widera, A.; Norouziyan, F.; Shen, W. C. "Mechanisms of TfR-mediated transcytosis and sorting in epithelial cells and applications toward drug delivery*" Adv. Drug Deliv. Rev.* **2003**, *55*, 1439-1466.

59. Wu, D.; Pardridge, W. M. "Central nervous system pharmacologic effect in conscious rats after intravenous injection of a biotinylated vasoactive intestinal peptide analog coupled to a blood-brain barrier drug delivery system" *J. Pharmacol. Exp. Ther.* **1996**, *279*, 77-83. Wu, D.; Pardridge, W. M. "Neuroprotection with noninvasive neurotrophin delivery to the brain" *PNAS U S A* **1999**, *96*, 254-259. Song, B. W.; Vinters, H. V.; Wu, D.; Pardridge, W. M. "Enhanced neuroprotective effects of basic fibroblast growth factor in regional brain ischemia after conjugation to a blood-brain barrier delivery vector" *J. Pharmacol. Exp. Ther.* **2002**, *301*, 605-610.

60. Kurihara, A.; Pardridge, W. M. "Imaging brain tumors by targeting peptide radiopharmaceuticals through the blood-brain barrier" *Cancer Res.* **1999**, *59*, 6159-6163. Aktas, Y.; Yemisci, M.; Andrieux, K.; Gursoy, R. N.; Alonso, M. J.; Fernandez-Megia, E.; Novoa-Carballal, R.; Quinoa, E.; Riguera, R.; Sargon, M. F.; Celik, H. H.; Demir, A. S.; Hincal, A. A.; Dalkara, T.; Capan, Y.; Couvreur, P. "Development and brain delivery of chitosan-PEG nanoparticles functionalized with the monoclonal antibody OX26" *Bioconj. Chem.* **2005**, *16*, 1503-1511.

61. Kobayashi, T.; Ishida, T.; Okada, Y.; Ise, S.; Harashima, H.; Kiwada, H. "Effect of transferrin receptor-targeted liposomal doxorubicin in P-glycoprotein-mediated drug resistant tumor cells" *Int. J. Pharmac.* **2007**, *329*, 94-102.

CHAPTER 2

SYNTHESIS OF CAGED GARCINIA XANTHONE ANALOGUES

Section 2.1 Introduction

The tropical trees of the genus *Garcinia*, found in lowland rainforests of Southeast Asia, are widely known for their use in folk medicines.[1] Efforts to identify the bioactive ingredients from these plants have yielded a family of natural products structurally characterized by a xanthone backbone in which the C ring has been converted into a caged tricyclic structure. Plant-specific substitutions and oxidations of this motif produce several subfamilies, such as the morellins (**1**, **2**),[2] the gaudichaudiones (**3**, **4**),[3] and the gambogins (**5**, **6**)[4] (Figure 1).

The ability of several caged *Garcinia* xanthones to selectively inhibit tumor cell proliferation and exhibit potent cytotoxicity at low μM concentrations has been well documented.[5] Moreover, gaudichaudione A (**3**) and gambogic acid (**5**) displayed strong growth inhibitory activities against both parental murine leukemic P388 and P388/doxorubicin-resistant cell lines, suggesting that they are not subjects of the multidrug-resistance mechanism that is typical of several relapsed cancers.[6] In addition, **5** displays antitumor activity in animal models and has an appropriate therapeutic window for clinical applications as an anticancer agent.[7]

A recent study reported that gambogic acid binds to the Bcl-2 family of proteins resulting in apoptosis presumably by blocking the antiapoptotic activity of these proteins.[8] Earlier mode-of-action studies have suggested that this compound binds to the transferrin receptor 1 (TfR1) and that this binding correlates with the induction of apoptosis.[9] Structure-activity relationship studies have proposed that the caged motif plays an essential role in the cytotoxicity.[10]

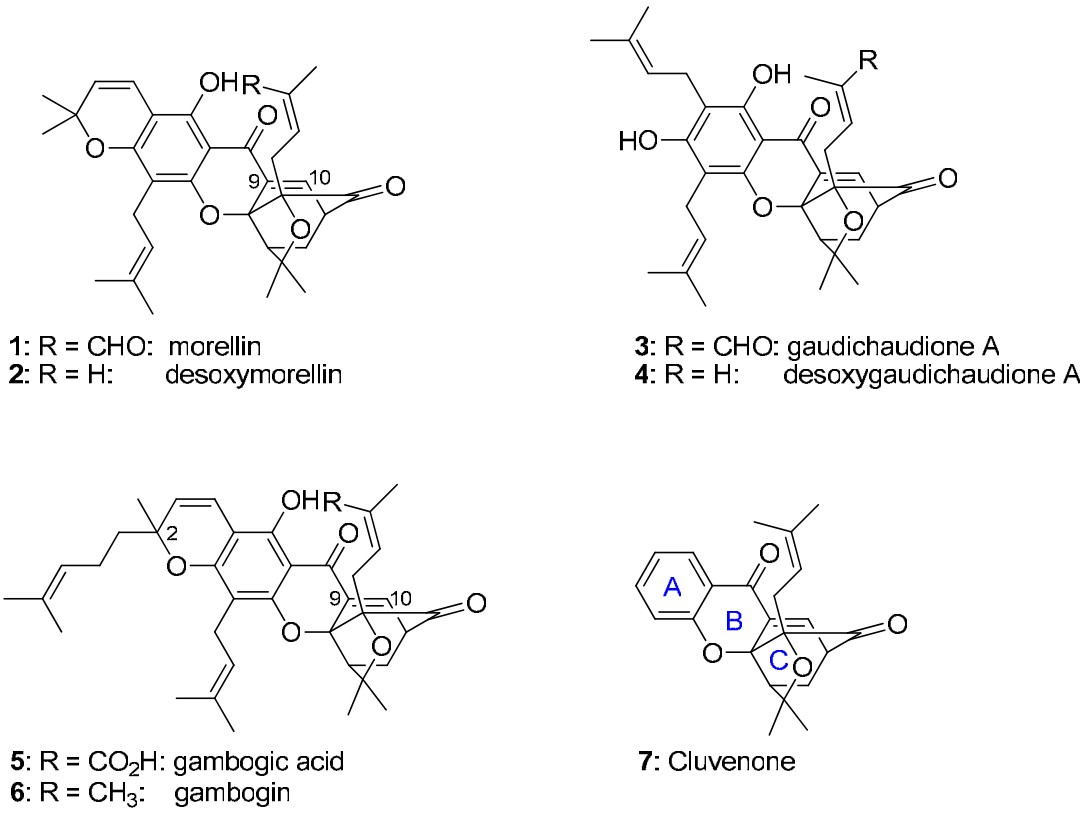

Figure 1. Chemical structures of selected caged *Garcinia* xanthones

Inspired by the therapeutic potential of the caged *Garcinia* xanthones, we developed a chemical strategy that allows access to these natural products and related analogues, such as cluvenone (**7**).[11,12] This strategy relies on a biomimetic Claisen/Diels-Alder/Claisen reaction cascade that produces the caged motif from a reverse prenylated xanthone.[13,14] Moreover, we have found that cluvenone (**7**) maintains the activity exhibited by the more structurally complex natural products of this family.[12] We have also shown that this compound is equally cytotoxic to HL-60 cells and the multidrug-resistant clone, HL-60/ADR, at low μM concentrations, attesting to the pharmacologically promising caged *Garcinia* xanthone motif. Herein, we report our studies on the evaluation of the pharmacophoric motif of these compounds. We also

present a new Pd(0)-catalyzed method for the reverse prenylation (installation of 1,1-dimethyl-2-propenyl units) of catechols, the synthetic precursors of the caged scaffolds. This reaction led to a synthesis of several caged *Garcinia* analogues and to an optimized synthesis of cluvenone (**7**).

Section 2.2 Synthesis of BC and C Ring Caged Analogues

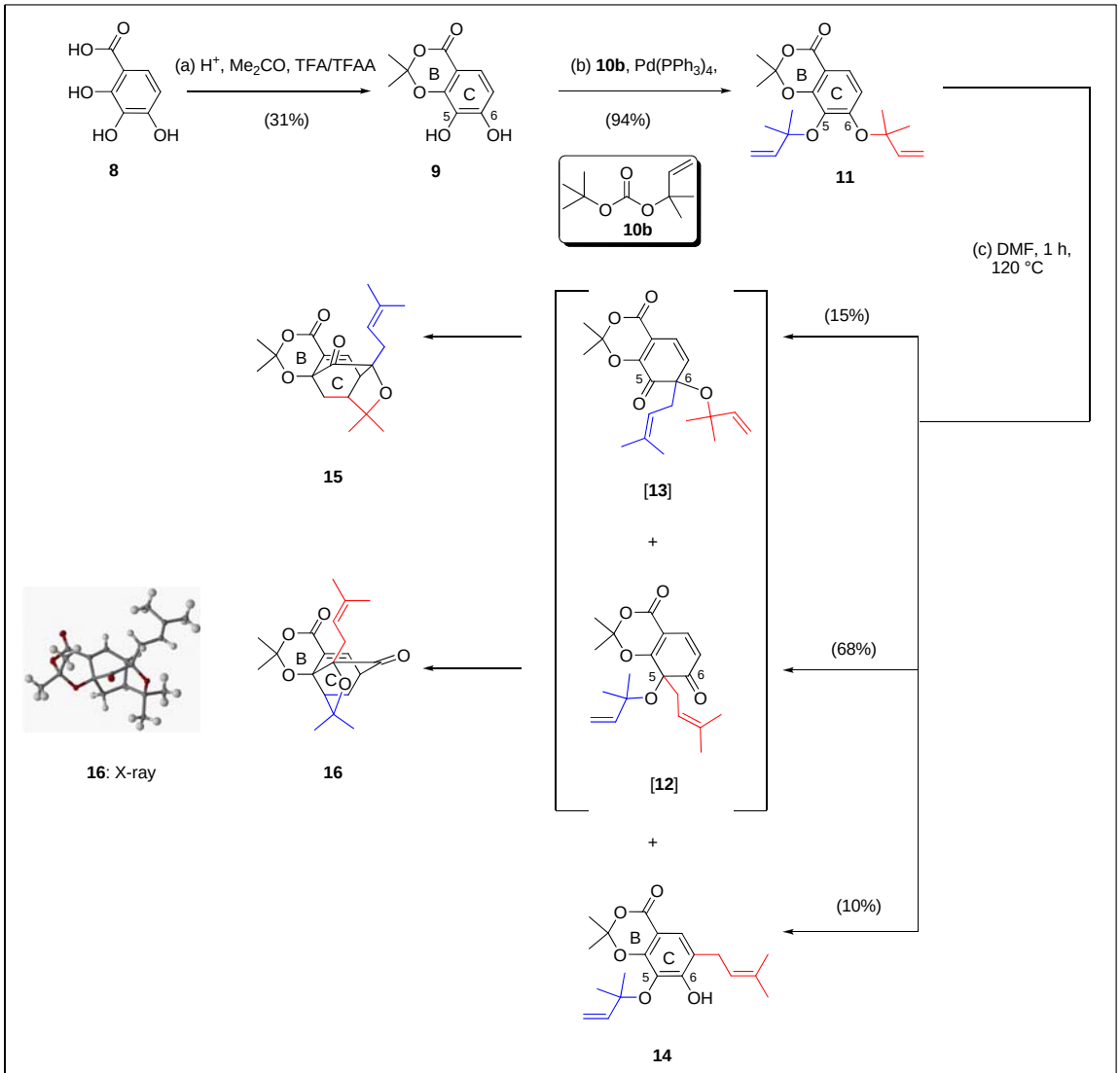

Scheme 1. Synthesis of BC ring caged analogues containing structural motif **9**. *Reagents and conditions*: (a) 6.0 equiv. $(CH_3)_2CO$, 20 equiv. TFA, 10 equiv. TFAA, 19 h, 0 °C, 31%; of **9**, 60% RSM; (b) 10 equiv. t-butyl 2-methylbut-3-en-2-yl carbonate (**10b**), 10 mol% $Pd(PPh_3)_4$, THF, 20 min, 0 °C, 94%; (c) DMF, 1 h, reflux, 120 °C, **14**: 10%, **15**: 68%, **16**: 15%.

Our initial studies aimed to produce analogues of the caged *Garcinia* xanthones lacking the A ring. With this in mind, commercially available 2,3,4-trihydroxybenzoic acid (**8**) was treated with acetone in the presence of TFA/TFAA (Scheme 1). To minimize formation of diprotected products, the reaction was performed at 0 °C and

produced dioxanone **9** in 31% yield together with starting material **8** (60% yield). Initial efforts to convert **9** to **11** were based on a previously reported two-step sequence that involves propargylation using 2-chloro-2-methyl butyne followed by Lindlar reduction of the resulting alkynes.[13] However, this two-step process proved to be tedious and difficult to streamline. To overcome this problem we decided to develop an alternative method for the one-step introduction of the 1,1-dimethyl-2-propenyl unit (reverse prenyl group) to a catechol motif. Support for this reaction came from a report on the reverse prenylation of a substituted phenol using 1,1-dimethylpropenyl isobutyl carbonate (**10a**) under Pd(0) catalysis.[15] Using 1,1-dimethylpropenyl isobutyl carbonate (**10a**), we obtained the desired compound **11** (62-69% yield) together with significant amounts of isobutyl addition products (5-10%). We hypothesized that these side products could be formed through a Mitsunobu-type reaction between isobutanol, triphenyl prosphine and catechol **9**. To minimize their formation we tested the allylation reaction with 1,1-dimethylpropenyl *t*-butyl carbonate (**10b**). In this case we observed the formation of **11** as the only product which was isolated in 94% yield. Similar yields (90-92%) were obtained using the unexplored bis(1,1-dimethylpropenyl)carbonate (**10c**).[16] We also evaluated this reaction under Rh(I) catalysis but did not observe the formation of any prenylation product.[17]

Heating of **11** in DMF (120 °C, 1 h) gave rise to two caged compounds **15** and **16** in 68% and 15% yields, respectively (Scheme 1). Under these conditions did we also observe the formation of phenol **14**, arising from a Claisen rearrangement of **11** in 10% yield. The formation of compounds **15** and **16** can be explained by considering an intramolecular Diels-Alder cycloaddition of intermediates **12** and **13,** respectively, which

have been formed via a Claisen rearrangement of **11**. The observed site-selectivity of this reaction cascade (C5 versus C6 allylation) parallels our previous observations, favoring the formation of the regular caged structure **15** versus the neo isomer **16**.[12,13] It is worth noting that, upon additional heating at 120 °C, phenol **14** produced caged compounds **15** and **16**, supporting the reversibility of the Claisen rearrangement.[18,19]

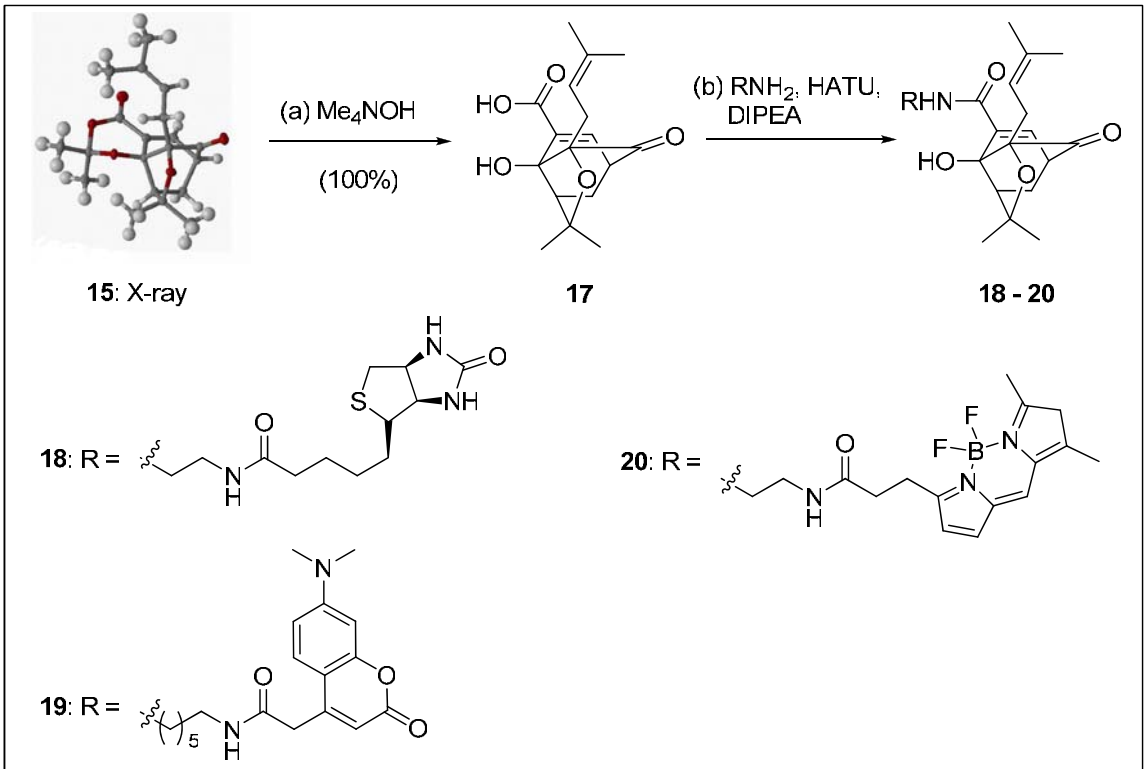

Scheme 2. Synthesis of C ring caged analogues containing structural motif **8** with amide side chains. *Reagents and conditions*: (a) excess 10% NMe_4OH (aq), MeOH, 24 h, 25 °C, 100%; (b) 2.0 equiv. DIPEA, 1.2 equiv. HATU, CH_2Cl_2, 24 h, 25 °C, 18: 54%, 19: 59%, 20: 68%.

Deprotection of the acetonide unit of compound **15** can open the B ring producing C-ring caged analogues. To this end, exposure of **15** to 10% aqueous Me_4NOH in MeOH provided the optimum saponification conditions and produced the desired β-hydroxy acid **17** in quantitative yield (Scheme 2). This compound was converted to amides **18-20** in good yields using standard amide coupling protocols.

In a similar manner, reaction of pyrrogallol **21** with acrylonitrile formed nitrile **22** (Scheme 3). Reflux of **22** in the presence of H_2SO_4 (50% aq.) produced dihydroxychromanone **23** (16% combined yield).[20] The Pd(0)-catalyzed reverse prenylation of **23** with **10b** formed compound **24** (89% yield), which upon heating gave rise to caged motif **26** in 91% yield. In this case we did not detect the formation of the neo caged structure.

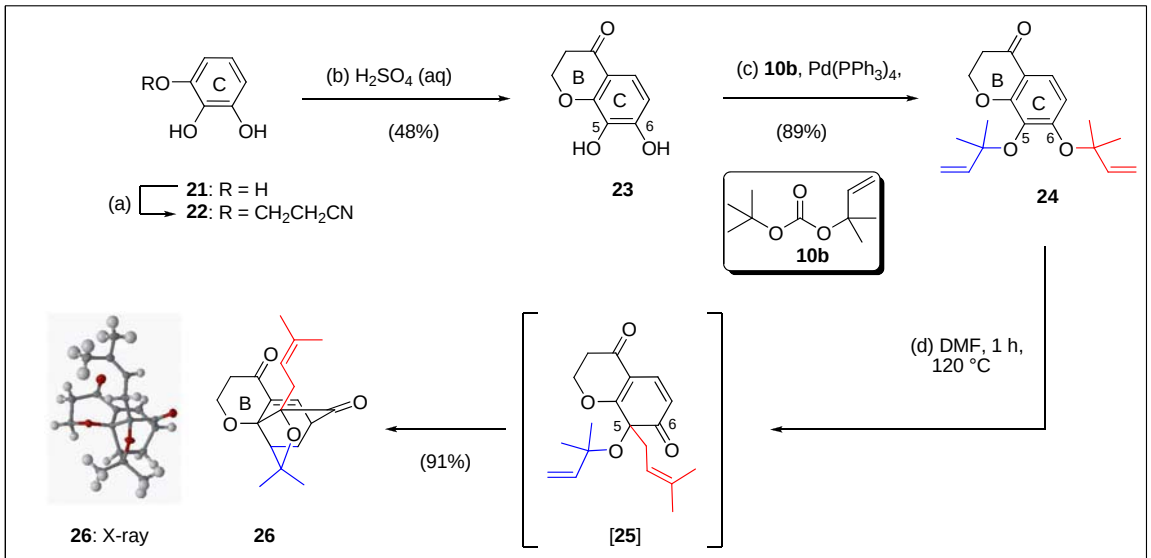

Scheme 3. Synthesis of BC ring caged analogues containing structural motif **23**. Reagents and conditions: (a) 3.4 equiv. acrylonitrile, 0.3 equiv. NaOMe, 7 h, reflux, 76 °C, 34%; (b) excess 50% (w/w) H_2SO_4 (aq), 3 h, reflux, 105 °C, 48%; (c) 10 equiv. t-butyl 2-methylbut-3-en-2-yl carbonate (**10b**), 10 mol% $Pd(PPh_3)_4$, THF, 4 h, 0 °C, 89%; (d) DMF, 1.5 h, reflux, 120 °C, 91%.

Section 2.3 Improved Synthesis of Cluvenone and Synthesis of Related Allylic Oxidation Products

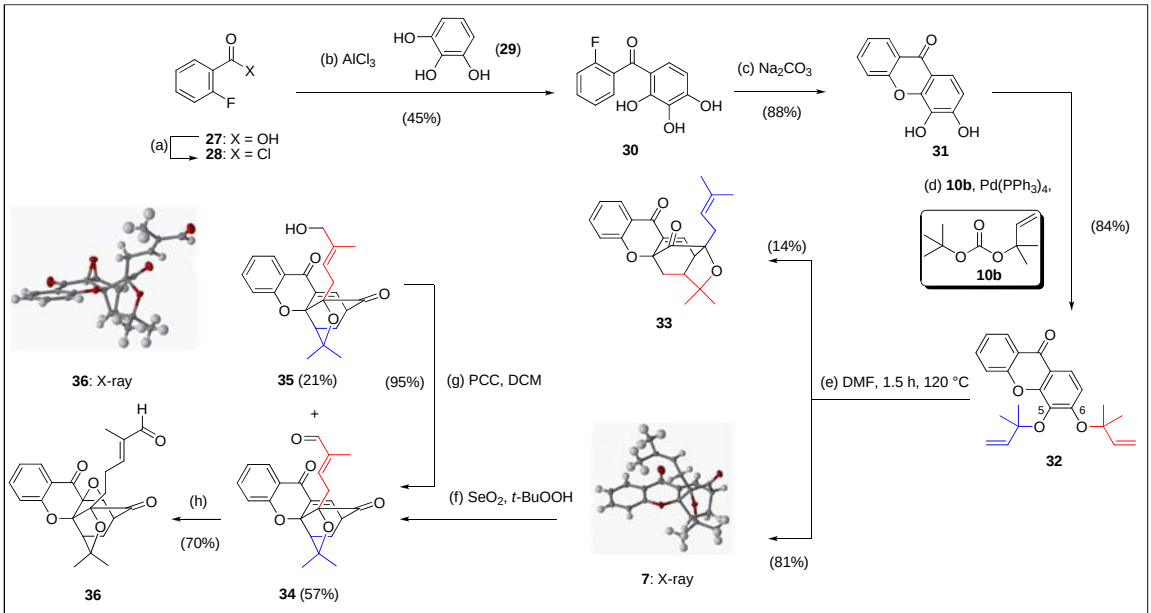

Scheme 4: Improved synthesis of ABC ring caged analogues containing structural motif **31** and synthesis of related allylic oxidation products. *Reagents and conditions*: (a) 1.2 equiv. ClCOCOCl (2.0 M in DCM), DCM, DMF (cat.), 1.5 h, 0 to 25 °C, 87%; (b) 2.0 equiv. **29**, 2.9 equiv. $AlCl_3$, chloroform, DCM, 12 h, 25 °C; then 4 h, reflux, 60 °C, 45%; (c) 1.5 equiv. Na_2CO_3, DMF, 3.5 h, reflux, 90 °C, 86%; (d) 10.0 equiv. t-butyl 2-methylbut-3-en-2-yl carbonate **10b**, 10 mol% $Pd(PPh_3)_4$, THF, 2.5 h, 5 °C, 84%; (e) DMF, 1.5 h, reflux, 120 °C, **7**: 81%, **33**: 14%; (f) 5 mol% SeO_2, 1.8 equiv. *t*-BuOOH, DCM, 19 h, 25 °C, **34**: 57%, **35**: 21%; (g) 1.5 equiv. PCC, DCM, 30 min, 25 °C, 95% (h) 3.0 equiv. $NaClO_2$, 3.0 equiv. $NaHPO_4oH_2O$, 8.0 equiv. 2-methyl-2-butene, t-BuOH/H_2O (2:1), 4 h, 0 °C, 70%.

An improved synthesis of cluvenone (**7**), featuring the Pd(0)-catalyzed reverse prenylation reaction, is shown in Scheme 4. The tricyclic xanthone **31** was prepared in two steps: (a) a Friedel-Crafts acylation of pyrrogalol (**29**) with 2-fluorobenzoyl chloride (**28**) in the presence of $AlCl_3$ and (b) a base-induced cyclization of the resulting benzophenone **30** (2 steps, 34% combined yield). Pd(0)-catalyzed reverse prenylation of **31** using 1,1-dimethylpropenyl *t*-butyl carbonate (**10b**) gave rise to compound **32** in 84% yield. The heat-induced Claisen/Diels-Alder reaction cascade furnished cluvenone **7** in 81% yield, along with small amounts of the neo caged xanthone **33** (14% yield).

With compound **7** in hand we explored an allylic oxidation reaction (Scheme 4). Treatment of **7** with SeO_2 and *t*-BuOOH produced aldehyde **34** (57% isolated yield) as the main product together with alcohol **35** (21%). The latter compound was converted to **34** upon PCC oxidation in 95% yield. However, all attempts to oxidize aldehyde **34** to the corresponding acid met with failure. In all these cases the characteristic signal corresponding to the C10 proton disappeared, indicating a substitution of the enone bond. Under relatively mild oxidation conditions ($NaClO_2$) we were able to isolate epoxide **36** in 70% yield. This observation supports the expected reactivity of the C9-C10 enone motif as a conjugate electrophile.

Section 2.4 Synthesis of Caged Garcinia Xanthone Analogues Modified at the C9-C10 Enone Bond

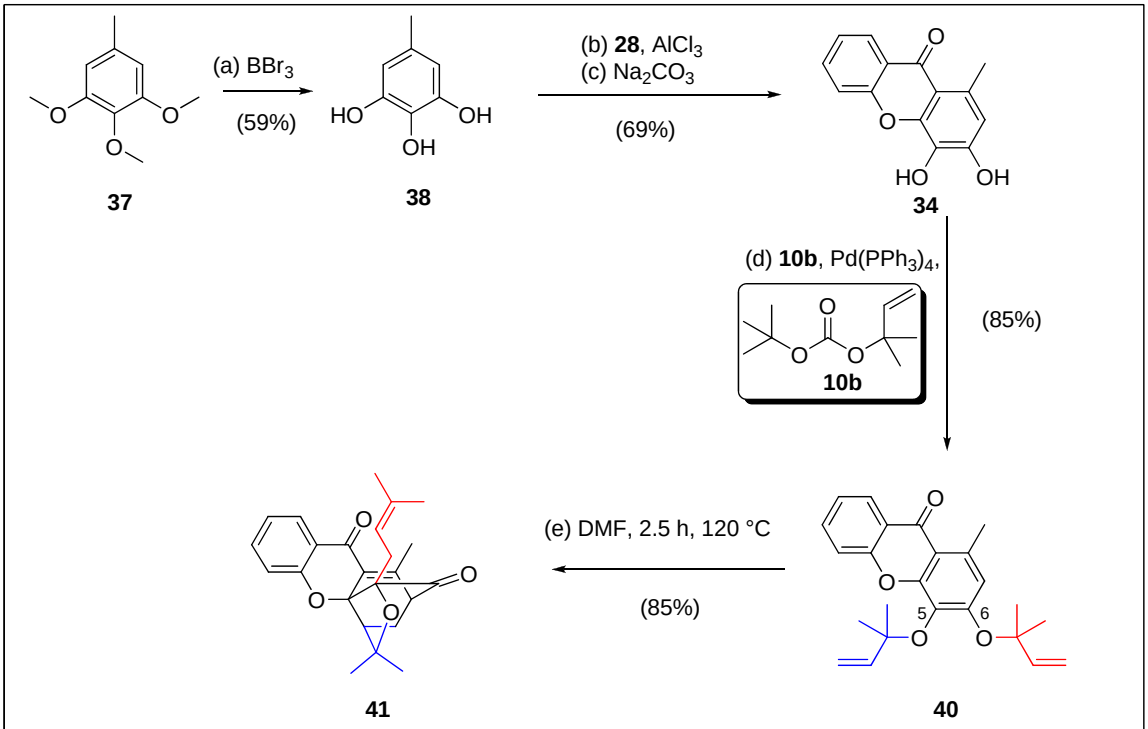

Scheme 5. Synthesis of ABC ring caged analogues containing structural motif **39**. *Reagents and conditions*: (a) excess BBr_3, DCM, 3 h, 0 to 25 °C, 59%; (b) 1.5 equiv. **28**, 2.0 equiv. $AlCl_3$, chloroform, DCM, 1.5 h, 25 °C; then 6 h, 60 °C; (c) 1.5 equiv. Na_2CO_3, DMF, 69% (over two steps); (d) 10.0 equiv. t-butyl 2-methylbut-3-en-2-yl carbonate **10b**, 10 mol% $Pd(PPh_3)_4$, THF, 6 h, 25 °C, 76%; (e) DMF, reflux, 2.5 h, 120 °C, 85%.

It has been suggested that the C9-C10 double bond of the caged *Garcinia* xanthones plays an essential role in the bioactivity of these molecules.[10a] For instance, conjugate reduction of the enone motif has yielded compounds that are of reduced cytotoxicity. This has been tentatively attributed to their decreased ability to serve as conjugate electophiles. However, the C9-C10 conjugate reduction affects the chemical structure of the caged xanthone motif, which in turn could be responsible for the lack of activity. To further test this hypothesis, we sought to evaluate the bioactivity of the C10

methylated analogue **41**. This compound was prepared as shown in Scheme 5. Commercially available 1,2,3-trimethoxy-5-methylbenzene (**37**) was demethylated with excess BBr_3 to form polyphenol **38** in 59% yield.[21] Friedel-Crafts acylation of **38** with 2-fluorobenzoyl chloride (**28**) in the presence of $AlCl_3$ followed by Na_2CO_3-induced cyclization of the resulting benzophenone produced xanthone **39** in 69% combined yield. The Pd(0)-catalyzed reverse prenylation with carbonate **10b** gave rise to compound **40** which, upon heating, underwent the Claisen/Diels-Alder reaction cascade to form caged xanthone **41** in 85% yield (Scheme 5).

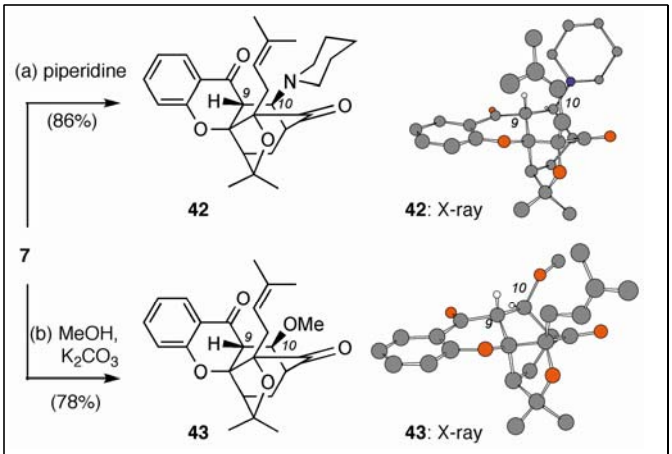

Scheme 6. Preparation of the caged xanthonoid derivatives from cluvenone **7**. *Reagents and conditions*: (a) 4.0 equiv piperidine, DCM, 4 h, 25 °C, 86%; (b) 4.0 equiv K_2CO_3, 4.0 equiv MeOH, THF, 4 h, 25 °C, 78%.

We have also treated cluvenone (**7**) with piperidine and MeOH under basic conditions. These reactions led to the formation of the conjugate addition products **42** and **43** that were isolated in 86% and 78% yield, respectively (Scheme 6). The chemical structure of these compounds was determined via X-ray analysis and indicated that the conjugate addition proceeded in a syn fashion across the C9-C10 enone bond.

Section 2.5 Synthesis of Amide Analogues of Gambogic Acid

To evaluate the bioactivity of the carboxylic acid functionality of gambogic acid (**5**) we prepared the amide derivatives **44-46**. These compounds contain affinity and fluorescent probes and can be used for studies related to receptor binding assays and subcellular localization of the caged *Garcinia* xanthones. The amide coupling reaction proceeded in high yields using the DIPEA and HATU protocol (Scheme 7).

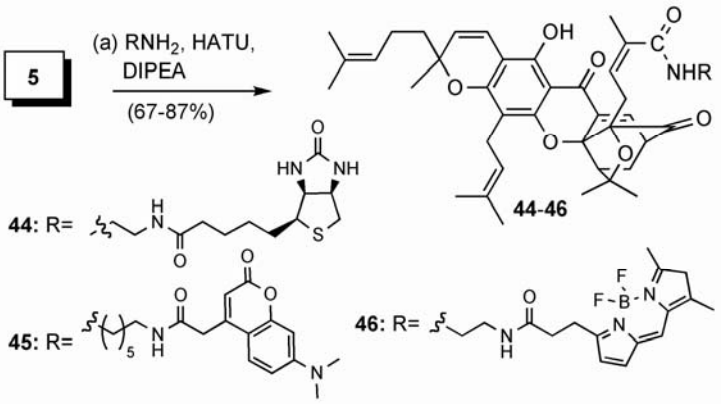

Scheme 7. Synthesis of amide analogues of gambogic acid **5**. *Reagents and conditions*: (a) 2.0 equiv. DIPEA, 1.2 equiv. HATU, CH_2Cl_2, 24 h, 25 °C, **44**: 67%, **45**: 87%, **46**: 77%.

Section 2.6 Cell Proliferation Studies

The ability of the synthesized caged *Garcinia* xanthones to inhibit cancer cell growth was evaluated in a multidrug-resistant promyelocytic leukemia cell line, HL-60, using a ^{3}H-thymidine incorporation assay. Cells were incubated with increasing concentrations of the compounds for 48 h, and then pulsed with ^{3}H-thymidine for 6 h. Gambogic acid (**5**) and cluvenone (**7**) were the most active among all compounds tested and exhibited an IC_{50} value of 0.5 and 0.4 μM, respectively (Table 1). Similar activity was observed for the amide analogues of gambogic acid (compounds **44**, **45**

and **46**, entries 18-20, respectively) as well as for the oxidized analogues of cluvenone (compounds **34** and **35**). Gambogin (**6**) also exhibited a low μM activity. These results suggest that: (a) the dihydropyran motif of **5** and **6** is not needed for the bioactivity and (b) the carboxylic acid of **5** can be functionalized without loss of bioactivity. In contrast, the intact ABC caged ring structure is important for the bioactivity. For instance, compounds **15**, **16** and **17** induce less than 10% growth inhibition at up to 10 μM concentrations.

Table 1. Inhibition of cell proliferation by caged Garcinia xanthones and analogues in multi-drug resistant promyelocytic leukemia cells

entry	Compound	IC_{50}/ μM HL-60/ADR
1	gambogic acid (**5**)	0.5
2	gambogin (**6**)	1.1
3	cluvenone (**7**)	0.4
4	**15**	ND*
5	**16**	ND*
6	**17**	ND*
7	**18**	20.1
8	**19**	20.7
9	**20**	27.3
10	**26**	10.4
11	**33**	1.3
12	**34**	0.7
13	**35**	0.8
14	**36**	2.5
15	**41**	5.1
16	**42**	2.8
17	**43**	2.5
18	**44**	1.1
19	**45**	0.3
20	**46**	0.6

*Less than 10% inhibition at 10.0 μM

Similarly, the C-ring amide analogues **18**-**20** have IC_{50} values greater than 20 μM, while compound **26**, which lacks the A ring, has an IC_{50} value of 10 μM. Compound **33**, containing the neo caged structure, has a low micromolar activity (IC_{50} value of 1.3 μM) but is about 3 times less potent than cluvenone (**7**) and related compounds with the regular caged motif. On the other hand, substitution of the C9-C10 enone functionality decrease substantially the bioactivity. For instance, compound **41** is almost 10 times less active than cluvenone (**7**), while compounds **36**, **42**, and **43** are about 5 times less active than **7**. A similar cytotoxicity pattern has been reported for gambogoic acid derivative, the conjugate addition product of **5** with methanol.[22] These results demonstrate the significance of the C9-C10 enone functionality for the bioactivity of these compounds. This may be due to its reactivity as a conjugate electrophile.

Section 2.7 Apoptosis studies

To determine whether the mechanism of cytotoxicity of these compounds involves the induction of apoptosis, a cell death detection ELISA which measures histone-associated DNA fragments was performed. These studies were performed with cluvenone (**7**) and are shown in Figure 2. Compound **7** induced apoptosis, after 7 h of treatment of HL-60 and HL-60/ADR cells, in a dose-dependent manner with EC_{50} of 0.25 and 0.32 μM, respectively. These results are comparable to the apoptotic effect of gambogic acid and related caged *Garcinia* natural products. Specifically, the EC_{50} values of **5** in human breast cancer cells T47D, human colon cancer cells HCT116 and hepatocellular carcinoma cancer cells SNU398 are reported to be about 0.7 μM.[10b] More importantly, the similar EC_{50} observed for cluvenone (**7**) in the HL-60 and HL-60/ADR

cells parallels our previous observations[12] and confirms that its cytotoxicity is not affected by the expression of P-glycoprotein which renders the HL-60/ADR cell lines multidrug-resistant.[24]

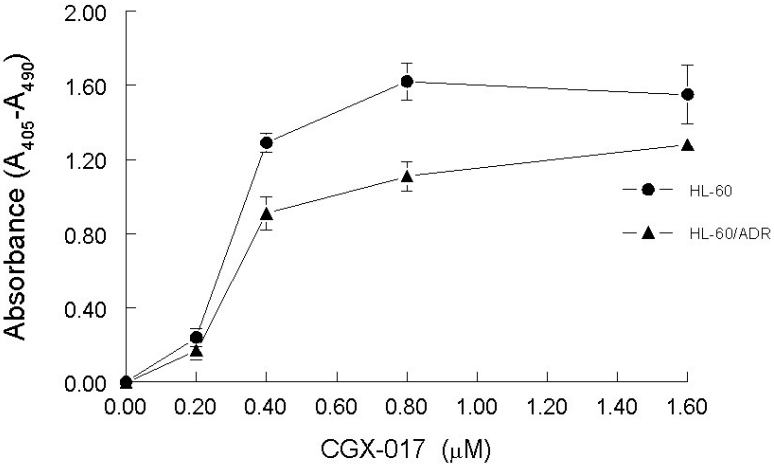

Figure 2: Induction of apoptosis by cluvenone (CGX-017 or **7**) in promyelocytic leukemia cells

Apoptosis induced in HL60/ADR cells by cluvenone (**7**) was also visualized by fluorescence microscopy after staining with Alexa Fluor® 488 annexin V and propidium iodide (PI) (Figure 3). The green-fluorescent Alexa Fluor® 488 annexin V detects the externalization of phosphatidylserine, a hallmark of apoptosis (Figure 3, middle column).[24] The red-fluorescent propidium iodide stains DNA during advanced stages of apoptosis and necrosis (Figure 3, right column). Cells in the left column of Figure 3 have been visualized by differential interference contrast (DIC) microscopy. While untreated live cells show little or no fluorescence (Figure 3, top row), cluvenone-treated cells undergoing early stages apoptosis show only green fluorescence after staining with both probes (Figure 3, middle row). In the middle row is also evident the membrane blebbing, which is characteristic of apoptosis.[24] Cluvenone-treated cells undergoing late stage

apoptosis, at which point DNA becomes accessible to staining by PI, display both green and red fluorescence (Figure 3, bottom row). In this row is the chromatin fragmentation also evident.

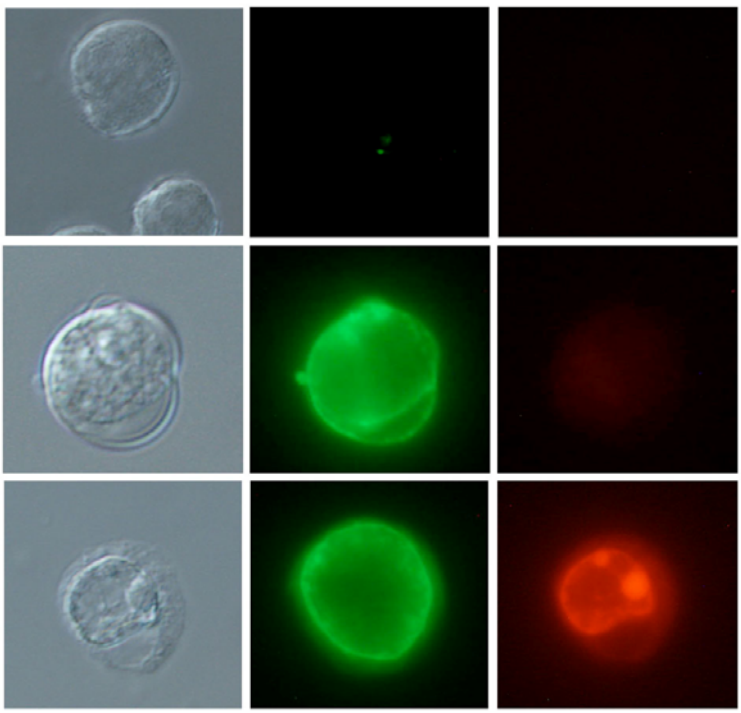

Figure 3. Induction of apoptosis in HL-60/ADR cells by cluvenone (7) visualized by differential interference contrast microscopy (left column) and fluorescence microscopy (middle and right column). Control unreated cells are shown in the top row. Treated cells undergoing early and late stage apoptosis are shown in the middle and bottom row respectively.

Section 2.8 Conclusions

We present herein a study aiming to identify the pharmacophoric motif of the caged *Garcinia* xanthones. Our results indicate that the minimum bioactive motif of these compounds is represented by the intact ABC ring containing the C-ring caged structure. Abbreviation of this motif results in substantial loss of activity. The C9-C10 enone functionality is also important to the activity, while the C5 prenyl group can be oxidized and functionalized without loss of bioactivity. In fact, this site could be used for

modifications that will improve the solubility and pharmacology of these compounds. We have also developed a method for the reverse prenylation (installation of 1,1-dimethyl-2-propenyl units) of catechols. This reaction proceeds in excellent yields under Pd(0)-catalysis using 1,1-dimethylpropenyl *t*-butyl carbonate (**10b**) or bis(1,1-dimethylpropenyl)carbonate (**10c**) as the prenylation reagents. Application of this reaction led to an improved synthesis of lead analogue cluvenone (**7**). In this study, we have also demonstrated that cluvenone (**7**) induces cell death via apoptosis and has similar cytotoxicity in multidrug-resistant and sensitive leukemia cells. These results support our previous findings on the pharmacological potential of the caged *Garcinia* xanthones, enhance our understanding of the structure-activity relationship, and pave the way for the preparation of therapeutically relevant agents.

Section 2.9 Experimental Section

Section 2.9.1 General techniques

Gambogic acid (**5**), $Pd(PPh_3)_4$, and 2-fluorobenzoic acid (**27**) were purchased from Gaia Chemical Corporation (Gaylordsville, CT), Strem Chemicals, Inc. (Newburyport, MA), and TCI America (Portland, OR), respectively. Biotin ethylenediamine hydrobromide and BODIPY FL EDA were purchased from Invitrogen (Carlsbad, CA). The rest of the reagents were obtained (Aldrich, Acros) at highest commercial quality and used without further purification except where noted. All reagents were commercially obtained (Aldrich, Acros) at highest commercial quality and used without further purification except where noted. Air- and moisture-sensitive liquids and solutions were transferred via syringe or stainless steel cannula. Organic solutions

were concentrated by rotary evaporation below 45 °C at approximately 20 mmHg. All non-aqueous reactions were carried out under anhydrous conditions with flame-dried glassware within an argon atmosphere in dry, freshly distilled solvents, unless otherwise noted. Tetrahydrofuran, diethyl ether, dichloromethane, toluene, and benzene were purified by passage through a bed of activated alumina. Dimethylformamide and dimethylsulfoxide were distilled from calcium hydride under reduced pressure (20 mmHg) and stored over 4Å molecular sieves until needed. Yields refer to chromatographically and spectroscopically (^{1}H NMR, ^{13}C NMR) homogeneous materials, unless otherwise stated. Reactions were monitored by thin-layer chromatography (TLC) carried out on 0.25 mm E. Merck silica gel plates (60F-254) and visualized under UV light and/or developed by dipping in solutions of 10% ethanolic phosphomolybdic acid (PMA) or p-anisaldehyde and applying heat. E. Merck silica gel (60, particle size 0.040-0.063 mm) was used for flash chromatography. Preparative thin-layer chromatography separations were carried out on 0.25 or 0.50 mm E. Merck silica gel plates (60F-254). NMR spectra were recorded on Varian Mercury 400 and/or Unity 500 MHz instruments and calibrated by using the residual non-deuterated solvent as an internal reference. The following abbreviations were used to explain the multiplicities: s = singlet, d = doublet, t = triplet, q = quartet, m = multiplet, b = broad. IR spectra were recorded on a Nicolet 320 Avatar FT-IR spectrometer and values are reported in cm^{-1} units. High resolution mass spectra (HRMS) were recorded on a VG 7070 HS mass spectrometer under chemical ionization (CI) conditions or on a VG ZAB-ZSE mass spectrometer under fast atom bombardment (FAB) conditions. X-ray data were recorded on a Bruker SMART APEX 3 kW sealed tube X-ray diffraction system.

Section 2.9.2 Experimental Procedures and Data

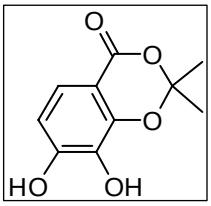

7,8-Dihydroxy-2,2-dimethyl-4*H*-benzo[d][1,3]dioxin-4-one 9. To a suspension of 2, 3, 4-trihydroxybenzoic acid **8** (0.99 g, 6.4 mmol) in TFA (9.5 mL) was added TFAA (10.0 mL, 64.0 mmol) followed by dry acetone (2.8 mL, 38 mmol) at 0 ºC. After 19 h, the homogeneous reaction mixture was concentrated under reduced pressure to half its volume and subsequently stirred with EtOAc (50 mL) and aqueous saturated $NaHCO_3$ (50 mL) in a 500 mL Erlenmeyer flask. The aqueous and ethyl acetate layers were then separated and the aqueous layer was back-extracted with EtOAc (2 x 25 mL). The combined ethyl acetate layers were dried over $MgSO_4$, filtered and concentrated by rotary evapor ation. The crude material was purified through flash column chromatography (silica, 50% EtOAc-hexane) to give the acetonide **9** (0.38 g, 31%). **9:** white solid; R_f = 0.14 (50% EtOAc-hexane); ^{1}H NMR (400 MHz, $CDCl_3$) δ 7.50 (d, *J* = 8.6 Hz, 1H), 6.72 (d, *J* = 8.6 Hz, 1H), 6.01 (s, 1H), 5.30 (s, 1H), 1.76 (s, 6H); ^{13}C NMR (100 MHz, $CDCl_3$) δ 161.9, 151.4, 144.4, 131.5, 122.4, 110.7, 107.5, 106.3, 26.0; HRMS calc. for $C_{10}H_{10}O_5$ $(M + H)^+$ 210.0523, found 210.0524.

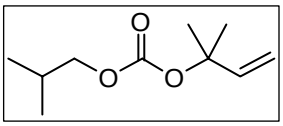

Isobutyl 2-methylbut-3-en-2-yl carbonate 10a. 2-Methyl-3-buten-2-ol (7.3 mL, 70 mmol) was dissolved in dry THF (125 mL) and stirred under argon at 0 ºC. To the clear solution was added 1.6 M *n*-BuLi in hexane (48.1 mL, 77.0 mmol) dropwise via syringe. After 30 min of continued stirring at 0 ºC, isobutyl chloroformate (13.7 mL, 105 mmol) was added dropwise to the reaction mixture. The reaction vessel was then allowed to gradually warm to room temperature and stirred for another 4 hours at room temperature. The reaction mixture was acidified

by addition of 1M HCl, extracted with diethyl ether (3 x 50 mL) and washed with water (20 mL). The combined organic layers were dried over $MgSO_4$, filtered, and concentrated by rotary evaporation to give isobutyl 2-methylbut-3-en-2-yl carbonate **10a** (13.9 mL, 100%). Further purification was not necessary. **10a**: colorless liquid; R_f = 0.60 (25% EtOAc-hexane); ^{1}H NMR (400 MHz, $CDCl_3$): δ 6.10 (dd, *J* = 17.5, 10.9 Hz, 1H), 5.22 (d, *J* = 17.5 Hz, 1H), 5.13 (d, *J* = 11.0 Hz, 1H), 3.85 (d, *J* = 6.7 Hz, 1H), 1.99-1.92 (m, 1H), 1.55 (s, 6H), 0.94 (s, 3H), 0.93 (s, 3H); ^{13}C NMR (100 MHz, $CDCl_3$) δ 153.8, 142.0, 113.7, 82.1, 73.5, 28.0, 26.4, 19.2.

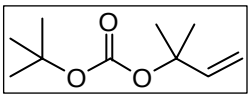

***tert*-Butyl 2-methylbut-3-en-2-yl carbonate 10b.** To a solution of 2-methyl-3-buten-2-ol (4.0 mL, 38 mmol) in dry THF (80 mL) under argon at -78 ^{o}C was added 1.6 M *n*-BuLi in hexane (26.3 mL, 42.1 mmol) dropwise via syringe. After stirring for 30 min, a solution of Boc_2O (8.35 g, 38.3 mmol) in THF (5 mL) was added to the reaction mixture. The reaction mixture was allowed to warm to room temperature and stirred for another 3 hours. The reaction mixture was then quenched with saturated aqueous NH_4Cl (20 mL) and extracted with diethyl ether (2 x 25 mL). The combined organic layers were washed with water and brine, dried over $MgSO_4$, filtered, and concentrated in vacuo. Purification by flash column chromatography (silica, 100% hexane) gave *tert*-butyl 2-methylbut-3-en-2-yl carbonate **10b** (1.8 g, 100%). **10b**: colorless liquid; R_f = 0.60 (25% EtOAc-hexane); ^{1}H NMR (400 MHz, $CDCl_3$): δ 6.11 (dd, *J* = 17.5, 10.9 Hz, 1H), 5.17 (d, *J* = 17.5 Hz, 1H), 5.09 (d, *J* = 10.9 Hz, 1H), 1.51 (s, 6H), 1.45 (s, 6H); ^{13}C NMR (100 MHz, $CDCl_3$) δ 152.1, 142.5, 113.2, 81.6, 81.6, 28.1, 26.6; HRMS calc. for $C_{10}H_{18}O_3$ $(M + Na)^+$ 209.1150, found 209.1148.

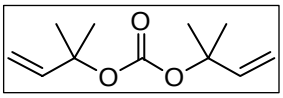

Bis(2-methylbut-3-en-2-yl) carbonate 10c: Carbonate **10c** was prepared in two steps as the following: 2-methyl-3-buten-2-ol (2.1 mL, 25 mmol) was dissolved in dry DCM (20 mL) in a 50 mL round-bottomed flask. To the stirring solution was added carbonyl diimidazole (5.0 g, 31.3 mmol) at room temperature. After 1 hour, the reaction mixture was washed with water (2 x 15 mL) and extracted with DCM (20 mL). The organic layer was dried over $MgSO_4$, filtered, and concentrated by rotary evaporation to yield 2-methylbut-3-en-2-yl 1*H*-imidazole-1-carboxylate (1.9 g, 84%) which was used in the next step without further purification. 2-methylbut-3-en-2-yl 1*H*-imidazole-1-carboxylate: colorless liquid; R_f = 0.48 (25% EtOAc-hexane); ^{1}H NMR (400 MHz, $CDCl_3$): δ 8.03 (s, 1H), 7.33 (s, 1H), 6.98 (s, 1H), 6.11 (dd, *J* = 17.4, 10.9 Hz, 1H), 5.27 (d, *J* = 17.4 Hz, 1H), 5.18 (d, *J* = 10.9 Hz, 1H), 1.64 (s, 6H); ^{13}C NMR (100 MHz, $CDCl_3$) δ 147.0, 140.6, 137.2, 130.5, 117.3, 115.0, 85.7, 64.4, 26.4. To a solution of 2-methyl-3-buten-2-ol (4.1 mL, 39 mmol) in dry THF (80 mL) under argon at -78 ^{o}C was added 1.6 M *n*-BuLi in hexane (26.7 mL, 42.7 mmol) dropwise via syringe. After stirring for 30 min at -78 ^{o}C, 2-methylbut-3-en-2-yl 1*H*-imidazole-1-carboxylate (6.7 mL, 38.8 mmol) was added. The reaction mixture was allowed to warm to room temperature and stirred for another 3 hours. The reaction mixture was then quenched with saturated aqueous NH_4Cl (20 mL) and extracted with diethyl ether (2 x 25 mL). The combined organic layers were washed with water (2 x 20 mL) and brine (20 mL), dried over $MgSO_4$, and concentrated in vacuo. Purification by flash column chromatography (silica, 100% hexane) gave bis(2-methylbut-3-en-2-yl) carbonate **10c** (7.7 g, 100%). **10c:** colorless liquid; R_f = 0.60 (25% EtOAc-hexane); ^{1}H

NMR (400 MHz, $CDCl_3$): δ 6.08 (dd, J = 17.5, 10.9 Hz, 2H), 5.15 (d, J = 17.5 Hz, 2H), 5.07 (d, J = 10.9 Hz, 2H), 1.46 (s, 12H); ^{13}C NMR (100 MHz, $CDCl_3$) δ 151.8, 142.2, 113.4, 81.9, 26.5

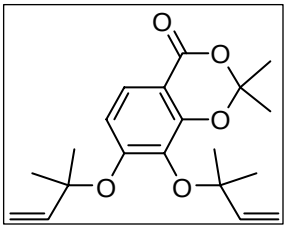

2,2-Dimethyl-7,8-bis(2-methylbut-3-en-2-yloxy)-4*H*-benzo[d][1,3]dioxin-4-one 11. To a 25 mL round-bottomed flask was added acetonide **9** (95 mg, 0.45 mmol) followed by THF (0.65 mL). The reaction vessel was degassed by argon and was placed in an ice bath. To the clear homogeneous solution was added *tert*-butyl 2-methylbut-3-en-2-yl carbonate **10b** (0.89 mL, 4.50 mmol) via syringe, followed by $Pd(PPh_3)_4$ (52.0 mg, 45.0 μmol). The reaction vessel was stirred under argon at 5 ºC for 20 min. The onset of a blue suspension indicated the formation of the desired product **11**. The solvent was removed by rotary evaporation and the crude material was purified through flash column chromatography (silica, 10% EtOAc-hexane) to yield the desired product **11** (146.5 mg, 94%). **11**: colorless oil; R_f = 0.61 (25% EtOAc-hexane); ^1H NMR (400 MHz, $CDCl_3$) δ 7.54 (d, J = 8.8 Hz, 1H), 6.81 (d, J = 8.9 Hz, 1H), 6.16 (m, 2H), 5.20 (m, 3H), 5.02 (d, J = 10.9 Hz, 1H), 1.72 (s, 3H), 1.55 (s, 3H), 1.47 (s, 3H); ^{13}C NMR (100 MHz, $CDCl_3$) δ 161.5, 158.6, 152.1, 143.9, 143.8, 135.6, 124.5, 114.3, 113.7, 113.0, 107.6, 106.4, 106.4, 83.3, 82.1, 27.4, 27.1, 26.1; HRMS calc. for $C_{20}H_{26}O_5$ $(M + H)^+$ 369.1672, found 369.1674.

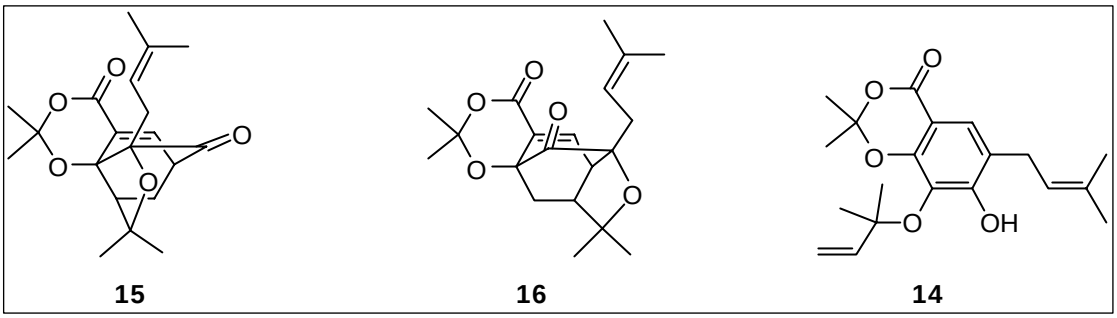

Caged bicycle 15 and neo-caged bicycle 16. Alkene **11** (99 mg, 0.28 mmol) was dissolved in dry DMF (1.8 mL) and the solution was stirred under argon at 120 ºC. After 1 hour, the reaction mixture was concentrated under reduced pressure. The crude material was purified by flash column chromatography (silica, 10-17% EtOAc-hexane) to yield the caged product **15** (67 mg, 68%), neo-caged product **16** (15 mg, 15%), and compound **14** (10 mg, 10%), respectively. **Caged product 15**: white solid; R_f = 0.10 (25% EtOAc-hexane); ^{1}H NMR (400 MHz, $CDCl_3$) δ 7.44 (d, *J* = 6.9 Hz, 1H), 4.41 (m, 1H), 3.42 (t, *J* = 4.3 Hz, 1H), 2.72 (dd, *J* = 13.8, 10.4 Hz, 1H), 2.63 (m, 1H), 2.50 (d, *J* = 9.7 Hz, 1H), 2.31 (dd, *J* = 13.6, 4.7 Hz, 1H), 1.69 (s, 3H), 1.67 (s, 3H), 1.62 (s, 3H), 1.54 (s, 3H), 1.53 (s, 3H), 1.44 (dd, *J* = 13.6, 9.3 Hz, 1H), 1.23 (s, 3H); ^{13}C NMR (100 MHz, $CDCl_3$) δ 203.2, 159.9, 139.0, 135.6, 128.1, 118.1, 105.1, 85.0, 84.9, 82.9, 48.6, 46.8, 30.2, 29.1, 28.8, 28.5, 28.0, 26.9, 25.9, 18.4; HRMS calc. for $C_{20}H_{26}O_5$ $(M + Na)^+$ 369.1672, found 369.1675. **Neo-caged product 16**: white solid; R_f = 0.30 (25% EtOAc-hexane); ^{1}H NMR (400 MHz, $CDCl_3$) δ 7.41 (d, *J* = 7.0 Hz, 1H), 4.95 (t, *J* = 7.0 Hz, 1H), 3.63 (dd, *J* = 7.0, 4.5 Hz, 1H), 2.36-2.25 (m, 4H), 1.69 (s, 3H), 1.68 (s, 3H), 1.64-1.61 (m, 1H), 1.59 (s, 3H), 1.43 (s, 3H), 1.31 (s, 3H), 1.29 (s, 3H); ^{13}C NMR (100 MHz, $CDCl_3$) δ 205.0, 159.2, 140.1, 136.7, 127.7, 117.2, 106.5, 83.6, 81.2, 80.1, 46.0, 45.5, 34.1, 30.7, 30.2, 28.6, 27.8, 27.0, 26.2, 18.2; HRMS calc. for $C_{20}H_{26}O_5$ $(M + Na)^+$ 369.1672, found 369.1686. **Phenol**

14: colorless oil; R_f = 0.52 (25% EtOAc-hexane);[1]H NMR (400 MHz, $CDCl_3$) δ 7.50 (s, 1H), 6.27 (s, 1H), 6.15 (dd, *J* = 17.5, 10.8 Hz, 1H), 5.35-5.25 (m, 2H), 5.17 (d, *J* = 10.9 Hz, 1H), 3.26 (d, *J* = 7.1 Hz, 1H), 1.74 (s, 3H), 1.72 (s, 6H), 1.69 (s, 3H) 1.48 (s, 6H); ^{13}C NMR (100 MHz, $CDCl_3$) δ 161.6, 156.0, 149.1, 143.3, 133.9, 130.0, 125.6, 123.1, 121.3, 114.6, 106.4, 105.8, 83.6, 27.9, 26.9, 26.1, 18.0; HRMS calc. for $C_{20}H_{26}O_5$ $(M + Na)^+$ 369.1672, found 369.1680.

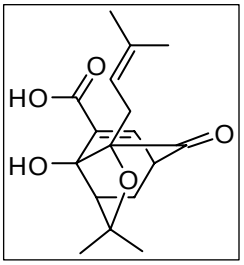

Carboxylic acid 17. To a 25 mL round-bottomed flask was added caged product **15** (41 mg, 0.12 mmol) followed by methanol (1.5 mL). The flask was placed in an ice bath and the solution was stirred at 0 ºC. To the stirring solution was then added 10% NMe_4OH (aq) (1.7 mL, 159 mmol) dropwise via syringe. The light yellow reaction mixture was allowed to warm to room temperature and further stirred at 25 ºC for another 30 min. Acetic acid (10 mL) was then added to neutralize the reaction mixture. The reaction mixture was partitioned between ethyl acetate (2 x 25 mL) and water (25 mL). The combined organic layers were dried over $MgSO_4$, filtered, and concentrated by rotary evaporation. The crude material was purified by recrystallization (DCM-hexane) to yield the acid **17** (37 mg, 100%). **17**: white solid; R_f = 0.11 (67% EtOAc-hexane); ^{1}H NMR (400 MHz, $CDCl_3$) δ 7.45 (d, *J* = 7.1 Hz, 1H), 4.64 (t, *J* = 6.4 Hz, 1H), 3.33 (t, *J* = 5.3 Hz, 1H), 2.69 (dd, *J* = 13.8, 9.8 Hz, 1H), 2.58 (dd, *J* = 13.8, 5.3 Hz, 1H), 2.25 (m, 2H), 1.60 (s, 6H), 1.57 (s, 3H), 1.40 (dd, *J* = 13.4, 9.6 Hz, 1H), 1.23 (s, 3H); ^{13}C NMR (100 MHz, $CDCl_3$) δ 204.7, 168.4, 142.0, 135.5, 130.7, 118.8, 85.0, 84.0, 83.5, 49.5, 47.1, 30.2, 29.2, 28.7, 27.1, 26.1, 18.0; HRMS calc. for $C_{17}H_{22}O_5$ $(M + Na)^+$ 329.1359, found 329.1362.

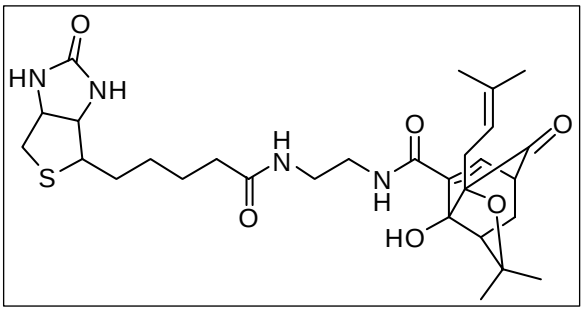

Biotin conjugate 18. To a solution containing acid **17** (5.4 mg, 17.6 μmol) and biotin ethylenediamine hydrobromide (7.1 mg, 19.4 μmol) in DCM (0.37 mL) was added DIPEA (6.13 μL, 35.2 μmol). Upon adding solid HATU (7.4 mg, 19.4 μmol) portionwise to the reaction mixture, the reaction mixture turned to pale yellow in color within 5 min. After 24 hours, the reaction mixture was partitioned between ethyl acetate (5 mL) and water (2 mL). The organic layer was washed with water (2 x 1 mL) and brine (2 mL). The combined organic layers were then dried over $MgSO_4$, filtered, and concentrated by rotary evaporation. The crude material was purified by preparative TLC (silica, 9% MeOH-EtOAc) to obtain the amide **18** (5.5 mg, 9.53 μmol, 54%). **18**: yellow solid; R_f = 0.28 (20% MeOH-EtOAc); ^{1}H NMR (400 MHz, $CDCl_3$) δ 7.84 (br s, 1H), 7.70 (br s, 1H), 7.08 (br s, 1H), 7.01 (br s, 1H), 6.89 (dd, *J* = 22.7, 7.0 Hz, 1H), 6.64 (d, *J* = 21.9 Hz, 1H), 6.60 (d, *J* = 8.4 Hz, 1H), 5.49 (d, *J* = 17.2 Hz, 1H), 4.72 (m, 1H), 4.54 (m, 1H), 4.33 (m, 1H), 3.50-3.33 (m, 4H), 3.23-3.14 (m, 2H), 2.94 (dd, *J* = 12.9, 4.9 Hz, 1H), 2.74 (d, *J* = 12.9 Hz, 1H), 2.67-2.18 (m, 5H), 2.80-2.30 (m, 16H), 1.20 (s, 3H); ^{13}C NMR (100 MHz, $CDCl_3$) δ 205.8, 174.5, 167.4, 156.1, 145.0, 135.4, 134.6, 131.9, 128.2, 124.2, 121.1, 118.8, 117.2, 85.3, 84.3, 83.2, 49.7, 46.3, 42.1, 39.4, 35.9, 30.3, 29.3, 28.6, 27.5, 26.2, 25.1, 18.0, 15.3, 11.6; HRMS calc. for $C_{29}H_{42}N_4O_6S$ $(M + Na)^+$ 597.2717, found 597.2728.

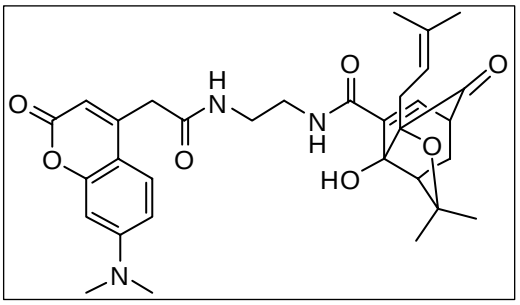

Coumarin conjugate 19. To a solution containing acid **17** (5.40 mg, 17.6 μmol) and coumarin diethyleneamine (5.58 mg, 19.4 μmol) in DCM (0.37 mL) was added DIPEA (6.13 μL, 35.2 μmol). Upon adding solid HATU (7.36 mg, 19.4 μmol) portionwise to the reaction mixture, the reaction mixture turned to pale yellow in color within 5 min. After 24 hours, the reaction mixture was partitioned between ethyl acetate (5 mL) and water (2 mL). The organic layer was washed with water (2 x 1 mL) and brine (2 mL). The combined organic layers were then dried over $MgSO_4$, filtered, and concentrated by rotary evaporation. The crude material was purified by preparative TLC (silica, 100% EtOAc) to obtain the amide **19** (6.0 mg, 59%). **19**: yellow solid; R_f = 0.17 (100% EtOAc); ^{1}H NMR (400 MHz, $CDCl_3$) δ 7.48 (br s, 1H), 7.45 (br s, 1H), 6.90 (br s, 1H), 6.68 (d, *J* = 7.0 Hz, 1H), 6.60 (dd, *J* = 9.1, 2.5 Hz, 1H), 6.46 (d, *J* = 2.5 Hz, 1H), 6.30 (br s, 1H), 6.00 (br s, 1H), 4.69 (t, *J* = 7.6 Hz, 1H), 3.64 (s, 2H), 3.52-3.13 (m, 5H), 3.06 (s, 6H), 2.60 (dd, *J* = 14.0, 9.0 Hz, 1H), 2.47 (dd, *J* = 13.8, 6.3 Hz, 1H), 2.16 (m, 2H), 1.58 (s, 3H), 1.53 (s, 3H), 1.49 (s, 3H), 1.27 (m, 1H), 1.19 (s, 3H); ^{13}C NMR (100 MHz, $CDCl_3$) δ 205.3, 169.8, 167.0, 165.8, 161.8, 156.1, 153.2, 149.2, 135.3, 134.7, 132.7, 125.4, 118.4, 110.5, 109.2, 108.0, 98.2, 84.7, 84.4, 83.0, 49.4, 46.1, 40.6, 40.5, 40.4, 40.1, 30.1, 29.7, 29.0, 28.2, 27.3, 25.9, 17.8; HRMS calc. for $C_{32}H_{39}N_3O_7$ $(M + Na)^+$ 600.2680, found 600.2688.

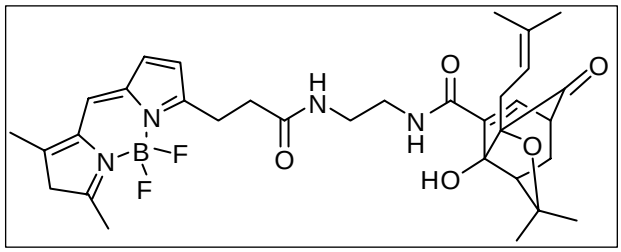

BODIPY conjugate 20. To a solution containing acid **17** (4.0 mg, 13.1 μmol) and BODIPY FL EDA (4,4-difluoro-5,7-dimethyl-4-bora-3a,4a-diaza-s-indacene-3-propionyl ethylenediamine) (5.3 mg, 14.4 μmol) in DCM (0.27 mL) was added DIPEA (4.56 μL, 26.2 μmol). Upon adding solid HATU (5.9 mg, 15.6 μmol) portionwise to the reaction mixture, the reaction mixture turned to pale yellow in color within 5 min. After 4 hours, the reaction mixture was partitioned between ethyl acetate (5 mL) and water (2 mL). The organic layer was washed with water (2 x 1 mL) and brine (2 mL). The combined organic layers were then dried over $MgSO_4$, filtered, and concentrated by rotary evaporation. The crude material was purified by preparative TLC (silica, 100% EtOAc) to obtain the amide **20** (5.60 mg, 68%). **20**: red solid; R_f = 0.62 (100% EtOAc); ^{1}H NMR (400 MHz, $CDCl_3$) δ 7.54 (br s, 1H), 7.11 (s, 1H), 6.92 (s, 1H), 6.87 (d, J = 3.8 Hz, 1H), 6.69 (d, J = 7.0 Hz, 1H), 6.26 (br s, 1H), 6.24 (d, J = 3.8 Hz, 1H), 6.15 (s, 1H), 4.64 (t, J = 6.9 Hz, 1H), 3.40-3.10 (m, 6H), 2.71-2.56 (m, 4H), 2.56 (s, 3H), 2.27 (s, 3H), 2.18-2.15 (m, 2H), 1.59 (s, 6H), 1.51 (s, 3H), 1.36-1.27 (m, 1H), 1.19 (s, 3H); ^{13}C NMR (100 MHz, $CDCl_3$) δ 205.8, 174.5, 167.4, 161.4, 156.1, 145.0, 135.4, 134.6, 131.9, 128.2, 124.2, 121.1, 118.8, 117.2, 85.3, 84.3, 83.2, 49.7, 46.3, 42.1, 39.4, 35.9, 30.3, 29.3, 28.6, 27.5, 26.2, 25.1, 18.0, 15.3, 11.6; HRMS calc. for $C_{33}H_{41}BF_2N_4O_5$ $(M + Na)^+$ 645.3030, found 645.3043.

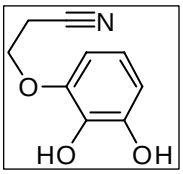

3-(2,3-Dihydroxylphenoxy)propanenitrile 22. To a 250 mL round-bottomed flask was added pyrogallol **21** (10.0 g, 79.3 mmol) and acrylonitrile (14.7 g, 278 mmol) followed by NaOMe (4.3 g, 79.3 mmol). The reaction vessel was then equipped with a reflux condenser and stirred under argon at 78 ºC for 7 hours. The onset of a dark black color indicated the formation of the 3-(2,3-dihydorxylphenoxy)propanenitrile **22**. The reaction mixture was then cooled to 25 ºC and the excess acrylonitrile was removed by rotary evaporation. The residue was extracted with ethyl acetate (5 x 100 mL), and the combined organic layers were dried over $MgSO_4$, filtered, and concentrated by rotary evaporation. The crude material was purified through flash column chromatography (silica, 40% EtOAc-hexane) to yield the nitrile **22** (4.5 g, 32%). **22**: off-white solid; R_f = 0.43 (50% EtOAc-hexane); ^{1}H NMR (400 MHz, DMSO-d6) δ 6.55 (t, J = 8.0 Hz, 1H), 6.44 (m, 2H), 4.11 (t, J = 6.0 Hz, 2H), 2.94 (t, J = 6.0 Hz, 2H); ^{13}C NMR (100 MHz, DMSO-d6) δ 146.8, 146.2, 135.0, 119.0, 118.3, 109.8, 106.0, 64.2, 18.1; HRMS calc. for $C_9H_9NO_3$ $(M + Na)^+$ 202.0471, found 202.0475.

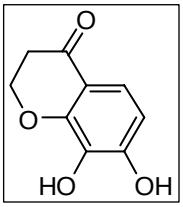

7,8-Dihydroxychroman-4-one 23. To a 100 mL round-bottomed flask containing 3-(2,3-dihydroxylphenoxy)propanenitrile **22** (2.05 g, 11.8 mmol) was added slowly dropwise, via the addition funnel, aqueous sulfuric acid (50% v/v, 42 mL). The reaction vessel was then equipped with a reflux condenser and stirred under argon at 105 ºC for 3 hours. The cooled solution was diluted with water (50 mL) and extracted with ethyl acetate (4 x 100 mL). The organic layers were washed with water, brine, and dried over $MgSO_4$. The combined organic layers were then filtered and concentrated by rotary evaporation. The crude material was

purified through flash column chromatography (silica, 60-70% EtOAc-hexane) to yield 7,8-dihydroxychroman-4-one **23** (0.98 g, 48%). **23**: off-white solid; R_f = 0.38 (70% EtOAc-hexane); ^{1}H NMR (400 MHz, DMSO-d6) δ 7.15 (dd, *J* = 8.7, 1.3 Hz, 1H), 6.49 (dd, *J* = 8.6, 1.3 Hz, 1H), 4.48 (t, *J* = 6.3 Hz, 2H), 2.67 (t, *J* = 6.3 Hz, 2H); ^{13}C NMR (100 MHz, DMSO-d6) δ 190.3, 152.0, 151.3, 132.7, 117.4, 114.5, 109.6, 67.1, 37.1; HRMS calc. for $C_9H_8O_4$ $(M + H)^+$ 181.0495, found 181.0494.

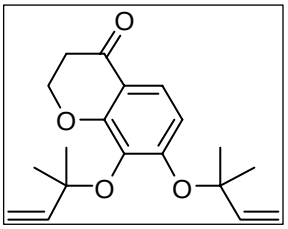

7,8-Bis(2-methylbut-3-en-2-yloxy)chroman-4-one 24. To a 25 mL round-bottomed flask was added 7,8-dihydroxychroman-4-one **23** (50 mg, 0.28 mmol) followed by dry THF (1.5 mL). The flask was degassed by argon and was placed in an ice water bath. To the yellow homogeneous solution was added *tert*-butyl 2-methylbut-3-en-2-yl carbonate **10b** (522 mg, 2.80 mmol), via syringe, followed by $Pd(PPh_3)_4$ (32 mg, 0.028 mmol). The reaction vessel was stirred under argon at 5 ºC for 2 hours. The onset of a yellow suspension indicated the formation of the alkene **24**. The solvent was removed by rotary evaporation and the crude material was purified through flash column chromatography (silica, 30-40% EtOAc-hexane) to yield 7,8-bis(2-methylbut-3-en-2-yloxy)choman-4-one **24** (79 mg, 89%). **24**: yellow oil; R_f = 0.52 (30 % EtOAC-hexane); ^{1}H NMR (400 MHz, $CDCl_3$) δ 7.49 (d, *J* = 9.0 Hz, 1H), 6.72 (d, *J* = 9.0, 1H), 6.19 (dd, *J* = 17.4, 10.6 Hz, 1H), 6.12 (dd, *J* = 17.6, 10.9 Hz, 1H), 5.13 (m, 3H), 4.98 (dd, *J* = 10.9, 1.1 Hz, 1H), 4.47 (t, *J* = 6.5 Hz, 2H), 2.71 (t, *J* = 6.6 Hz, 2H), 1.51 (s, 6H), 1.47 (s, 6H); ^{13}C NMR (100 MHz, $CDCl_3$) δ 191.2, 157.8, 143.7, 135.8, 121.7, 116.7, 113.8, 113.6, 112.5, 82.8, 81.8, 67.1, 37.4, 27.1, 26.7; HRMS calc. for $C_{19}H_{24}O_4$ $(M + Na)^+$ 339.1567, found 339.1569.

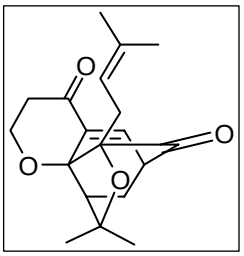

Caged chromanone 26. A solution of compound **24** (36 mg, 0.11 mmol) in DMF (1.5 mL) was heated at 120 ºC for 1.5 hours. The onset of a brown color indicated the formation of the caged xanthone **26**. The reaction mixture was then cooled to 25 ºC and the solvent was removed by rotary evaporation. The crude material was purified through flash column chromatography (silica, 50-55 % EtOAc-hexane) to yield the caged product **26** (33 mg, 91%). **26**: white solid; R_f = 0.21 (30 % EtOAc-hexane); ^{1}H NMR (400 MHz, $CDCl_3$) δ 7.25 (d, *J* = 6.6 Hz, 1H), 4.41 (m, 1H), 4.17 (ddd, *J* = 12.1, 6.5, 1.4 Hz, 1H), 3.94 (dt, *J* = 12.3, 2.9 Hz, 1H), 3.34 (m, 1H), 2.63 (d, *J* = 8.6 Hz, 1H), 2.50 (dd, *J* = 12.4, 6.5 Hz, 1H), 2.42 (dd, *J* = 2.9, 1.4 Hz, 1H), 2.37 (m, 1H), 2.31 (dd, *J* = 13.6, 4.5 Hz, 1H), 1.59 (s, 3H), 1.53 (s, 3H), 1.48 (s, 3H), 1.32 (m, 1H), 1.23 (s, 3H); ^{13}C NMR (100 MHz, $CDCl_3$) δ 203.9, 192.0, 136.9, 135.4, 133.8, 119.2, 87.4, 84.2, 82.9, 60.0, 46.2, 44.5, 38.1, 30.1, 28.8, 27.7, 25.5, 17.9; HRMS calc. for $C_{19}H_{24}O_4$ $(M + Na)^+$ 339.1567, found 339.1571.

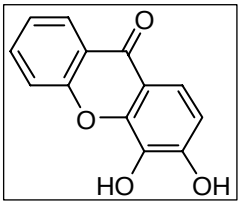

3,4-Dihydroxy-9*H*-xanthen-9-one 31. To a clean, dried 250 mL round-bottomed flask was added 2-fluorobenzoic acid **27** (5.09 g, 36.3 mmol). The flask containing 2-fluorobenzoic acid **27** and a magnetic stir bar was placed under high vacuum for about 10 min. The flask was carefully sealed and DCM (100 mL) was added by using a syringe under argon. The flask was then placed in an ice bath and the reaction mixture was stirred at 0 ºC. To the stirring solution of 2-fluorobenzoic acid **27** and DCM was added a solution of oxalyl chloride (2.0 M in dichloromethane, 21.0 mL, 42.0 mmol) dropwise, via syringe, followed by a

catalytic amount of DMF. The ice bath was removed and the reaction mixture was stirred at room temperature for 1.5 hours. The solution was concentrated by rotary evaporation under argon to yield a colorless oil, 2-fluorobenzoyl chloride **28** (5.01 g, 87%). To a mixture of pyrogallol **29** (6.48 g, 51.3 mmol), aluminum chloride (14.6 g, 110 mmol), chloroform (80 mL), and DCM (200 mL) in a 1 L round-bottomed flask was added a solution of 2-fluorobenzoyl chloride **28** in DCM (10 mL) dropwise via syringe. The reaction mixture was stirred at room temperature under argon for 17 hours. The reaction vessel was then equipped with a reflux condenser and stirred under argon at 80 ºC for another 4 hours. The cooled, red homogeneous solution was acidified with 1N HCl (300 mL). The reaction mixture was then partitioned between water and ethyl acetate (3 x 200 mL). The aqueous layer was back-extracted with ethyl acetate (2 x 200 mL) until the color of the aqueous layer was almost clear. The combined organic layers were dired over $MgSO_4$, filtered, and concentrated to yield (2-fluorophenyl)(2,3,4-trihydroxy-phenyl)methanone **30** (3.54 g, 45%). To a 500 mL round-bottomed flask containing sodium carbonate (2.27 g, 21.4 mmol) and DMF (100 mL) was added (2-fluorophenyl)(2,3,4-trihydroxyphenyl)-methanone **30**. The reaction vessel was the equipped with a reflux condenser and stirred under argon at 90 ºC for 4 hours. The dark reaction mixture was cooled to room temperature and acidified with 1 N HCl (300 mL). The reaction mixture was then partitioned between water and ethyl acetate (3 x 150 mL). The aqueous layer was back extracted with ethyl acetate (5 x 150 mL). The combined brown organic layers were dried over $MgSO_4$, filtered, and concentrated by rotary evaporation. The crude material was purified through flash column chromatography (silica, 50-60% EtOAc-hexane) to yield 3,4-dihydroxy-9*H*-xanthen-9-one **31** (2.79 g,

86%). **31**: off-white solid; R_f = 0.42 (90% Et_2O-hexane); ^1H NMR (400 MHz, DMSO-d6) δ 10.52 (br s, 1H), 9.46 (br s, 1H), 8.15 (dd, *J* = 7.9, 1.5 Hz, 1H), 7.83 (ddd, *J* = 8.7, 7.2, 1.7 Hz,1H), 7.63 (dd, *J* = 8.4, 0.7 Hz, 1H), 7.56 (d, *J* = 8.6 Hz, 1H), 7.42 (t, *J* = 7.5 Hz, 1H), 6.94 (d, *J* = 8.8 Hz, 1H); ^{13}C NMR (100 MHz, DMSO-d6) δ 175.3, 155.5, 151.5, 146.3, 134.8, 132.6, 125.9, 123.9, 120.8, 118.0, 116.5, 114.7, 113.1; HRMS calc. for $C_{13}H_8O_4$ $(M + H)^+$ 229.0501, found 229.0509.

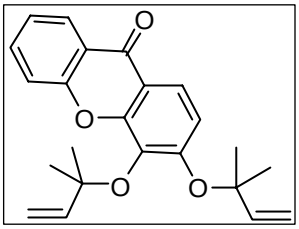

3,4-Bis(2-methylbut-3-en-2-yloxy)-9*H*-xanthen-9-one 32. To a 50 mL round-bottomed flask was added 3,4-dihydroxy-9*H*-xanthen-9-one **31** (56 mg, 0.24 mmol) followed by dry THF (1.5 mL). The flask was degassed by argon and was placed in an ice water bath. To the yellow homogeneous solution was added *tert*-butyl 2-methylbut-3-en-2-yl carbonate **10b** (455 mg, 2.4 mmol), via syringe, followed by $Pd(PPh_3)_4$ (28 mg, 0.024 mmol). The reaction vessel was stirred under argon at 5 ºC for 2 hours. The onset of a yellow suspension indicated the formation of the alkene **32**. The solvent was removed by rotary evaporation and the crude material was purified through flash column chromatography (silica, 10-15% EtOAc-hexane) to yield 3,4-bis(2-methylbut-3-en-2-yloxy)-9*H*-xanthen-9-one **32** (74 mg, 84%). **32**: yellow solid; R_f = 0.67 (30 % EtOAc-hexane); ^1H NMR (400 MHz, $CDCl_3$) δ 8.30 (dd, *J* = 8.0, 1.7 Hz, 1H), 7.92 (d, *J* = 9.1 Hz, 1H), 7.68 (ddd, *J* = 8.6, 7.1, 1.7 Hz, 1H), 7.49 (d, *J* = 7.9 Hz, 1H), 7.36 (ddd, *J* = 8.0, 7.2, 0.9 Hz, 1H), 7.12 (d, *J* = 8.9 Hz, 1H), 6.28 (dd, *J* = 17.5, 10.8 Hz, 1H), 6.18 (dd, *J* = 17.6, 10.9 Hz, 1H), 5.19 (m, 3H), 5.01 (dd, *J* = 10.9, 1.0 Hz, 1H), 1.58 (s, 6H), 1.56 (s, 6H); ^{13}C NMR (100 MHz, $CDCl_3$) δ 176.8, 156.9, 155.9, 152.4, 143.5, 143.4, 135.7, 134.3, 126.5, 123.7, 121.5, 121.0, 117.8,

117.1, 116.8, 114.1, 113.0, 83.5, 82.1, 27.1, 26.9; HRMS calc. for $C_{23}H_{24}O_4$ $(M + H)^+$ 365.1753, found 365.1740.

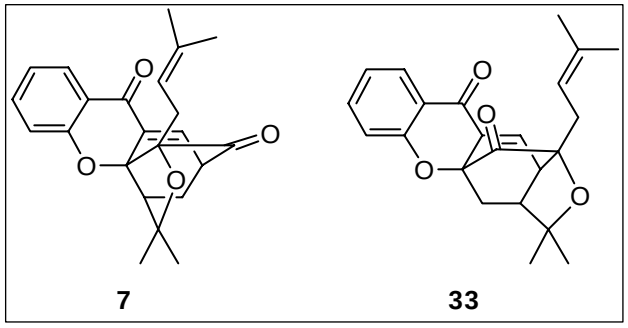

Caged xanthones 7 and 33. A solution of compound **31** (350 mg, 0.96 mmol) in DMF (6 mL) was refluxed at 120 ºC for 1.5 hours. The onset of a brown color indicated the formation of the xanthones **33** and **7**. The brown reaction mixture was then cooled to room temperature and the solvent was removed by rotary evaporation. The crude material was then purified by column chromatography (silica, 20-30% Et_2O-hexane) to yield a mixture of caged products **7** (285 mg, 81%) and **33** (50 mg, 14%). **7**: white solid; R_f = 0.28 (25% EtOAc-hexane); ^{1}H NMR (400 MHz, $CDCl_3$) δ 7.93 (dd, *J* = 8.0 Hz, 1.7 Hz, 1H), 7.51 (ddd, *J* = 8.9, 7.3, 1.7 Hz, 1H), 7.42 (d, *J* = 6.9 Hz, 1H), 7.05 (m, 2H), 4.39 (m, 1H), 3.48 (dd, *J* = 6.7 Hz, 4.6 Hz, 1H), 2.64 (m, 2H), 2.45 (d, *J* = 9.6 Hz, 1H), 2.33 (dd, *J* = 13.5 Hz, 4.6 Hz, 1H), 1.71 (s, 3H), 1.29 (m, 1H), 1.29 (s, 6H), 0.89 (s, 3H); ^{13}C NMR (100 MHz, $CDCl_3$) δ 203.0, 176.4, 159.5, 136.1, 134.8, 134.7, 133.7, 126.8, 121.8, 118.9, 118.9, 118.0, 90.2, 84.5, 83.4, 48.7, 46.7, 30.2, 29.0, 25.2, 25.0, 16.6; HRMS calc. for $C_{23}H_{24}O_4$ $(M + H)^+$ 365.1753, found 365.1765. **33**: yellow solid; R_f = 0.34 (25% EtOAc-hexane); ^{1}H NMR (400 MHz, $CDCl_3$) δ 7.91 (dd, *J* = 7.9, 1.7 Hz, 1H), 7.54 (m, 1H), 7.25 (d, *J* = 7.1 Hz, 1H), 7.18 (d, *J* = 8.5 Hz, 1H), 7.05 (ddd, *J* = 8.0, 7.3, 1.0 Hz, 1H), 5.02 (m, 1H), 3.76 (dd, *J* = 6.9, 4.6 Hz, 1H), 2.50 (m, 2H), 2.13 (m, 2H), 1.87 (dd, *J* = 13.2, 10.0 Hz, 1H), 1.71 (s, 3H), 1.59 (s, 3H), 1.38 (s, 3H), 1.34 (s, 3H); ^{13}C NMR (100 MHz, $CDCl_3$) δ

199.7, 175.4, 160.2, 136.5, 136.1, 135.9, 134.9, 127.0, 122.0, 119.2, 118.3, 117.3, 84.1, 83.7, 78.8, 44.8, 42.1, 33.1, 30.2, 29.7, 26.8, 26.0, 18.2; HRMS calc. for $C_{23}H_{24}O_4$ $(M + H)^+$ 365.1753, found 365.1766.

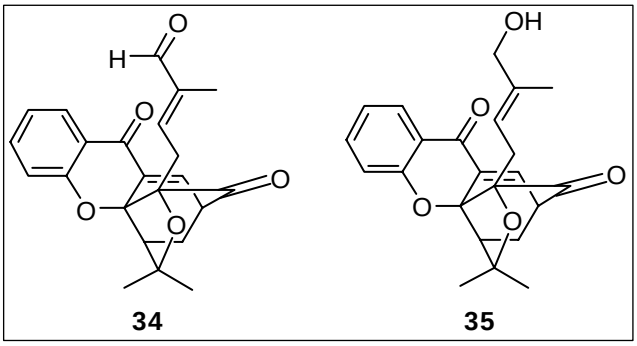

34 **35**

Aldehyde 34 and Alcohol 35. A solution of SeO_2 (0.67 mg, 6.00 μmol) and *t*BuOOH (5.5M in decane, 40.0 μL, 0.22 mmol) in DCM (1.4 mL) was prepared. To the stirring solution was added a solution of caged xanthone **7** (42.7 mg, 0.12 mmol) in DCM (0.5 mL) dropwsie, via syringe, at room temperature. After stirring for 19 hours at room temperature, the reaction mixture was dissolved in diethyl ether (10 mL) and washed with 10% KOH (10 mL), water (10 mL), and brine (10 mL). The ether layer was dried over $MgSO_4$, filtered, and concentrated by rotary evaporation. The crude yellow oil was purified through flash column chromatography to yield the aldehyde **34** (26 mg, 57%) and alcohol **35** (9.6 mg, 21%). **34**: white solid; R_f = 0.42 (17% EtOAC-hexane); ^{1}H NMR (400 MHz, $CDCl_3$): δ 9.22 (s, 1H), 7.91 (d, *J* = 7.8 Hz, 1H), 7.59 (d, *J* = 6.9 Hz, 1H), 7.53 (d, *J* = 7.5 Hz, 1H), 7.07 (t, *J* = 7.4 Hz, 1H), 6.94 (d, *J* = 8.4 Hz, 1H), 6.41 (t, *J* = 7.2 Hz, 1H), 3.55 (m, 1H), 2.82 (dd, *J* = 15.9, 7.5 Hz, 1H), 2.65 (dd, *J* = 15.9, 7.0 Hz, 1H), 2.56 (d, *J* = 9.5 Hz, 1H), 2.38 (dd, *J* = 13.6, 4.6 Hz, 1H), 1.76 (s, 3H), 1.42-1.36 (m, 1H), 1.34 (s, 3H), 1.18 (s, 3H); ^{13}C NMR (100 MHz, $CDCl_3$) δ 202.8, 194.8, 176.6, 159.5, 147.3, 140.3, 137.2, 136.6, 134.7, 127.6, 122.7 119.0, 118.2, 91.1, 84.4, 83.4, 48.9, 47.0, 30.3, 29.3, 29.2, 25.1, 8.8; HRMS calc. for $C_{23}H_{22}O_5(M + H)^+$ 379.1540, found 379.1550. **35**: white solid; R_f =

0.21 (17% EtOAC-hexane); ^{1}H NMR (400 MHz, $CDCl_3$): δ 7.93 (d, *J* = 8.2 Hz, 1H), 7.56 (t, *J* = 8.4 Hz, 1H), 7.54 (d, *J* = 6.9 Hz, 1H), 7.10-7.07 (m, 2H), 4.75-4.71 (m, 1H), 3.67-3.53 (m, 3H), 2.75-2.67 (m, 2H), 2.49 (d, *J* = 9.6 Hz, 1H), 2.37 (dd, *J* = 13.6, 4.7 Hz, 1H), 1.74 (s, 3H), 1.39-1.34 (m, 1H), 1.31(s, 3H), 0.94 (s, 3H); ^{13}C NMR (100 MHz, $CDCl_3$) δ 203.0, 178.8, 159.9, 138.1, 137.0, 135.4, 134.7, 127.4, 122.5, 119.8, 119.4, 118.3, 90.4, 84.7, 84.0, 68.4, 48.9, 47.2, 30.5, 29.3, 29.0, 25.2, 12.7; HRMS calc. for $C_{23}H_{24}O_5$ $(M + Na)^+$ 403.1516, found 403.1524.

Oxidation of alcohol 35 to aldehyde 34. A mixture of alcohol **35** (20 mg, 52.6 μmol) and PCC (17 mg, 78.9 μmol) in DCM (0.2 mL) was stirred at room temperature for 30 min. The reaction mixture was diluted with DCM and filtered through a pad of celite. The solvent was removed by rotary evaporation and the crude was purified by preparative TLC (silica, 50% EtOAc-hexane) to yield aldehyde **34** (19 mg, 95%).

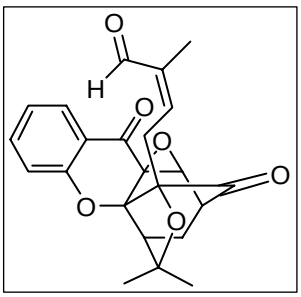

Epoxide 36. $NaH_2PO_4.H_2O$ (6.8 mg, 49.1 μmol) was added to a solution of **34** (6.2 mg, 16.4 μmol) in *t*BuOH/H_2O (2:1, 0.43 mL). The reaction mixture was stirred at room temperature to fully dissolve the white precipitate and the reaction vessel was placed in an ice bath. To the stirring solution in an ice bath was added 2-methylbut-2-ene (13.9 μL, 131.2 μmol) via syringe. After 30 min, $NaClO_2$ (4.4 mg, 49.1 μmol) was added to the reaction mixture. When the reaction was complete 4 hours later, the reaction mixture was partitioned between ethyl acetate (2 x 3 mL) and water (3 mL). The combined organic layers were dried over $MgSO_4$, filtered, and concentrated by rotary

evaporation. The crude material was purified through preparative TLC (silica, 50% EtOAc-Hexane) to yield the epoxide **36** (4.4 mg, 70%). **36**: white solid; R_f = 0.52 (50% EtOAc-hexane); ^{1}H NMR (400 MHz, $CDCl_3$): δ 9.48 (s, 1H), 7.97 (d, *J* = 7.9 Hz, 1H), 7.65 (t, *J* = 7.4 Hz, 1H), 7.20 (t, *J* = 7.7 Hz, 1H), 7.10 (d, *J* = 8.3 Hz, 1H), 7.01 (t, *J* = 8.1 Hz, 1H), 4.29 (d, *J* = 4.5 Hz, 1H), 3.12 (t, *J* = 4.6 Hz, 1H), 3.03-3.01 (m, 2H), 2.58 (d, *J* = 9.2 Hz, 1H), 2.23 (dd, *J* = 5.1, 14.5 Hz, 1H), 1.81-1.73 (m, 1H), 1.70 (s, 3H), 1.60 (s, 3H), 1.24 (s, 3H); ^{13}C NMR (100 MHz, $CDCl_3$) δ 204.3, 195.6, 184.5, 159.0, 150.3, 139.8, 138.2, 127.8, 123.4, 122.6, 119.4, 89.6, 88.7, 84.0, 59.8, 55.0, 46.9, 42.1, 30.2, 28.3, 27.9, 24.4, 9.5; HRMS calc. for $C_{23}H_{22}O_6$ $(M + Na)^+$ 417.1309, found 417.1313.

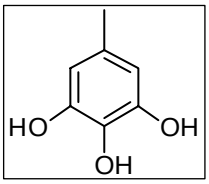

5-Methylbenzene-1,2,3-triol 38. To a 50 mL round-bottomed flask was added pyrogallol **29** (372 mg, 2.04 mmol) followed by DCM (4.0 mL). The flask was placed on an ice bath and 1.0 M solution of boron tribromide in DCM (6.5 mL, 6.52 mmol) was added dropwise, via syringe, while stirring over 10 min. The reaction vessel was then stirred under argon at room temperature for 3.5 hours. The reaction was quenched by adding water (10 mL), and the reaction mixture was extracted with ethyl acetate (3 x 20 mL). The combined organic layers were washed with water, brine, and dried over $MgSO_4$. The solution was then filtered and concentrated by rotary evaporation. The crude material was purified through flash column chromatography (silica, 60-70% EtOAc-hexane) to yield 5-methylbenzene-1,2,3-triol (170 mg, 59%). **38**: off-white solid; R_f = 0.32 (40% EtOAc-hexane); ^{1}H NMR (400 MHz, $CDCl_3$) δ 6.30 (s, 2H), 5.05 (s, 2H), 5.00 (s, 1H), 2.20 (s, 3H); ^{13}C NMR (100 MHz,

DMSO-d6) δ 145.9, 130.4, 127.2, 107.6, 20.6; HRMS calc. for $C_7H_8O_3$ (M) 140.0468, found 140.0470.

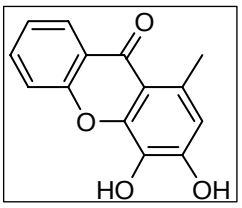

3,4-Dihydroxy-1-methyl-9*H*-xanthen-9-one 39. 2-Fluorobenzoyl chloride **28** (170 mg, 1.07 mmol) was added dropwise to a mixture of 5-methylbenzene-1,2,3-triol **38** (100 mg, 0.71 mmol), aluminum chloride (187 mg, 1.40 mmol), chloroform (2 mL) and dichloromethane (6 mL) in a 50 mL round-bottomed flask. The reaction mixture was stirred at room temperature under argon for 1.5 hours. The reaction vessel was then equipped with a reflux condenser and stirred under argon at 60 ºC for 6 hours. The cooled, red homogeneous solution was acidified with 1N HCl (15 mL). The reaction mixture was then partitioned between water and ethyl acetate (3 x 50 mL). The aqueous layer was back extracted with ethyl acetate (2 x 30 mL) until the color of the aqueous layer was almost clear. The combined organic layers were dired over $MgSO_4$, filtered, and concentrated to yield dark brown oil. The crude oil was then added to a 100 mL round-bottomed flask containing sodium carbonate (98 mg, 0.92 mmol) and DMF (4 mL). The reaction vessel was the equipped with a reflux condenser and stirred under argon at 90 ºC for 4 hours. The dark reaction mixture was cooled to room temperature and acidified with 1 N HCl (15 mL). The reaction mixture was then partitioned between water and ethyl acetate (3 x 50 mL). The aqueous layer was back extracted with ethyl acetate (2 x 30 mL). The combined brown organic layers were dried over $MgSO_4$, filtered, and concentrated by rotary evaporation. The crude material was purified through flash column chromatography (silica, 40-50% EtOAc-hexane) to yield the methyl xanthone **39** (120 mg, 70%). **39**: off-white solid; R_f = 0.21 (40% EtOAc-

hexane); ^{1}H NMR (400 MHz, DMSO-d6) δ 10.15 (br s, 1H), 9.34 (br s, 1H), 8.10 (dd, *J* = 7.9, 1.6 Hz, 1H), 7.76 (ddd, *J* = 8.6, 7.3, 1.7 Hz, 1H), 7.56 (d, *J* = 8.3 Hz, 1H), 7.38 (t, *J* = 7.5 Hz, 1H), 6.68 (s, 1H), 2.68 (s, 3H); ^{13}C NMR (100 MHz, DMSO-d6) δ 176.8, 154.6, 150.3, 147.4, 134.3, 131.1, 130.7, 126.0, 123.6, 121.8, 117.4, 115.2, 112.8, 22.4; HRMS calc. for $C_{14}H_{10}O_4$ $(M + H)^+$ 243.0652, found 243.0654.

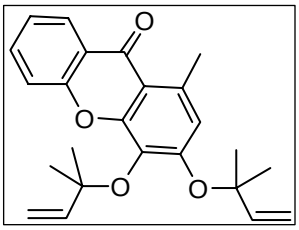

1-Methyl-3,4-bis(2-methylbut-3-en-2-yloxy)-9*H*-xanthen-9-one 40. To a 25 mL round-bottomed flask was added methyl xanthone **39** (46 mg, 0.19 mmol) followed by dry THF (1.5 mL). The flask was degassed by argon and was placed in an ice water bath. To the yellow homogeneous solution was added *tert*-butyl 2-methylbut-3-en-2-yl carbonate **10b** (354 mg, 1.9 mmol), via syringe, followed by $Pd(PPh_3)_4$ (22 mg, 0.019 mmol). The reaction vessel was stirred under argon at 5 ºC for 2 hours. The onset of a yellow suspension indicated the formation of the desired product **40**. The solvent was removed by rotary evaporation and the crude material was purified through flash column chromatography (silica, 10-15% EtOAc-hexane) to yield 1-methyl-3,4-bis(2-methylbut-3-en-2-yloxy)-9*H*-xanthen-9-one **40** (55 mg, 76%). **40**: yellow oil; R_f = 0.66 (30% EtOAc-hexane); ^{1}H NMR (400 MHz, $CDCl_3$) δ 8.24 (dd, *J* = 7.9, 1.5 Hz, 1H), 7.64 (ddd, *J* = 8.6, 7.2, 1.7 Hz, 1H), 7.43 (d, *J* = 8.4 Hz, 1H), 7.31 (t, *J* = 7.5 Hz, 1H), 6.86 (s, 1H), 6.28 (dd, *J* = 17.5, 10.9 Hz, 1H), 6.19 (dd, *J* = 17.6, 10.8 Hz, 1H), 5.18 (m, 3H), 5.01 (dd, *J* = 10.9, 1.0 Hz, 1H), 2.80 (s, 3H), 1.56 (s, 12H); ^{13}C NMR (100 MHz, $CDCl_3$) δ 178.4, 155.3, 155.0, 153.5, 143.8, 143.6, 136.3, 133.9, 126.5, 123.5, 122.5, 119.1, 117.3, 115.5, 113.9, 112.8,

83.1, 82.0, 27.2, 26.9, 23.5; HRMS calc. for $C_{24}H_{26}O_4$ $(M + H)^+$ 379.1904, found 379.1911.

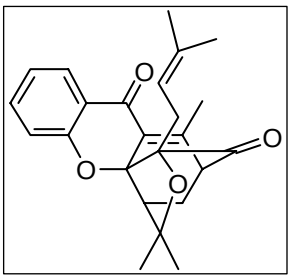

Caged xanthone 41. A solution of compound **40** (35 mg, 0.092 mmol) in DMF (1.5 mL) was refluxed at 120 ºC under argon for 2.5 hours. The onset of a yellow color indicated the formation of the methyl caged xanthone **41**. The reaction mixture was then cooled to room temperature and the solvent was removed by rotary evaporation. The crude material was purified through flash column chromatography (silica, 15-20% EtOAc-hexane) to yield the methyl caged xanthone **41** (30 mg, 85%). **41**: white solid; R_f = 0.56 (30 % EtOAc-hexane); ^{1}H NMR (400 MHz, $CDCl_3$) δ 7.87 (d, J = 7.7 Hz, 1H), 7.47 (m, 1H), 7.03 (m, 2H), 4.42 (t, J = 7.0 Hz, 1H), 3.18 (d, J = 4.4 Hz, 1H), 2.61 (m, 1H), 2.51 (s, 3H), 2.45 (d, J = 9.5 Hz, 1H), 2.28 (dd, J = 13.5, 4.7 Hz, 1H), 1.70 (s, 3H), 1.35 (s, 3H), 1.34 (m, 1H), 1.27 (s, 3H), 0.96 (s, 3H); ^{13}C NMR (100 MHz, $CDCl_3$) δ 203.6, 179.3, 158.3, 150.7, 135.5, 134.8, 126.8, 121.7, 120.6, 118.3, 117.6, 90.5, 84.8, 83.2, 55.8, 49.2, 30.3, 29.0, 28.6, 25.6, 24.9, 19.7, 16.7; HRMS calc. for $C_{24}H_{26}O_4$ $(M + H)^+$ 379.1904, found 379.1909.

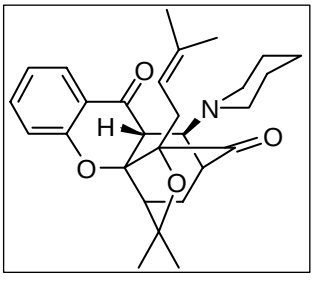

Piperidine addition product 42. A solution of compound **7** (7.1 mg, 0.019 mmol) in DCM (0.5 mL) was treated with piperidine (7 μL, 0.76 mmol) at 25 °C for 4 h. The crude material was purified through flash column chromatography (silica, 20-70% Et_2O-hexane) to yield adduct **42** (7.3 mg, 86%). **42**: white solid; R_f = 0.71

(70 % Et_2O-hexane); ^1H NMR (400 MHz, $CDCl_3$) δ 7.90 (d, J = 8 Hz, 1H), 7.56-7.52 (m, 1H), 7.08-7.01 (m, 2H), 5.23-5.50 (m, 1H), 3.36 (s, 1H), 3.26 (s, 1H), 3.15 (b, 1H), 2.91-2.78 (m, 3H), 2.53 (b, 1H), 2.45 (d, J = 8.8 Hz, 1H), 2.34-2.23 (b, 2H), 1.95 (dd, J = 14.8 Hz, 6.4 Hz, 1H), 1.93-1.84 (b, 1H), 1.68 (s, 3H), 1.62 (s, 3H), 1.51-1.40 (m, 6H), 1.37 (s, 3H), 1.13 (s, 3H); ^{13}C NMR (100 MHz, $CDCl_3$) δ 209.1, 191.7, 158.3, 136.4, 132.9, 127.0, 125.4, 121.4, 120.7, 118.3, 118.2, 89.4, 86.7, 81.5, 62.1, 51.3, 48.3, 43.4, 42.0, 30.4, 29.8, 28.0, 27.5, 26.0, 25.7, 24.6, 22.0, 18.1; HRMS calc. for $C_{28}H_{35}NO_4$ ($M + H^+$) 450.2639, found 450.2620.

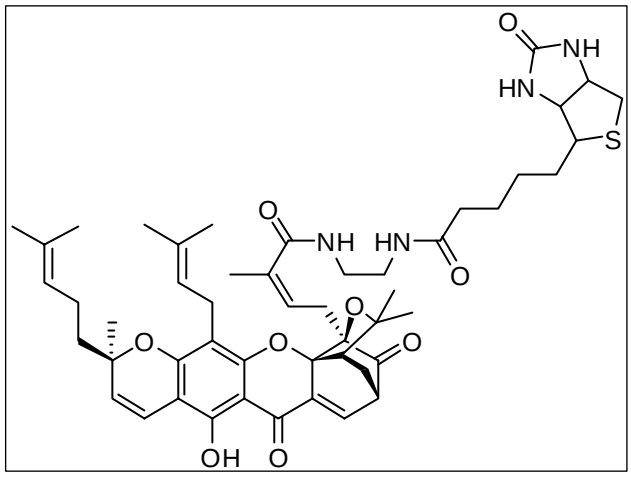

Biotin conjugate 44. To a solution containing gambogic acid (5.0 mg, 7.95 μmol) and biotin ethylenediamine hydrobromide (3.2 mg, 8.75 μmol) in DCM (0.34 mL) was added DIPEA (2.77 μL, 15.9 μmol) via syringe. Upon adding solid HATU (3.6 mg, 9.46 μmol) portionwise to the reaction mixture, the reaction mixture turned to pale yellow in color within 5 min. After 24 hours, the reaction mixture was diluted with ethyl acetate (5 mL) and washed with water (2 x 1 mL) and brine (2 mL). The organic layers were dried over $MgSO_4$, filtered and concentrated by rotary evaporation. The crude material was purified through preparative TLC (silica, 17% MeOH-EtOAc) to yield the biotin conjugate **44** (4.8 mg, 67%). **44**: yellow solid; R_f = 0.11 (17% MeOH-EtOAc); ^1H NMR (400 MHz, $CDCl_3$): δ 7.59 (d, J = 6.9 Hz, 1H), 6.90-7.05 (m, 2H), 6.68 (d, J = 10.2

Hz, 1H), 6.02 (br s, 1H), 5.47 (d, *J* = 10.3 Hz, 1H), 5.28 (m, 2H), 5.03 (m, 2H), 4.49 (m, 1H), 4.32 (m, 1H), 3.00-3.60 (m, 6H), 2.89 (dd, *J* = 12.8, 4.8 Hz, 1H), 2.72 (d, *J* = 13.1 Hz, 2H), 2.54 (d, *J* = 9.3 Hz, 1H), 2.34 (m, 2H), 2.20 (m, 2H), 2.03 (m, 1H), 1.77 (s, 3H), 1.73 (s, 3H), 1.68 (br s, 6H), 1.65 (m, 6H), 1.45 (s, 3H), 1.29 (s, 3H), 1.25 (s, 3H); ^{13}C NMR (100 MHz, $CDCl_3$) δ 205.1, 179.0, 174.0, 170.2, 163.9, 162.1, 157.9, 157.3, 136.0, 135.6, 133.2, 132.1, 125.2, 123.9, 122.1, 115.9, 108.0, 103.0, 100.6, 91.3, 84.6, 84.0, 81.8, 61.8, 60.4, 55.5, 49.1, 47.0, 42.3, 40.8, 40.0, 39.5, 35.9, 30.1, 29.9, 29.3, 29.1, 28.2, 28.1, 28.0, 25.9, 25.7, 25.4, 22.9, 21.8, 21.3, 18.4, 17.9; HRMS calc. for $C_{50}H_{64}N_4O_9S$ $(M + Na)^+$ 919.4286, found 919.4329.

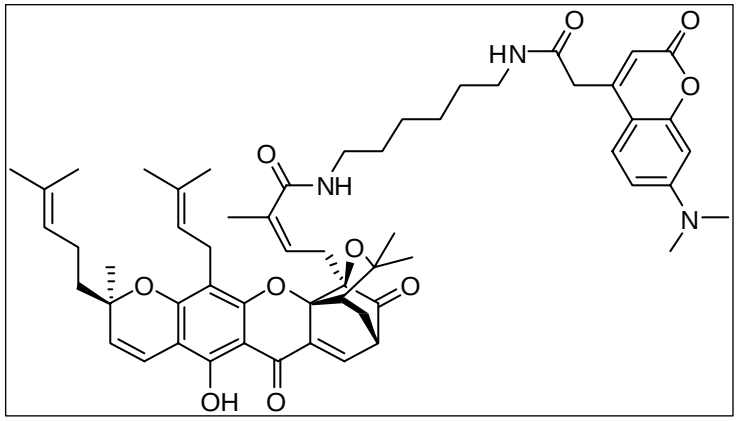

Coumarin conjugate 45. To a solution containing gambogic acid (5.8 mg, 9.22 μmol) and coumarin hexanediamine TFA salt (4.6 mg, 10.1 μmol) in DCM (0.30 mL) was added DIPEA (3.21 μL, 18.4 μmol). Upon adding solid HATU (4.2 mg, 10.9 μmol) portionwise to the reaction mixture, the reaction mixture turned to pale yellow in color within 5 min. After 24 hours, the reaction mixture was diluted with ethyl acetate (5 mL) and washed with water (2 x 1 mL) and brine (2 mL). The organic layers were dried over $MgSO_4$, filtered and concentrated by rotary evaporation. The crude material was then purified through preparative TLC (silica, 100% EtOAc) to yield the coumarin conjugate **45** (7.7 mg, 87%). **45**: yellow solid; R_f = 0.29 (100% EtOAc); ^{1}H NMR (400 MHz, $CDCl_3$): δ

7.49 (d, J = 9.1 Hz, 2H), 6.66 (d, J = 10.1 Hz, 1H), 6.60 (dd, J = 9.0, 2.4 Hz, 1H), 6.47 (s, 2H), 6.04 (s, 2H), 5.46 (d, J = 10.0 Hz, 1H), 5.30 (t, J = 8.2 Hz, 1H), 5.07-5.02 (m, 2H), 3.63 (s,2 H), 3.46 (t, J = 6.1 Hz, 1H), 3.33-3.19 (m, 5H), 3.03 (s, 6H), 2.55 (d, J = 9.2 Hz, 2H),, 2.38-2.29 (m, 2H), 2.08-2.01 (m, 2H), 1.77-1.25 (m, 36H); ^{13}C NMR (100 MHz, $CDCl_3$) δ 204.4, 178.9, 169.5, 168.1, 162.0, 157.9, 156.3, 153.3, 150.1, 135.9, 132.2, 132.1, 126.0, 125.1, 124.1, 123.9, 122.2, 115.9, 110.6, 109.4, 108.6, 108.1, 103.0, 100.5, 98.3, 91.3, 84.3, 83.7, 81.8, 49.2, 47.2, 42.3, 41.0, 40.3, 39.6, 38.9, 30.2, 29.9, 29.5, 29.3, 29.2, 29.0, 28.1, 26.1, 26.0, 25.9, 25.4, 22.9, 21.8, 21.5, 18.4, 17.9; HRMS calc. for $C_{57}H_{69}N_3O_{10}$ $(M + H)^+$ 956.5056, found 956.5069.

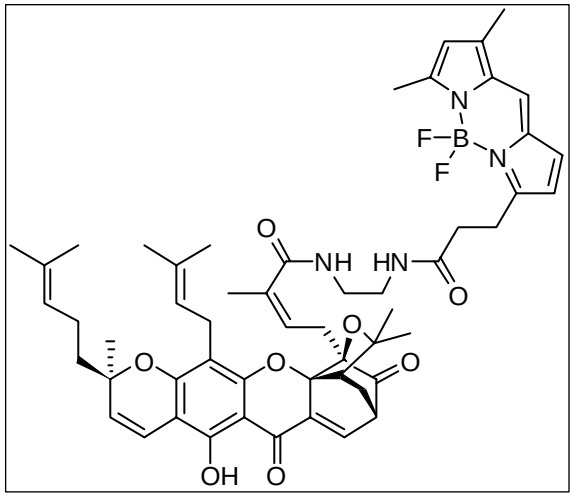

Amide 46. To a solution containing gambogic acid (6.1 mg, 9.70 μmol) and BODIPY FL EDA (3.95 mg, 10.7 μmol) in DCM (0.24 mL) was added DIPEA (3.38 μL, 19.4 μmol). Upon adding solid HATU (4.37 mg, 11.5 μmol) portionwise to the reaction mixture, the reaction mixture turned to pale yellow in color within 5 min. After 24 hours, the reaction mixture was diluted with ethyl acetate (5 mL) and washed with water (2 x 1 mL) and brine (2 mL). The organic layers were dried over $MgSO_4$, filtered and concentrated by rotary evaporation. The crude material was purified by preparative TLC (silica, 100% EtOAc) to yield the amide **46** (7.05 mg, 77%). **46**: red solid; R_f = 0.38 (100% EtOAc); ^{1}H NMR (400 MHz, $CDCl_3$): δ 7.51 (d, J = 6.9 Hz, 1H), 7.03 (s, 1H), 6.85 (d, J = 4.1 Hz, 1H),

6.68 (d, *J* = 10.2 Hz, 1H), 6.62 (m, 1H), 6.27 (d, *J* = 3.9 Hz, 1H), 6.09 (s, 1H), 3.49-3.15 (m, 7H), 2.64 (d, *J* = 6.9 Hz, 2H), 2.53 (s, 3H), 2.31-2.27 (m, 1H), 2.21 (s, 3H), 2.06-2.02 (m, 2H), 1.75-1.24 (m, 27H); ^{13}C NMR (100 MHz, $CDCl_3$) δ 204.8, 178.9, 172.4, 169.5, 162.0, 157.9, 157.3, 135.8, 133.3, 132.1, 128.8, 125.2, 124.9, 124.0, 123.9, 122.2, 120.4, 117.9, 115.9, 108.0, 103.0, 100.5, 91.3, 84.5, 84.0, 81.8, 49.1, 46.9, 42.3, 39.9, 39.8, 35.8, 30.1, 29.9, 29.2, 29.0, 28.1, 25.9, 25.4, 24.9, 22.9, 21.8, 21.4, 18.4, 17.9, 15.1, 11.5; HRMS calc. for $C_{54}H_{63}BF_2N_4O_8S$ $(M + H)^+$ 944.4816, found 944.4860.

Section 2.9.3 ^{3}H-Thymidine Incorporation Assay

Cells were plated in a 96-well plate at 10-20x10^3 cells/well in RPMI supplemented with 10% fetal bovine serum, 2 mM glutamine, 1% penicillin/streptomycin (complete medium). The caged *Garcinia* xanthones were added to the cells at increasing concentrations and 0.1% DMSO was added to control cells. Cells were incubated for 48h and then pulsed with ^{3}H-thymidine for 6 h. Incorporation of ^{3}H-thymidine was determined in a scintillation counter (Beckman Coulter Inc., Fullerton, CA) after cells were washed and deposited onto glass microfiber filters using a cell harvester M-24 (Brandel, Gaithersbur, MD).

Section 2.9.4 Apoptosis Assays

ELISA Assay. The compounds were dissolved in DMSO and further diluted in complete medium to obtain final concentrations as indicated. HL-60 and HL-60/ADR cells were seeded into each well of a 96-well cell culture plate at 10,000 cells per well and incubated at 37 °C for 7 h with the indicated concentrations of each compound.

Control samples were incubated in 0.1% DMSO. Each condition was in triplicate. The proapoptotic effect was detected by using the Cell Death Detection ELISA^{PLUS} kit (Roche Applied Science, Indianapolis, IN) according to the manufacturer's instructions. This kit constitutes a photometric enzyme-immunoassay for the qualitative and quantitative *in vitro* determination of cytoplasmic histone-associated-DNA-fragments (mono- and oligo-nucleosomes) after induced cell death. The absorption values A (A_{405nm}-A_{490nm}) measured give a quantitative indication of the induced amount of apoptosis.

Fluorescence Microscopy of Annexin V/PI Stained Cells. HL-60/ADR cells were plated in a 6-well plate at $1x10^6$ cell/ml (4 ml) and treated with 0.5 μM **7** while control cells received 0.1% DMSO. Cells were incubated overnight and then stained with Alexa Fluor 488 annexin V and propidium iodide using the Vybrant Apoptosis Assay Kit (Molecular Probes, Eugene, OR) according to manufacturer's recommendations. Cells were then viewed on an E800 Nikon (New York City, NY) research microscope equipped with an EXFO (Vanier, Canada) X-cite fluorescent 120W metal halide illuminator and imaged with a DMX 1200F Nikon fluorescence sensitive digital camera.

Section 2.9.5 ^{1}H NMR and ^{13}C NMR Spectra

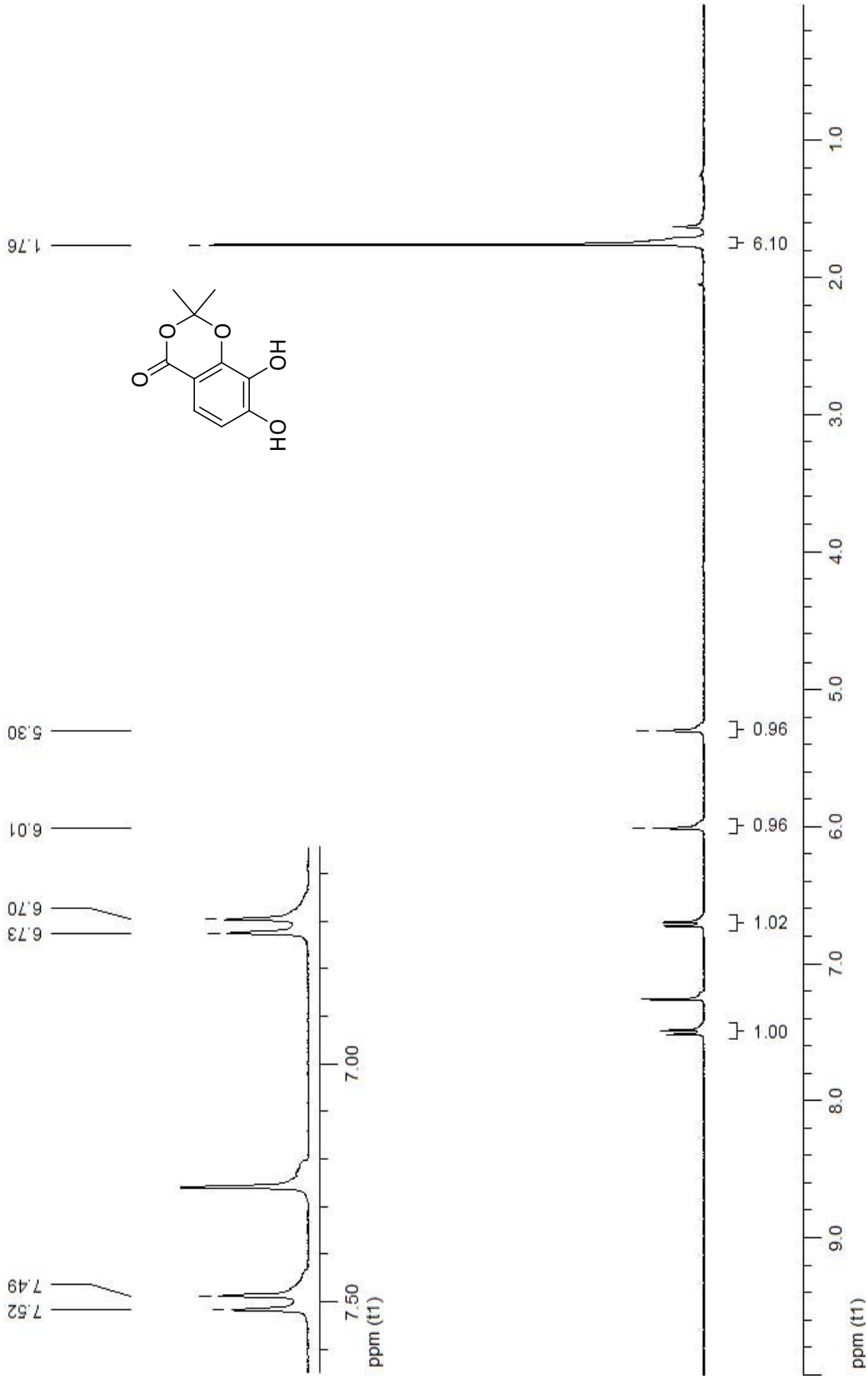

Spectrum 1: ^{1}H NMR ($CDCl_3$, 400 MHz) of compound 9.

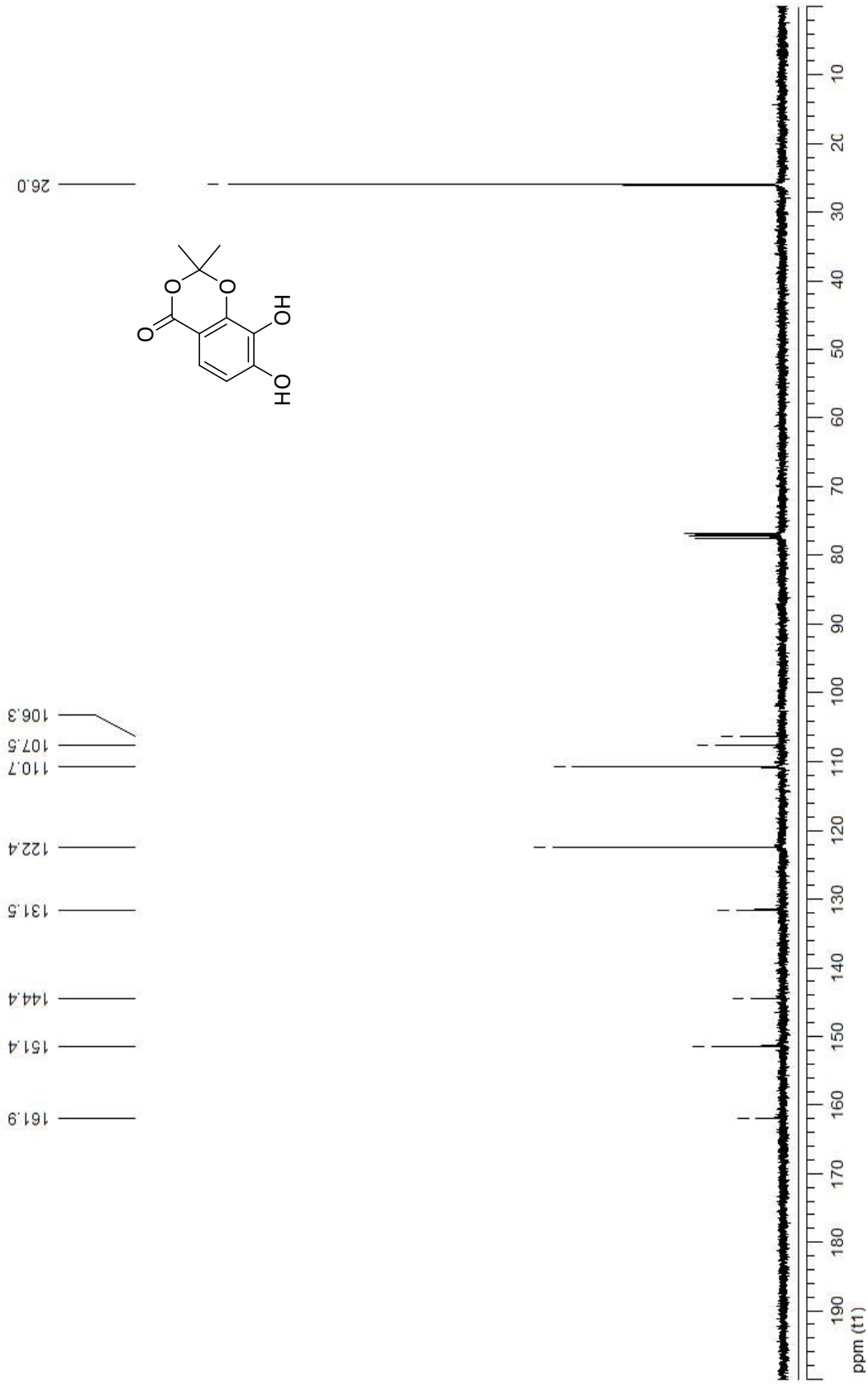

Spectrum 2: ^{13}C NMR ($CDCl_3$, 100 MHz) of compound 9.

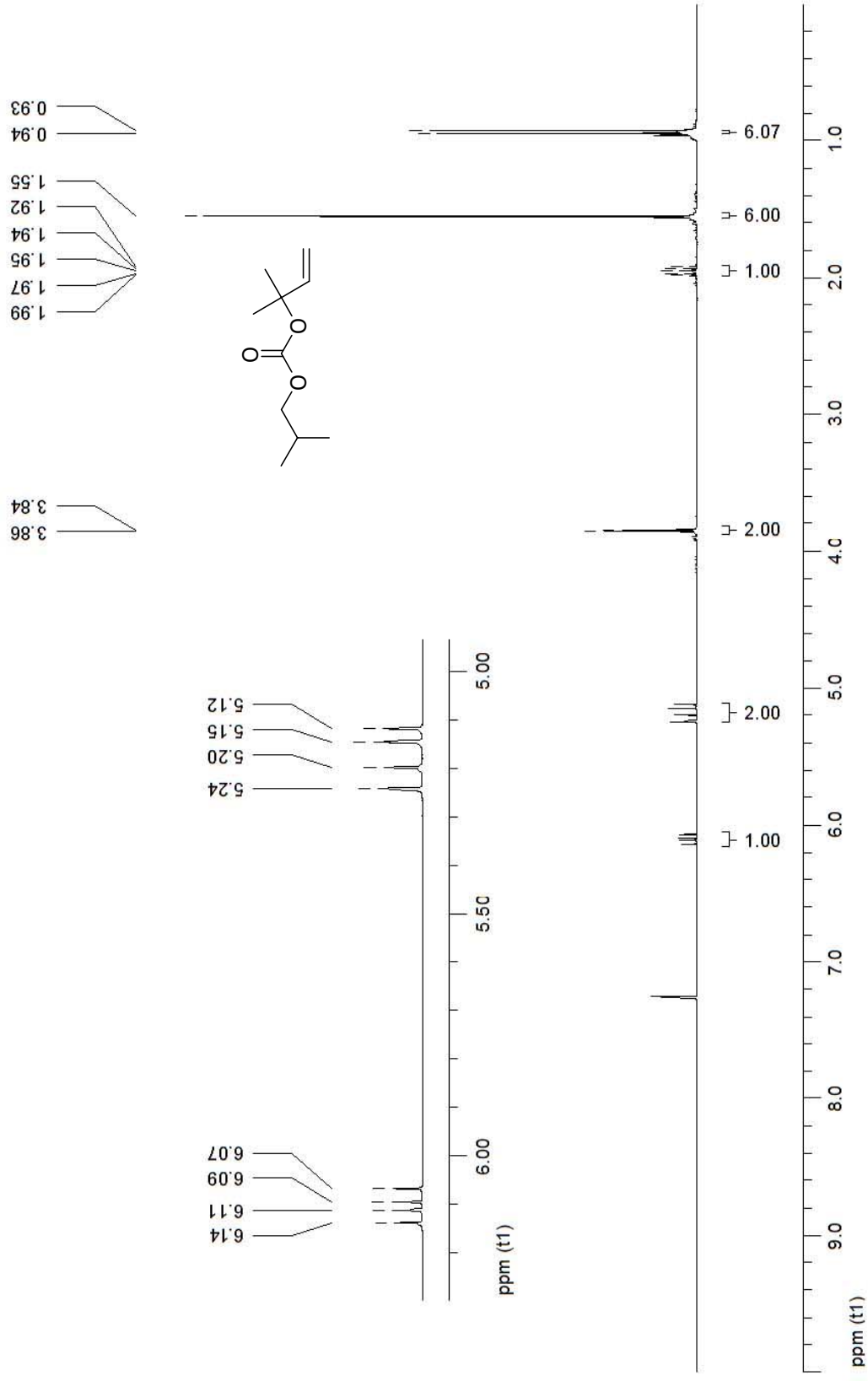

Spectrum 3: ^{1}H NMR ($CDCl_3$, 400 MHz) of compound 10a.

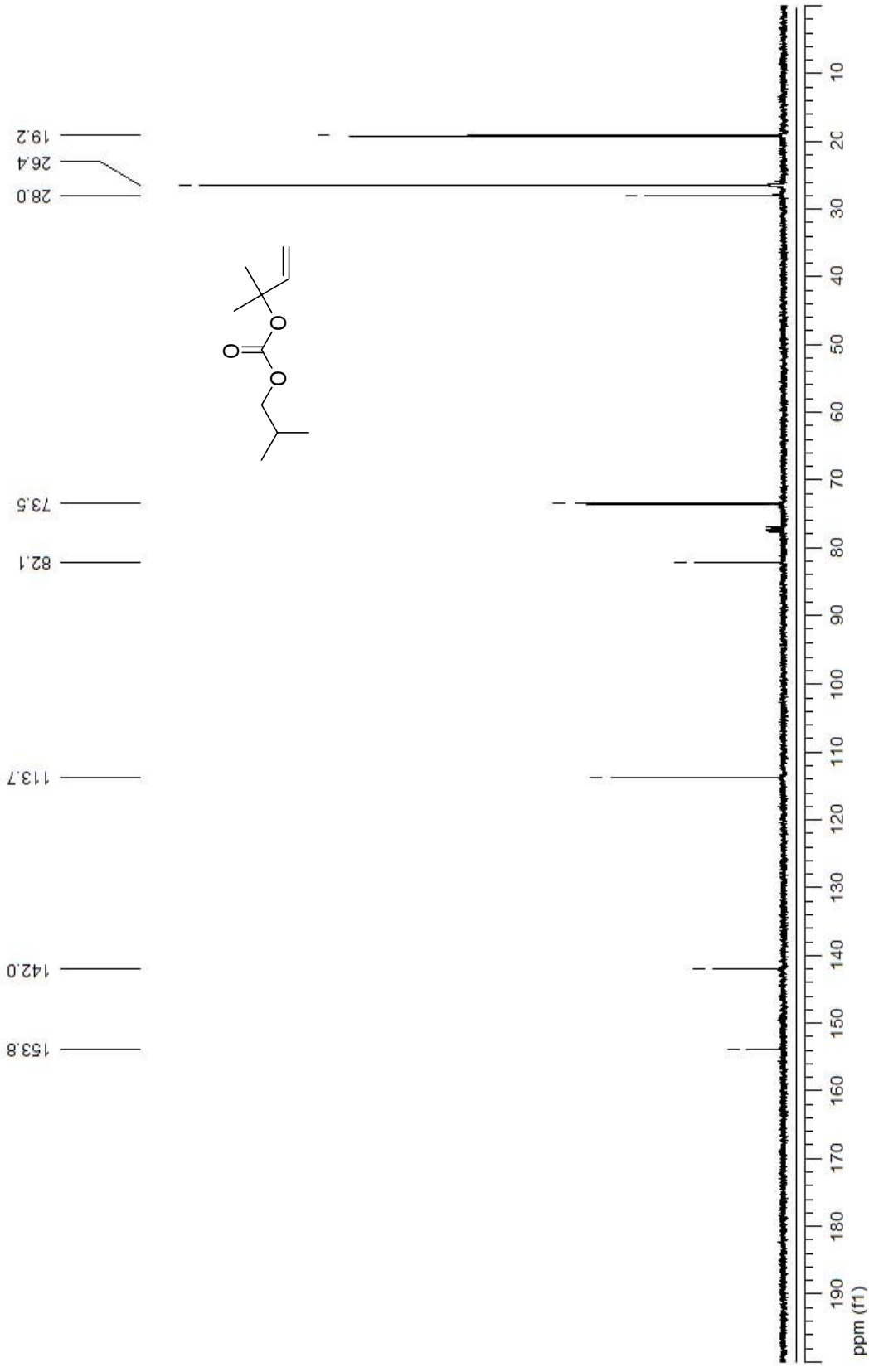

Spectrum 4: ^{13}C NMR ($CDCl_3$, 100 MHz) of compound 10a.

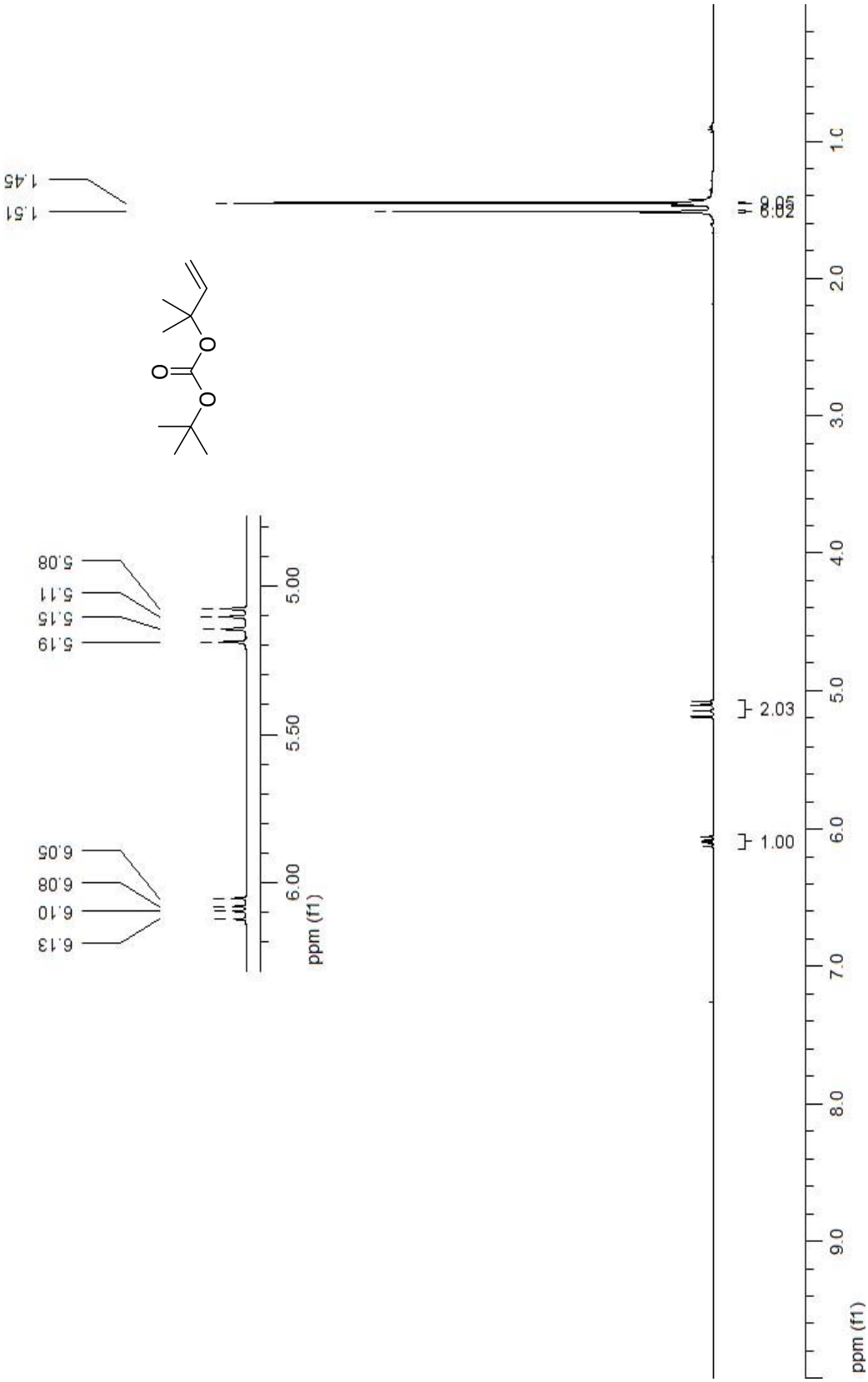

Spectrum 5: ^{1}H NMR ($CDCl_3$, 400 MHz) of compound 10b.

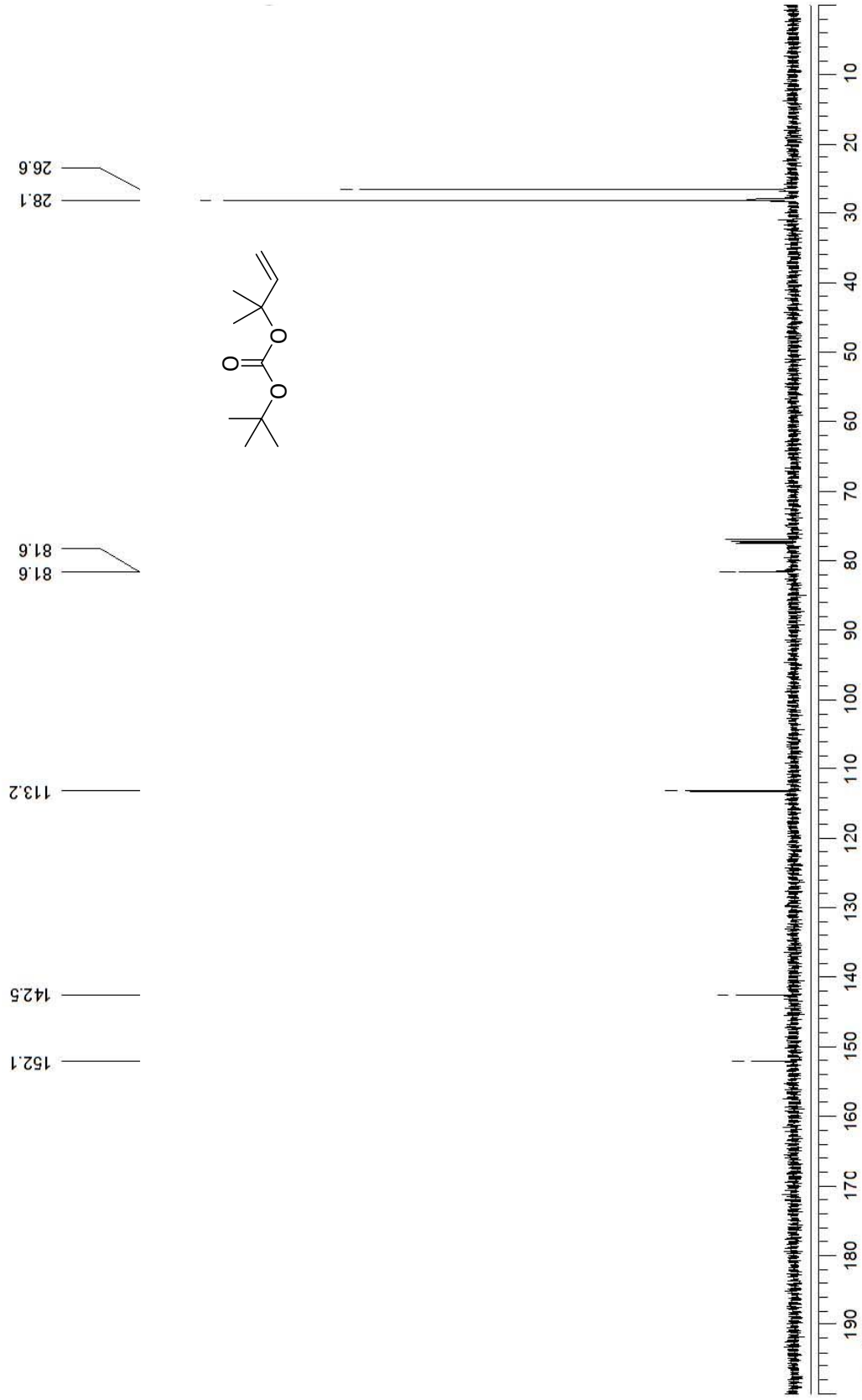

Spectrum 6: ^{13}C NMR ($CDCl_3$, 100 MHz) of compound 10b.

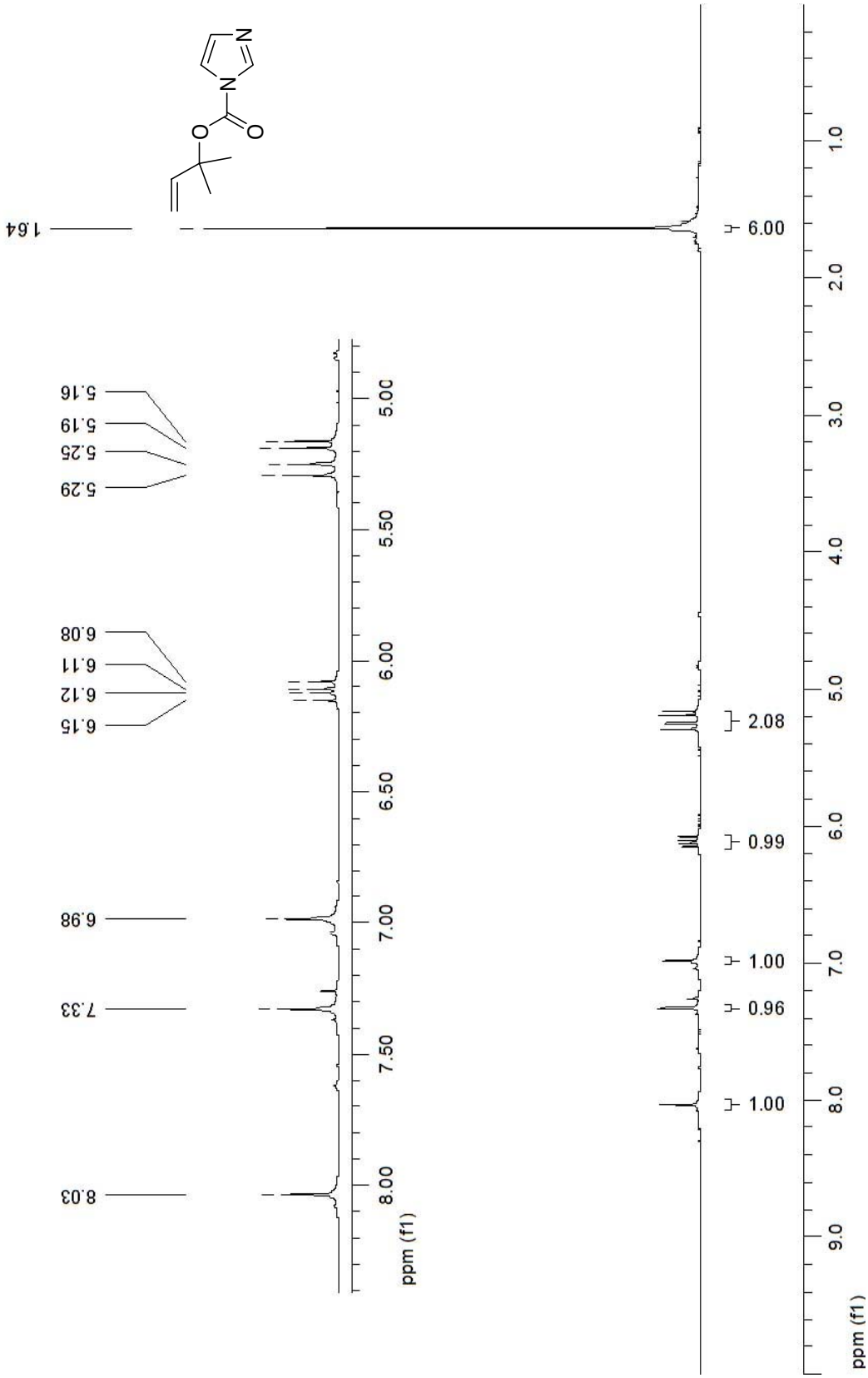

Spectrum 7: ^{1}H NMR ($CDCl_3$, 400 MHz) of precursor of compound 10c.

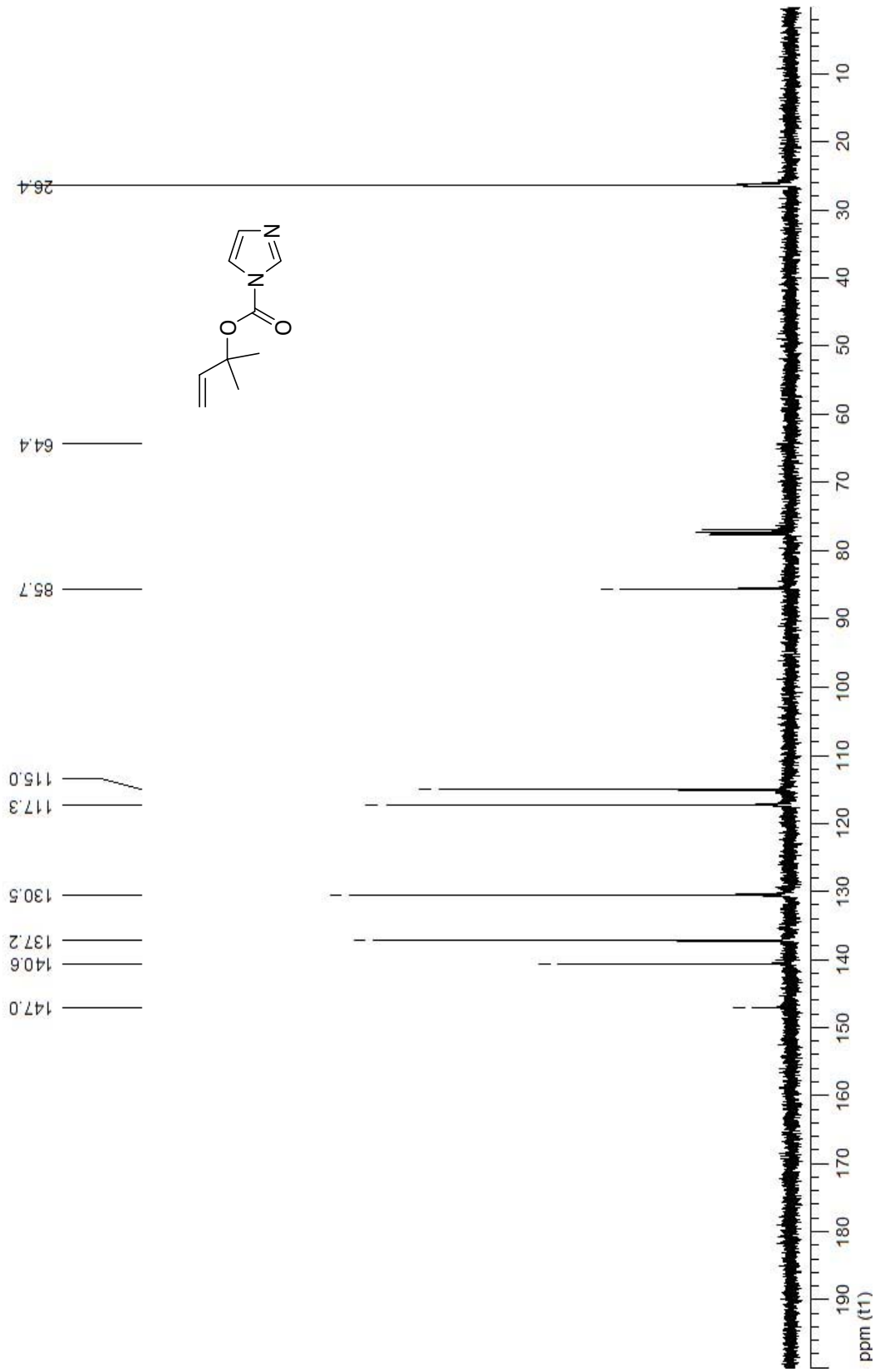

Spectrum 8: ^{13}C NMR ($CDCl_3$, 100 MHz) of precursor of compound 10c.

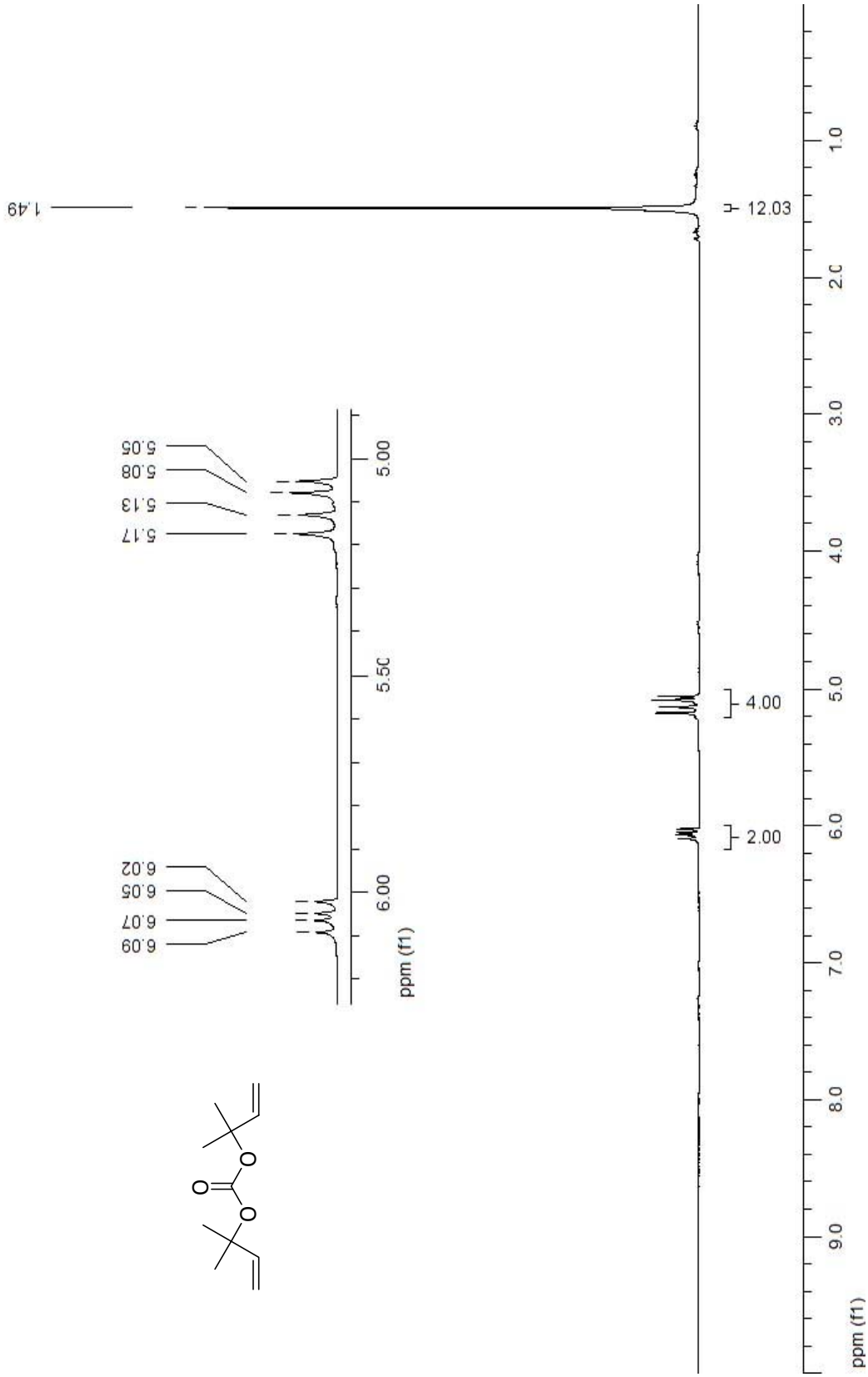

Spectrum 9: ^{1}H NMR ($CDCl_3$, 400 MHz) of compound 10c.

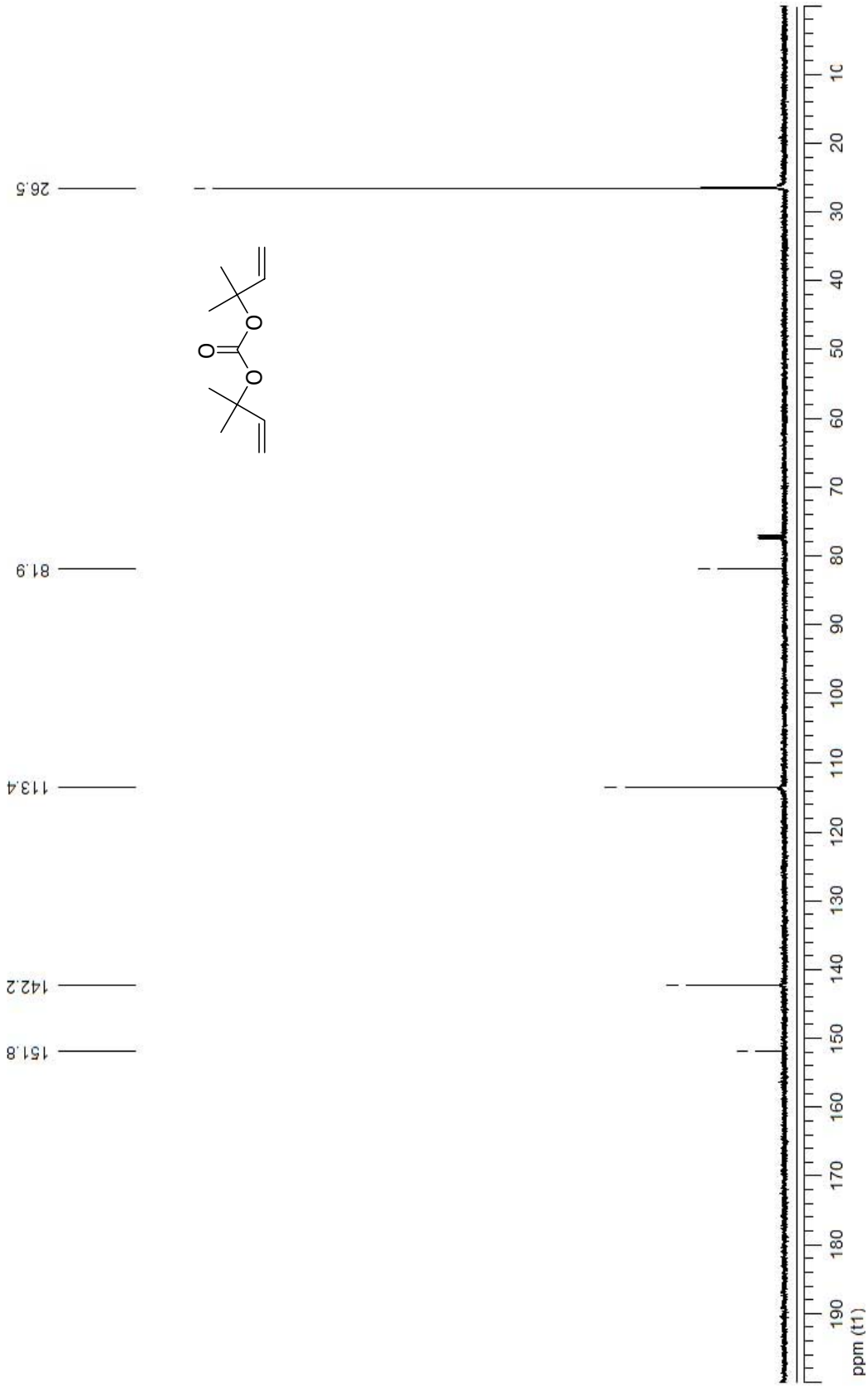

Spectrum 10: ^{13}C NMR ($CDCl_3$, 100 MHz) of compound 10c.

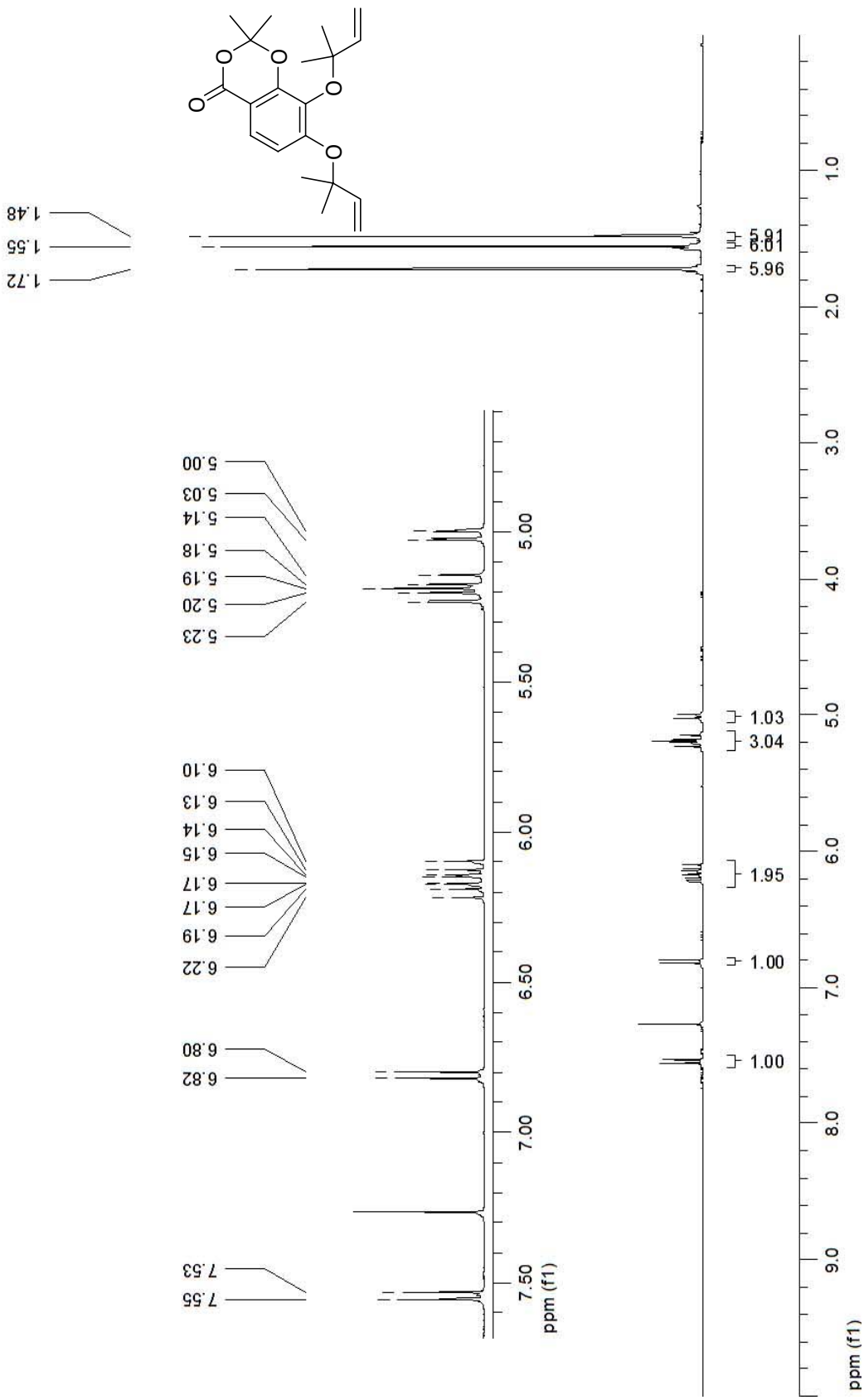

Spectrum 11: ^{1}H NMR ($CDCl_3$, 400 MHz) of compound 11.

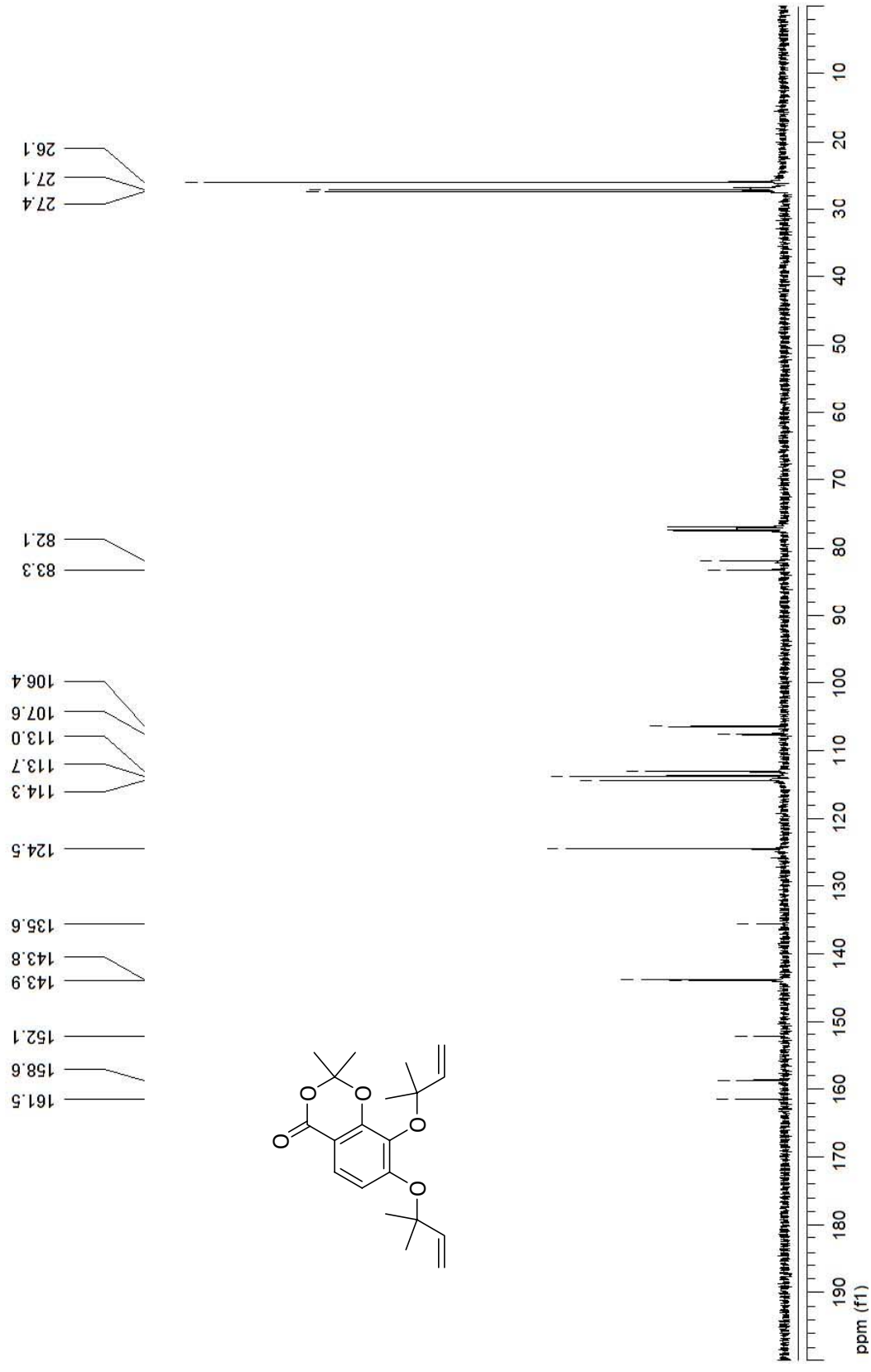

Spectrum 12: ^{13}C NMR ($CDCl_3$, 100 MHz) of compound 11.

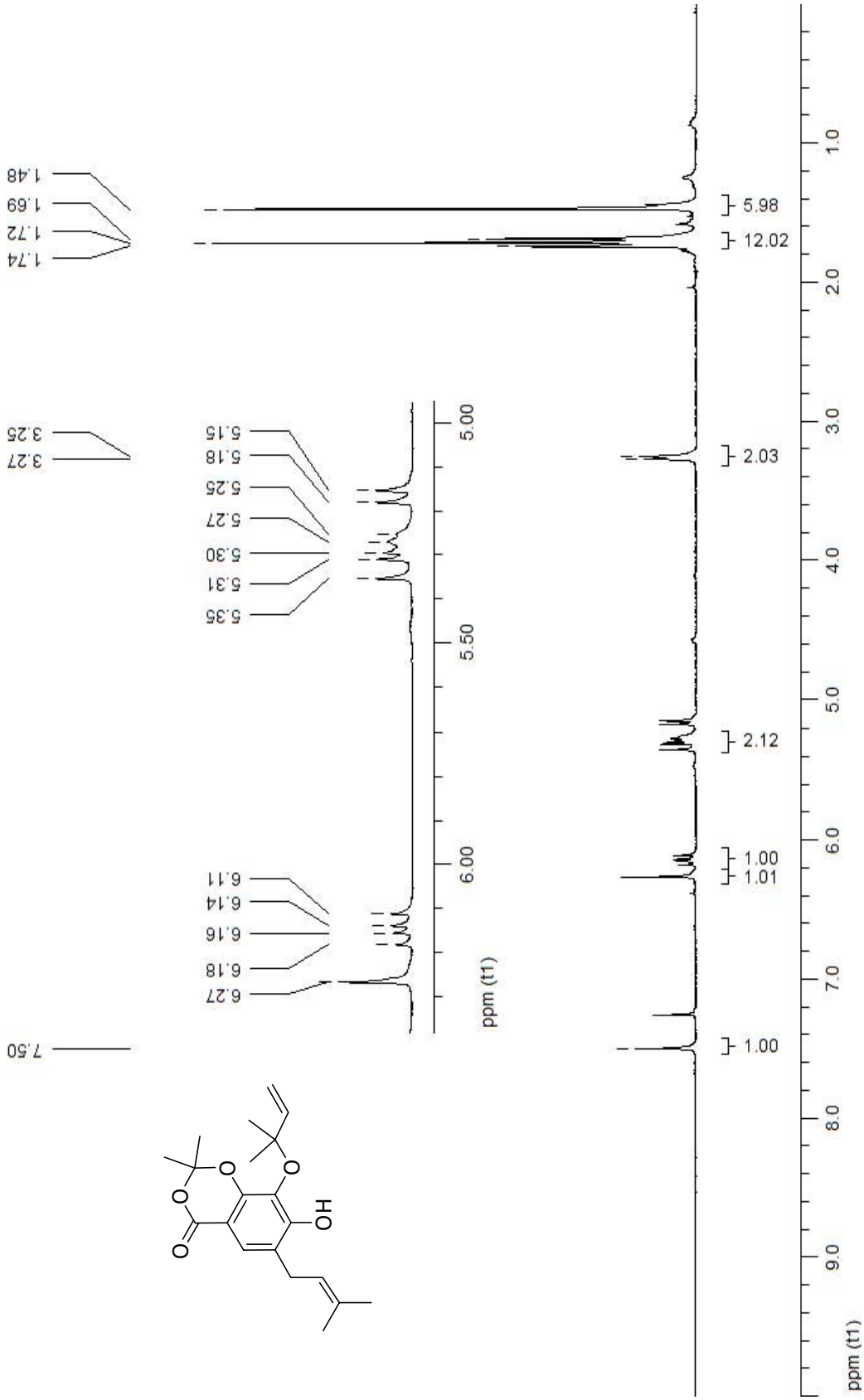

Spectrum 13: ^{1}H NMR ($CDCl_3$, 400 MHz) of compound 14.

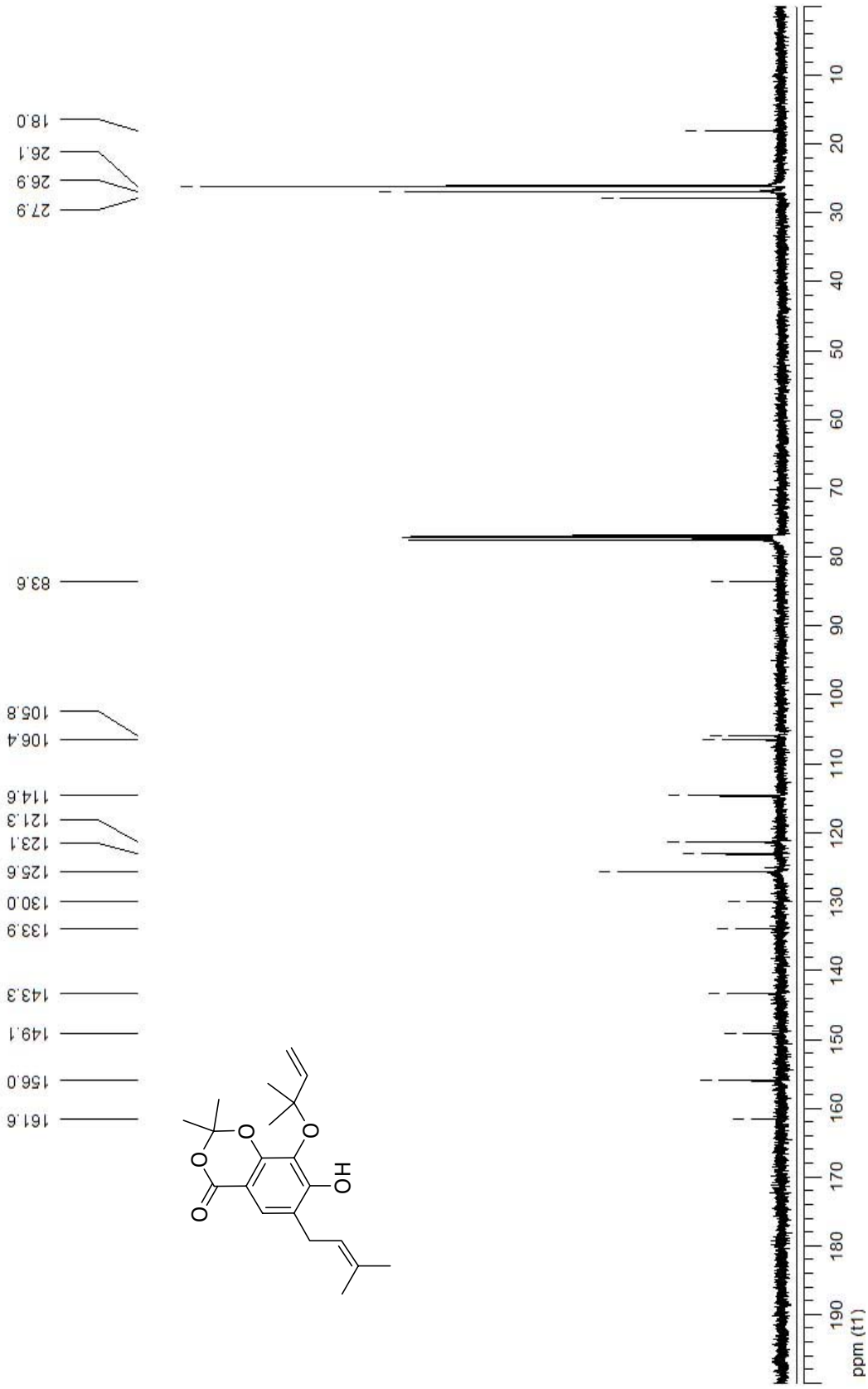

Spectrum 14: ^{13}C NMR ($CDCl_3$, 100 MHz) of compound 14.

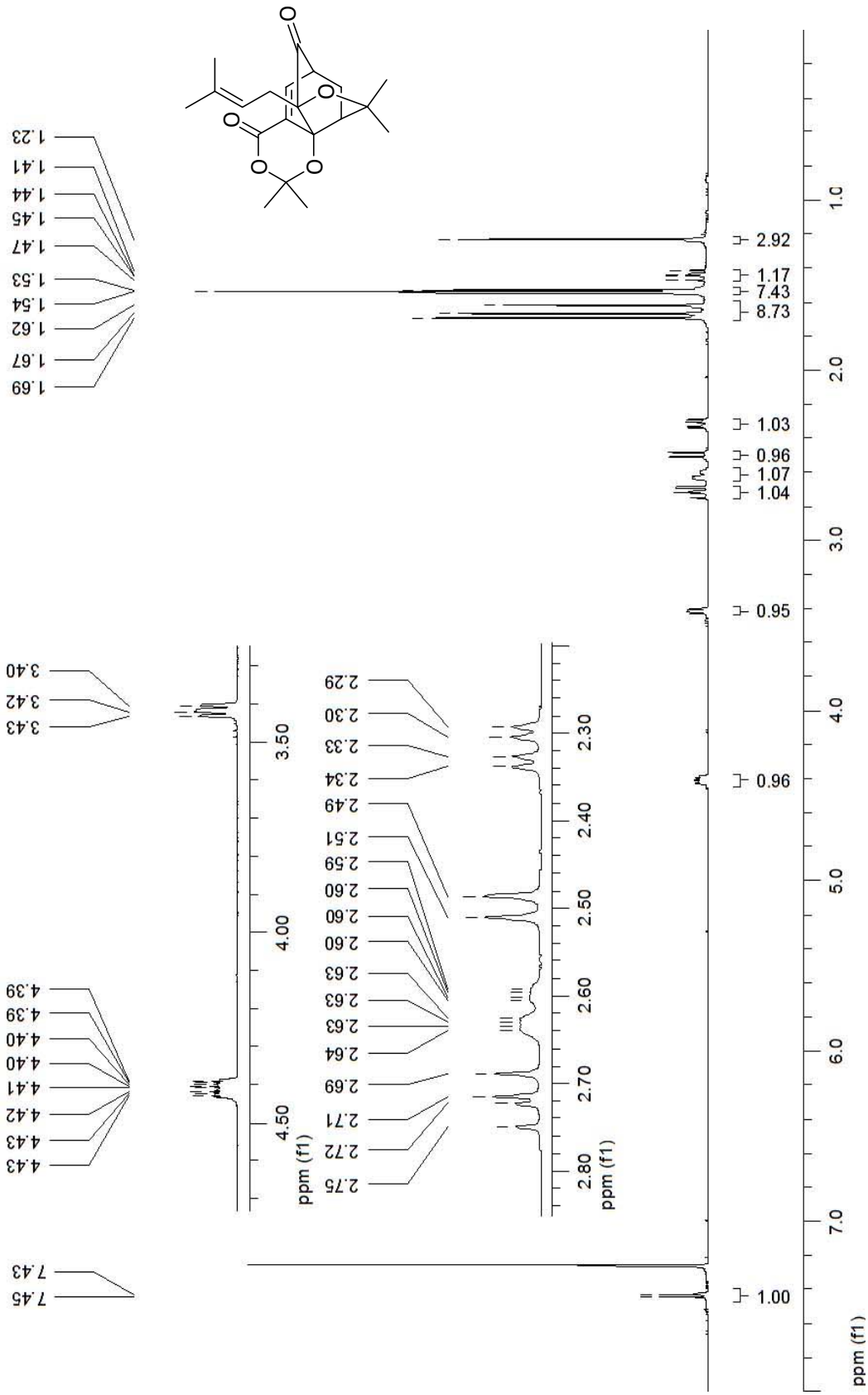

Spectrum 15: ^{1}H NMR ($CDCl_3$, 400 MHz) of compound 15.

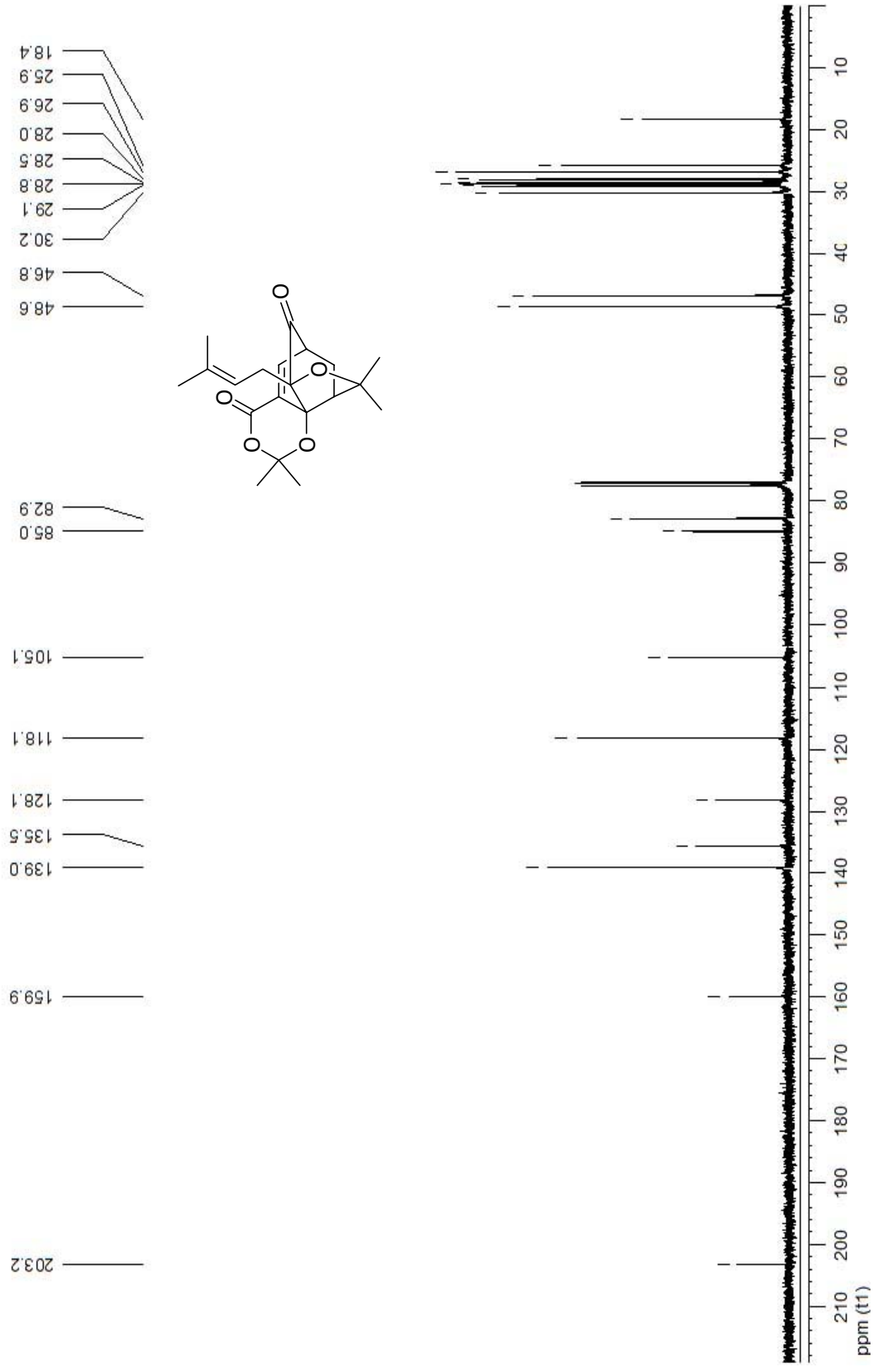

Spectrum 16: ^{13}C NMR ($CDCl_3$, 100 MHz) of compound 15.

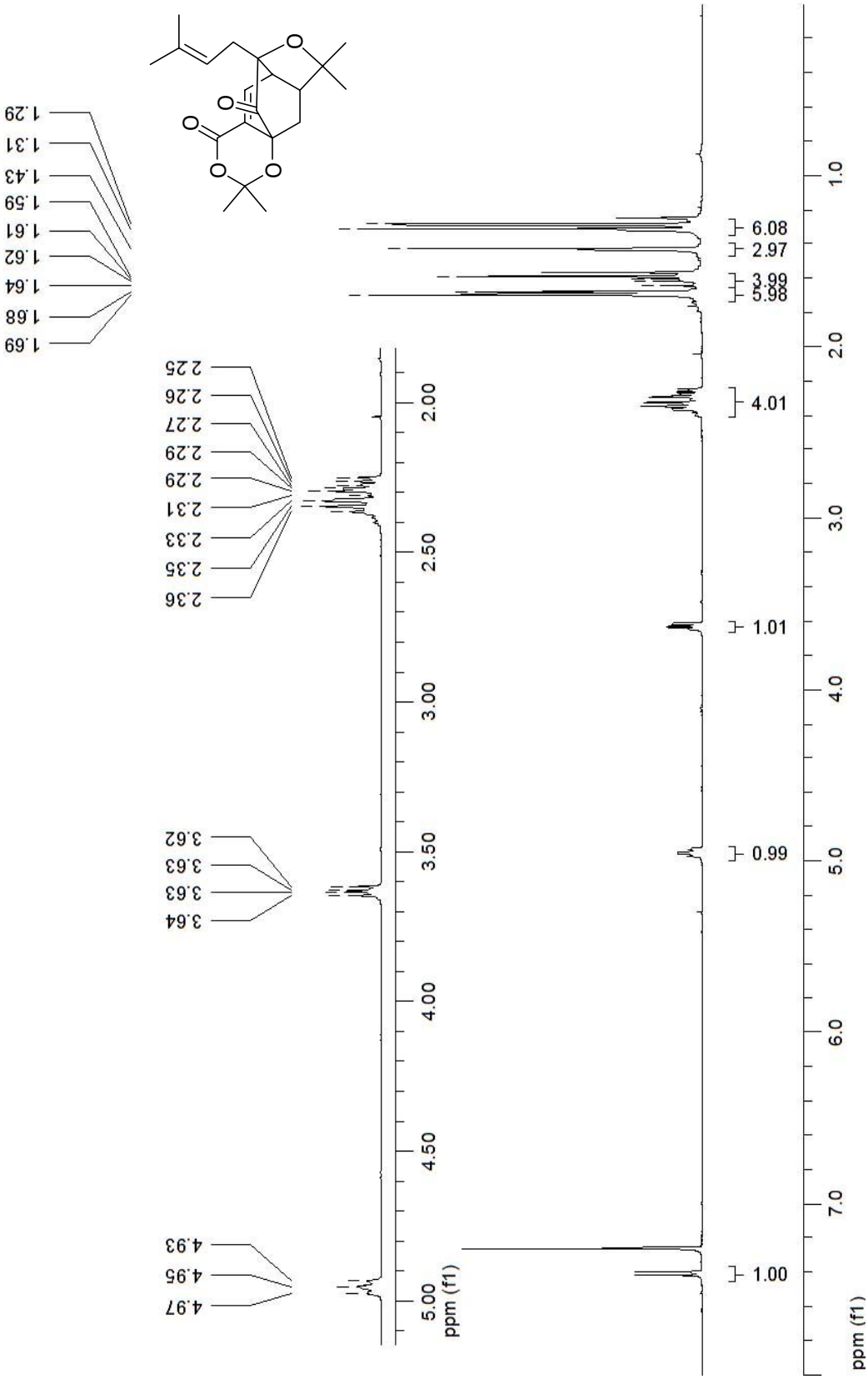

Spectrum 17: ^{1}H NMR ($CDCl_3$, 400 MHz) of compound 16.

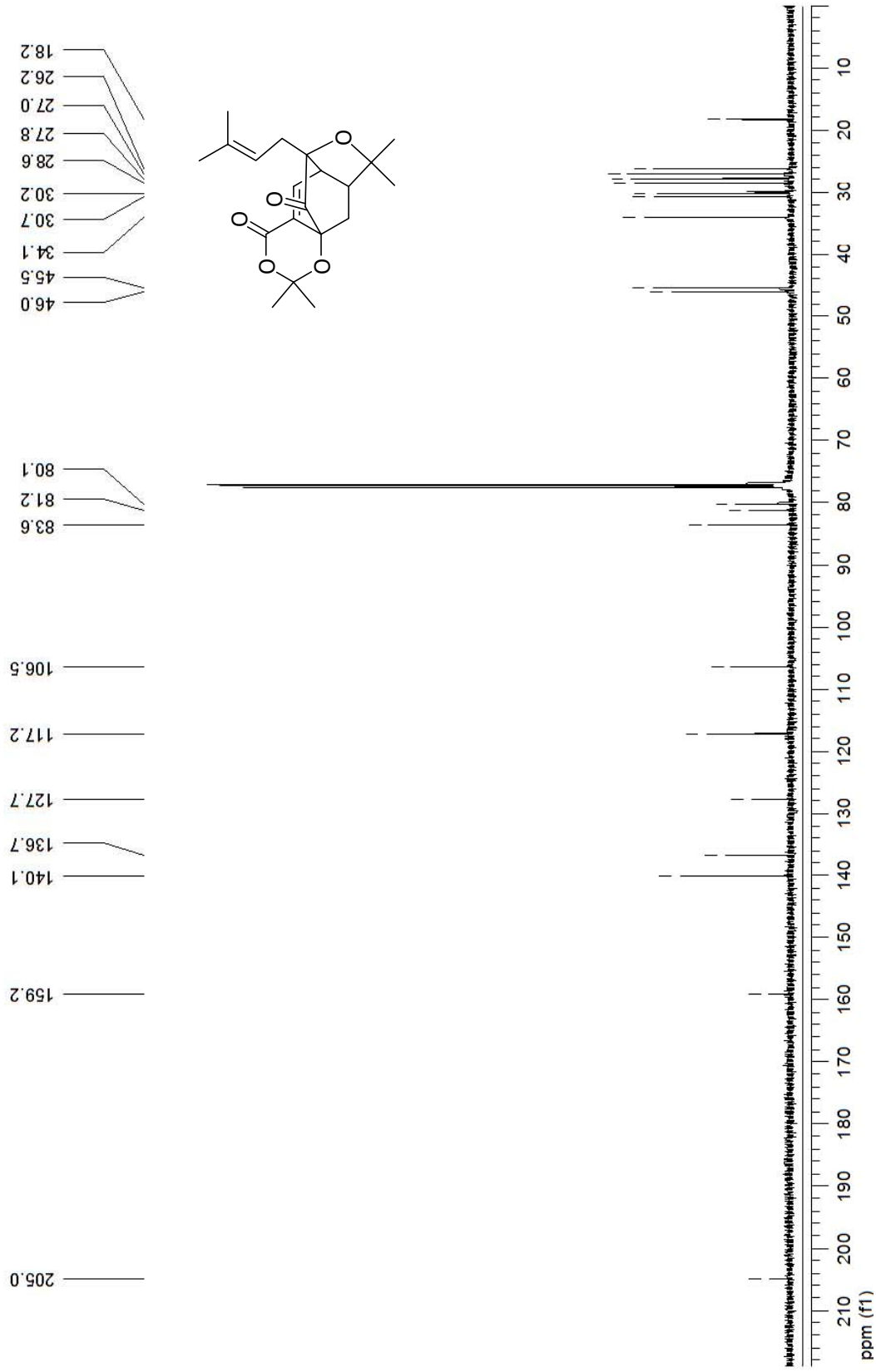

Spectrum 18: ^{13}C NMR ($CDCl_3$, 100 MHz) of compound 16.

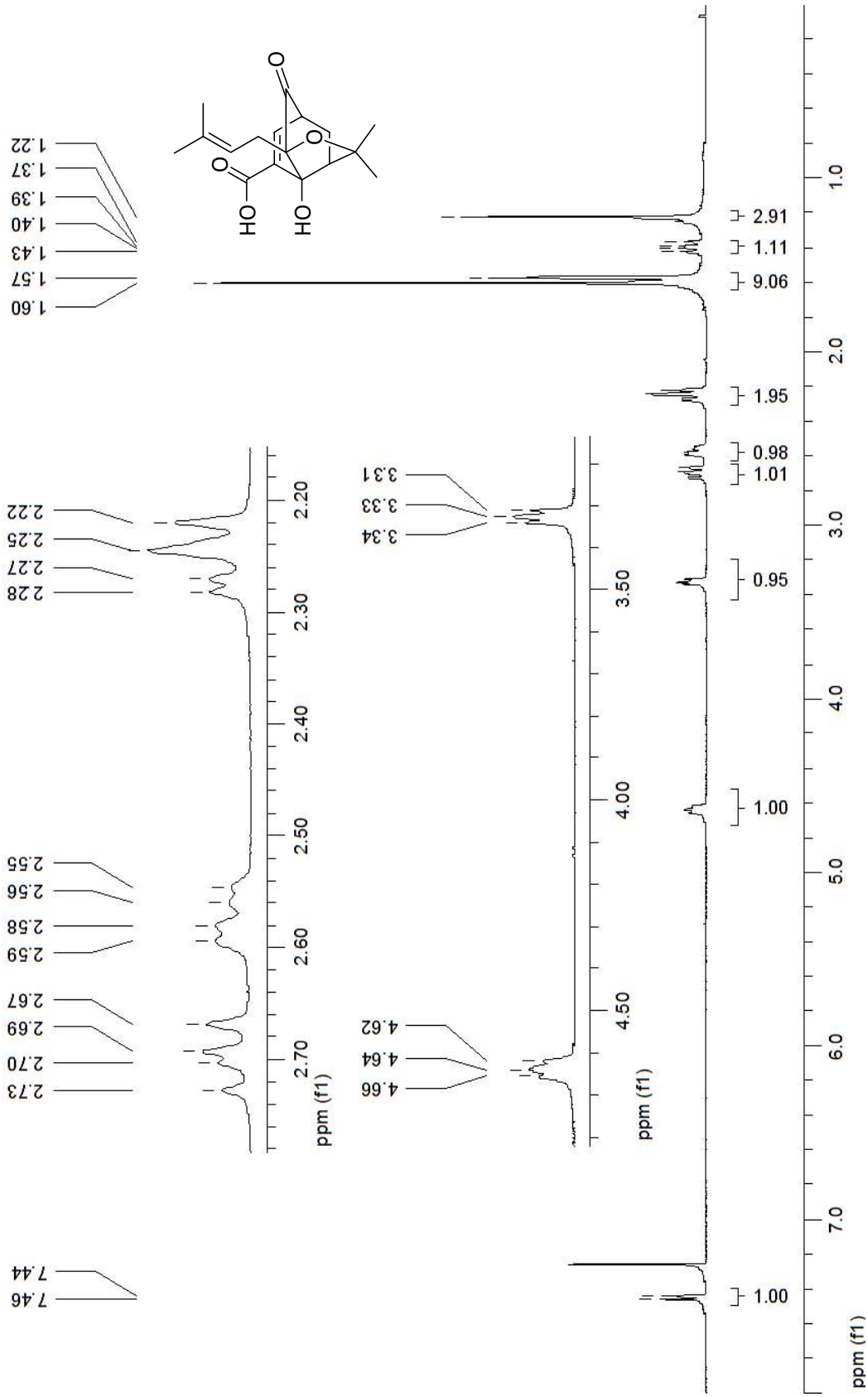

Spectrum 19: ^{1}H NMR ($CDCl_3$, 400 MHz) of compound 17.

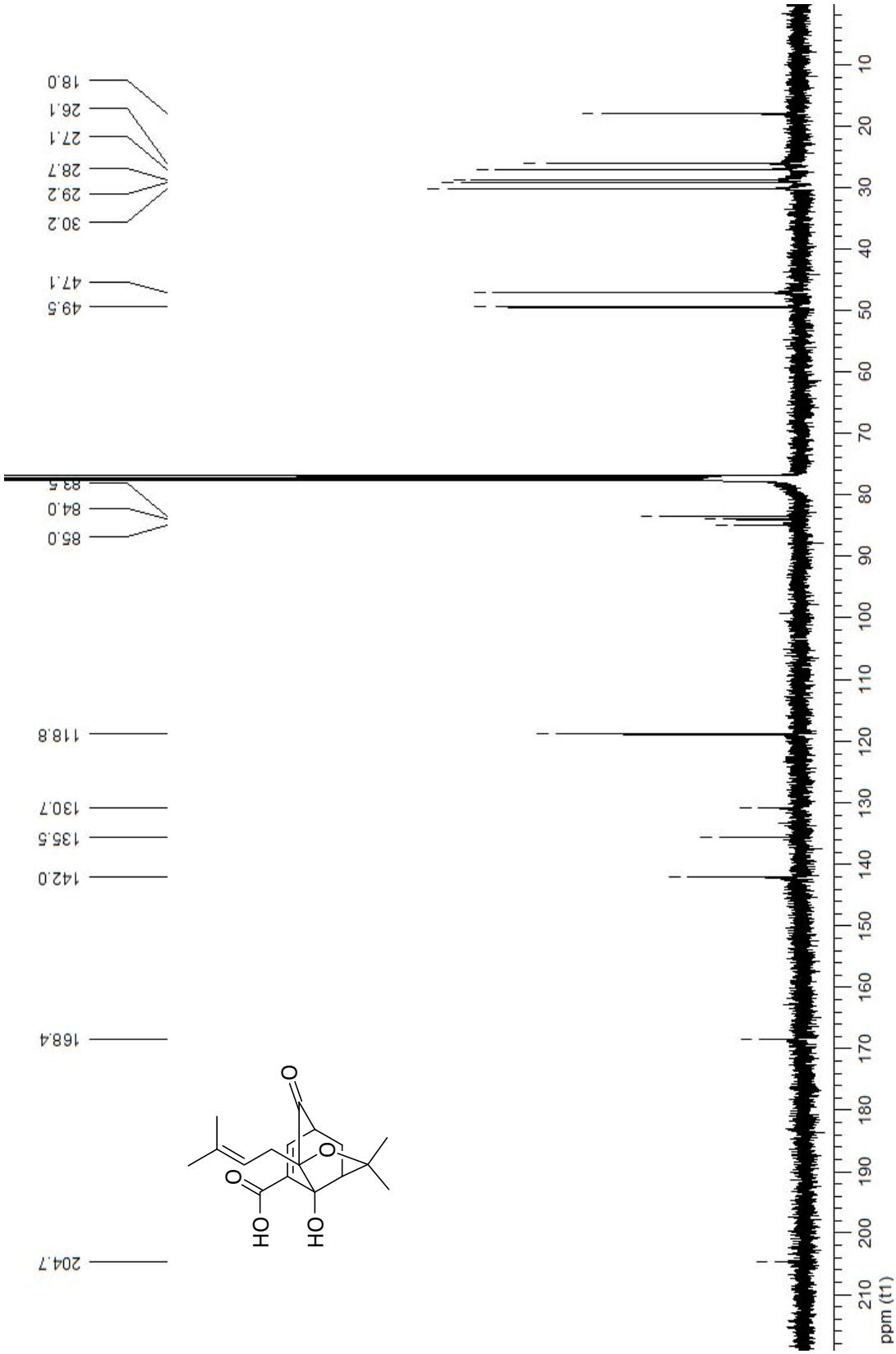

Spectrum 20: ^{13}C NMR ($CDCl_3$, 100 MHz) of compound 17.

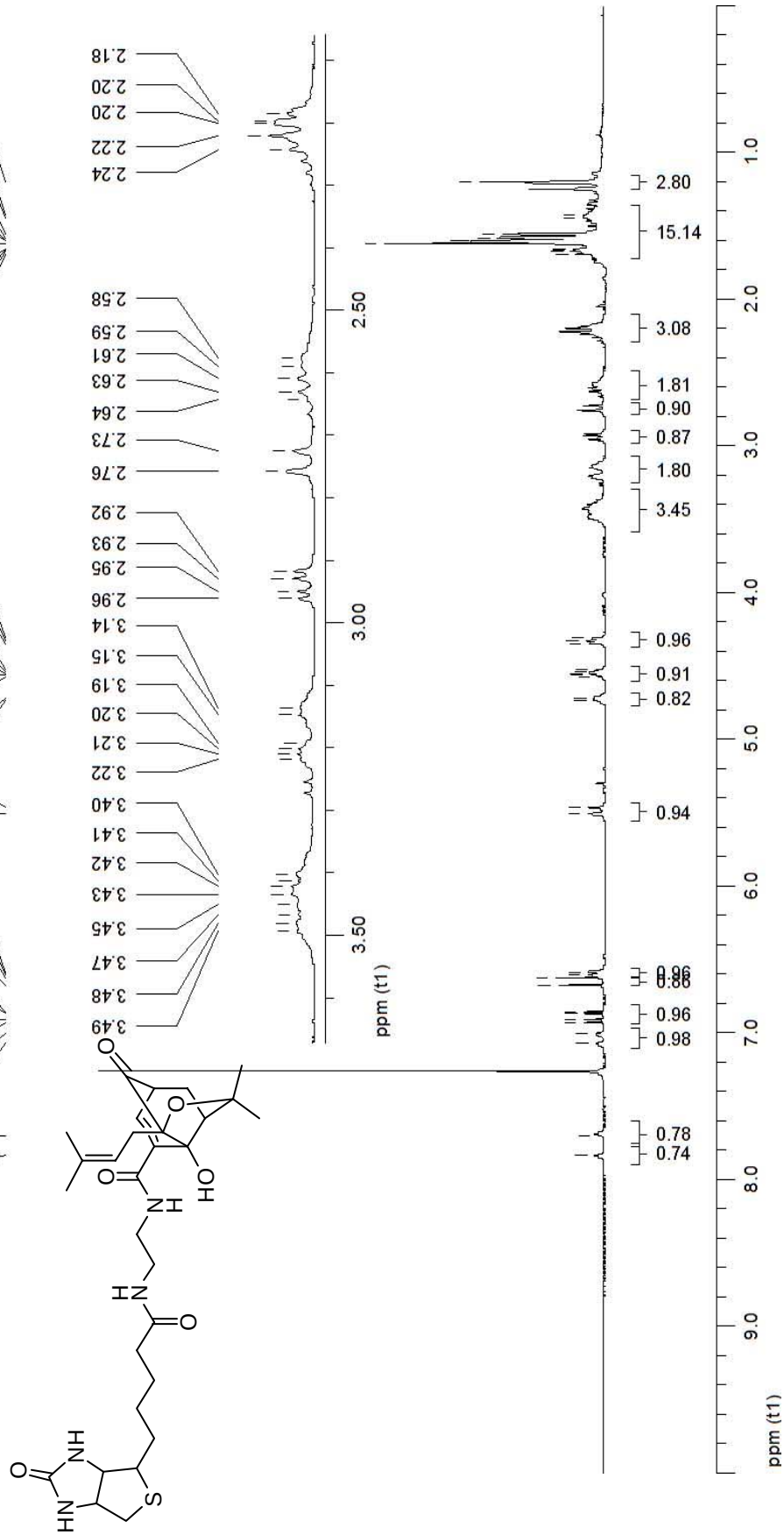

Spectrum 21: ^{1}H NMR ($CDCl_3$, 400 MHz) of compound 18.

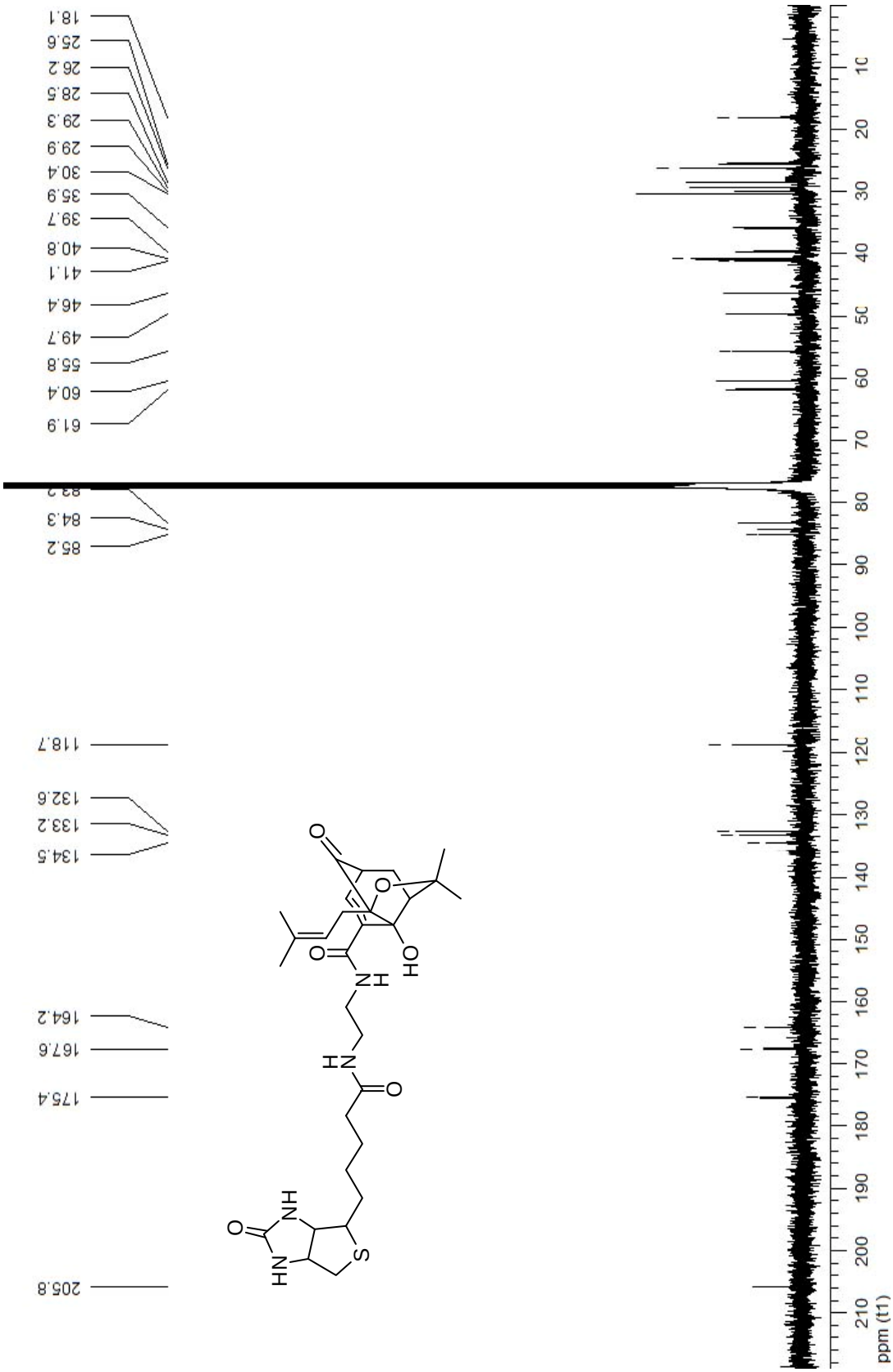

Spectrum 22: ^{13}C NMR ($CDCl_3$, 100 MHz) of compound 18.

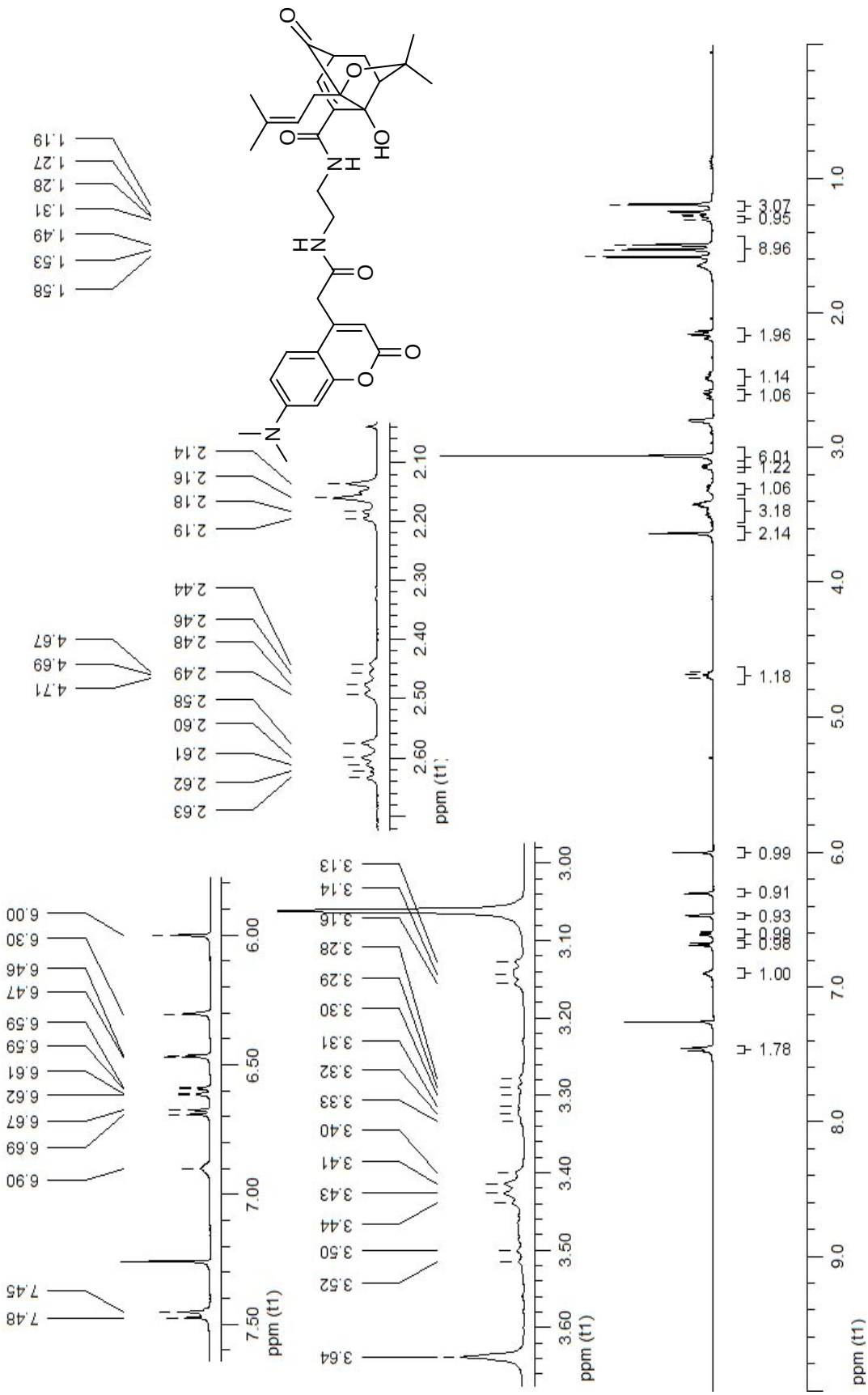

Spectrum 23: ^{1}H NMR ($CDCl_3$, 400 MHz) of compound 19.

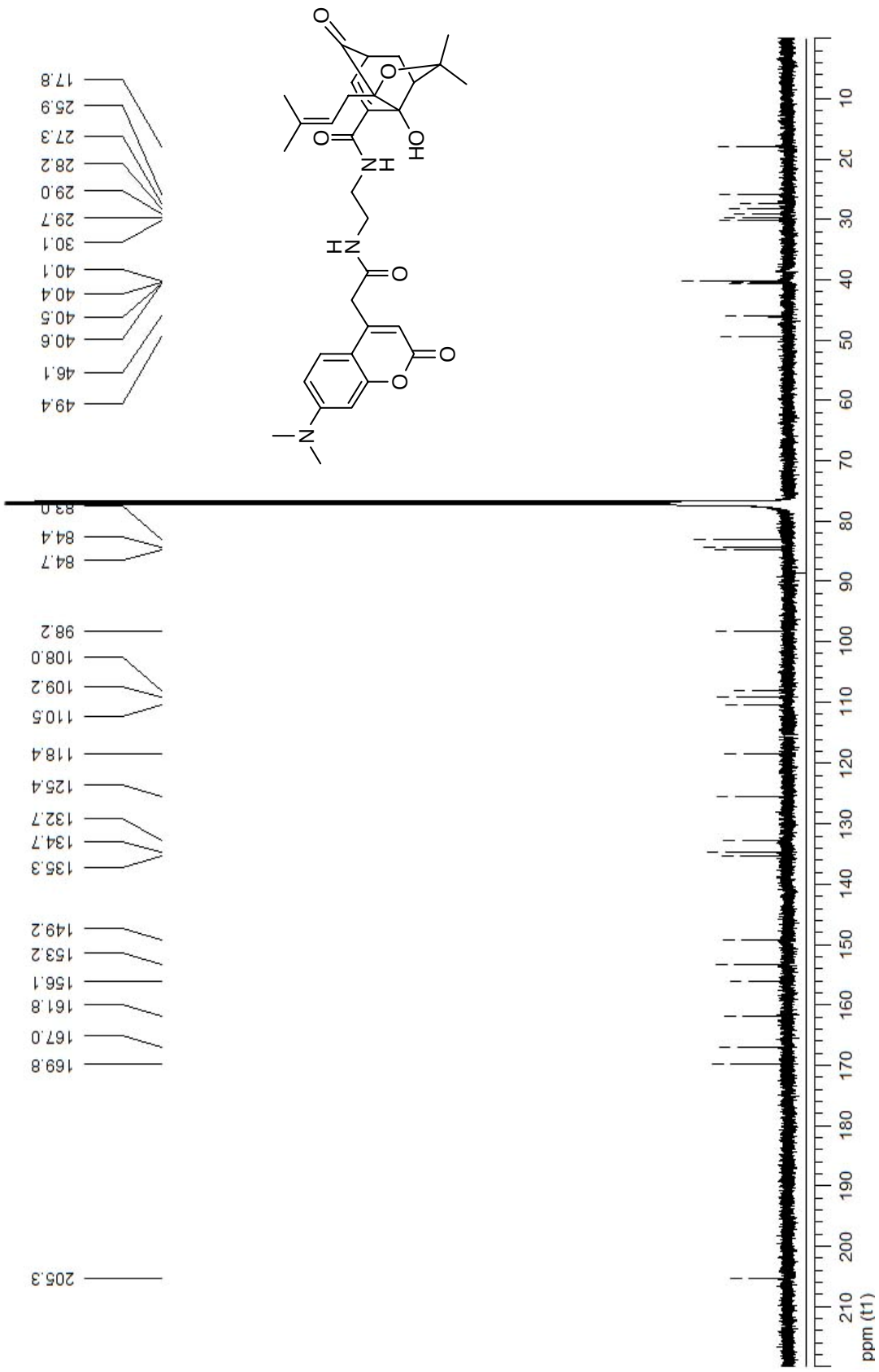

Spectrum 24: ^{13}C NMR ($CDCl_3$, 100 MHz) of compound 19.

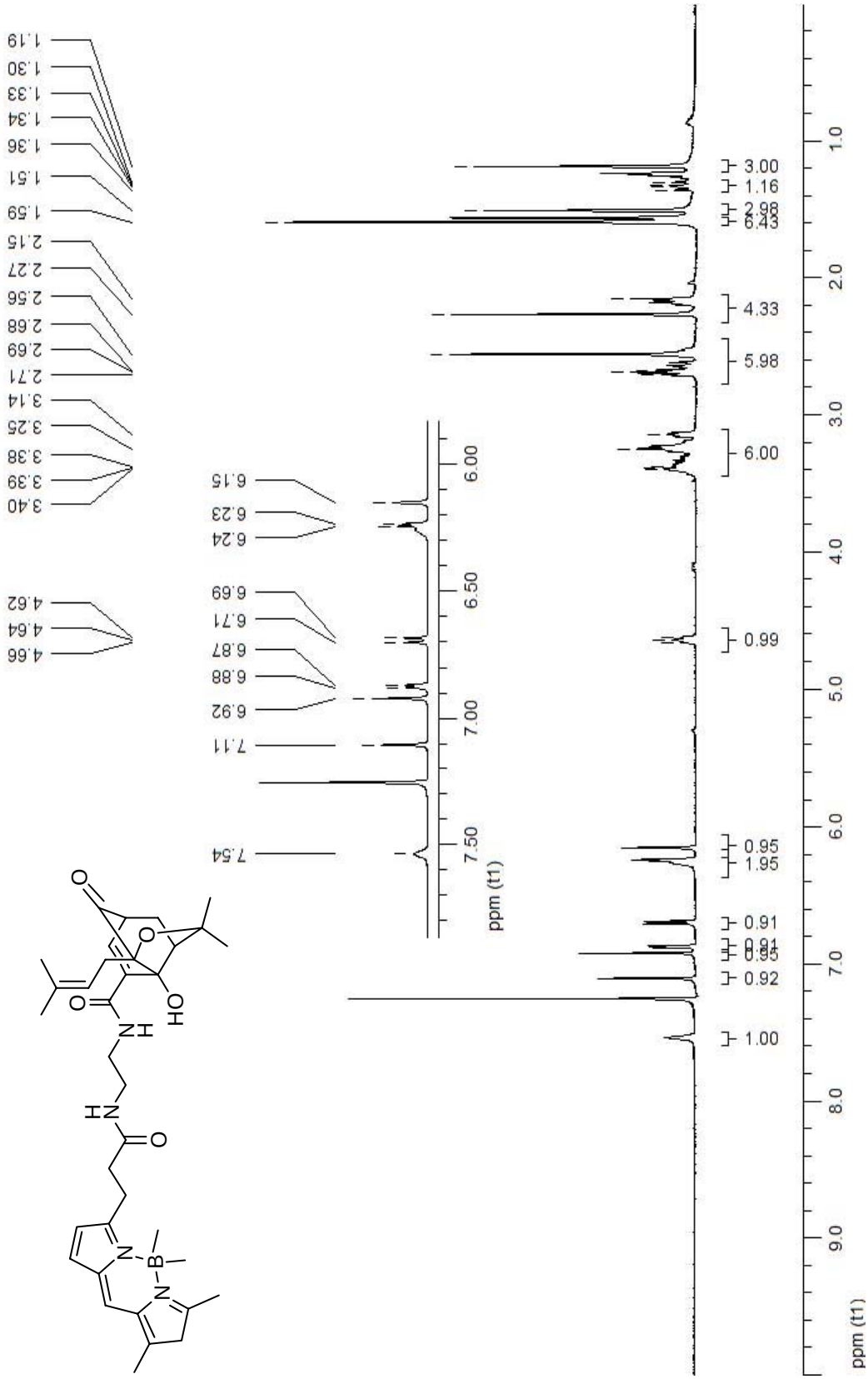

Spectrum 25: ^{1}H NMR ($CDCl_3$, 400 MHz) of compound 20.

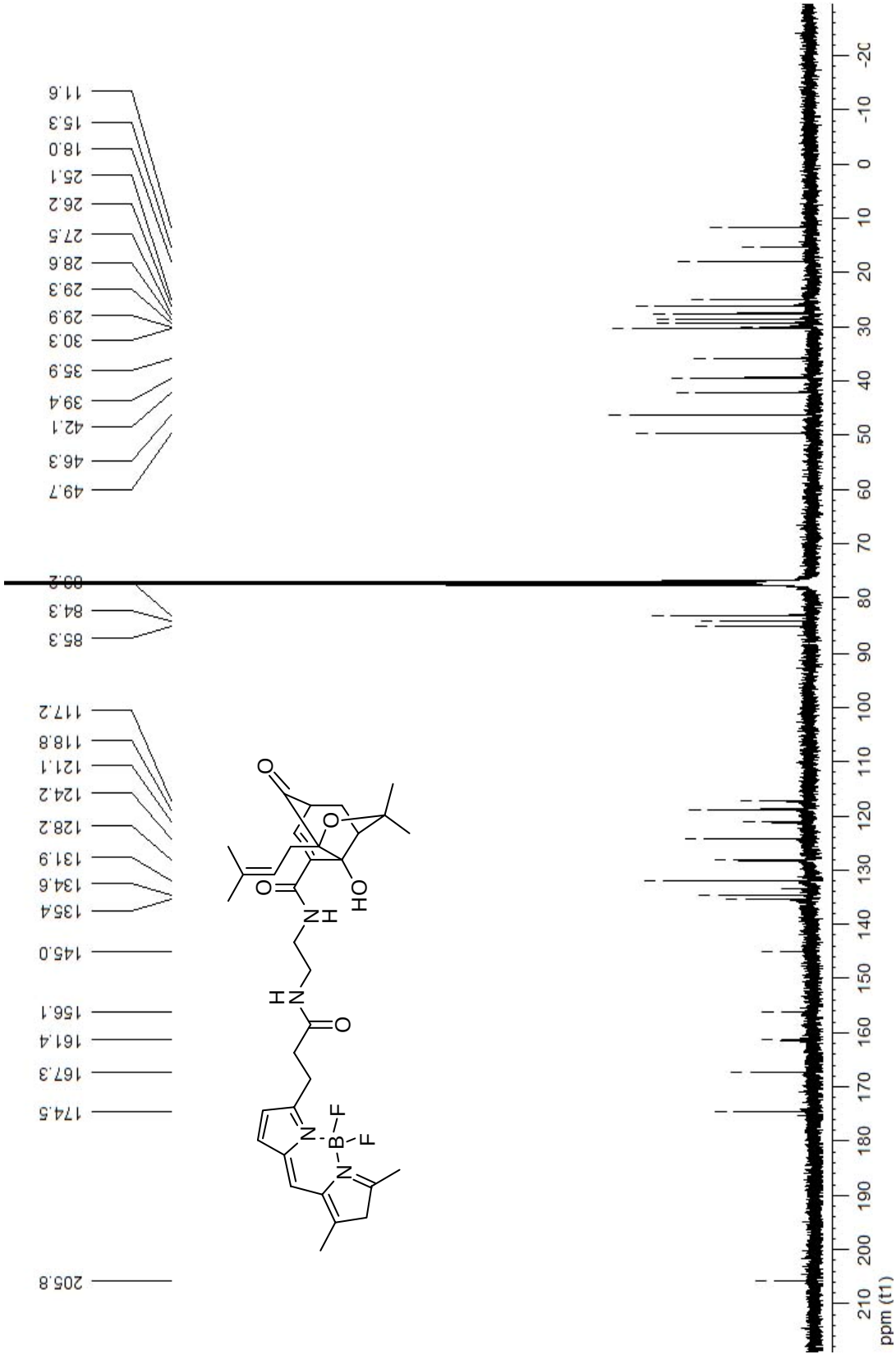

Spectrum 26: ^{13}C NMR ($CDCl_3$, 100 MHz) of compound 20.

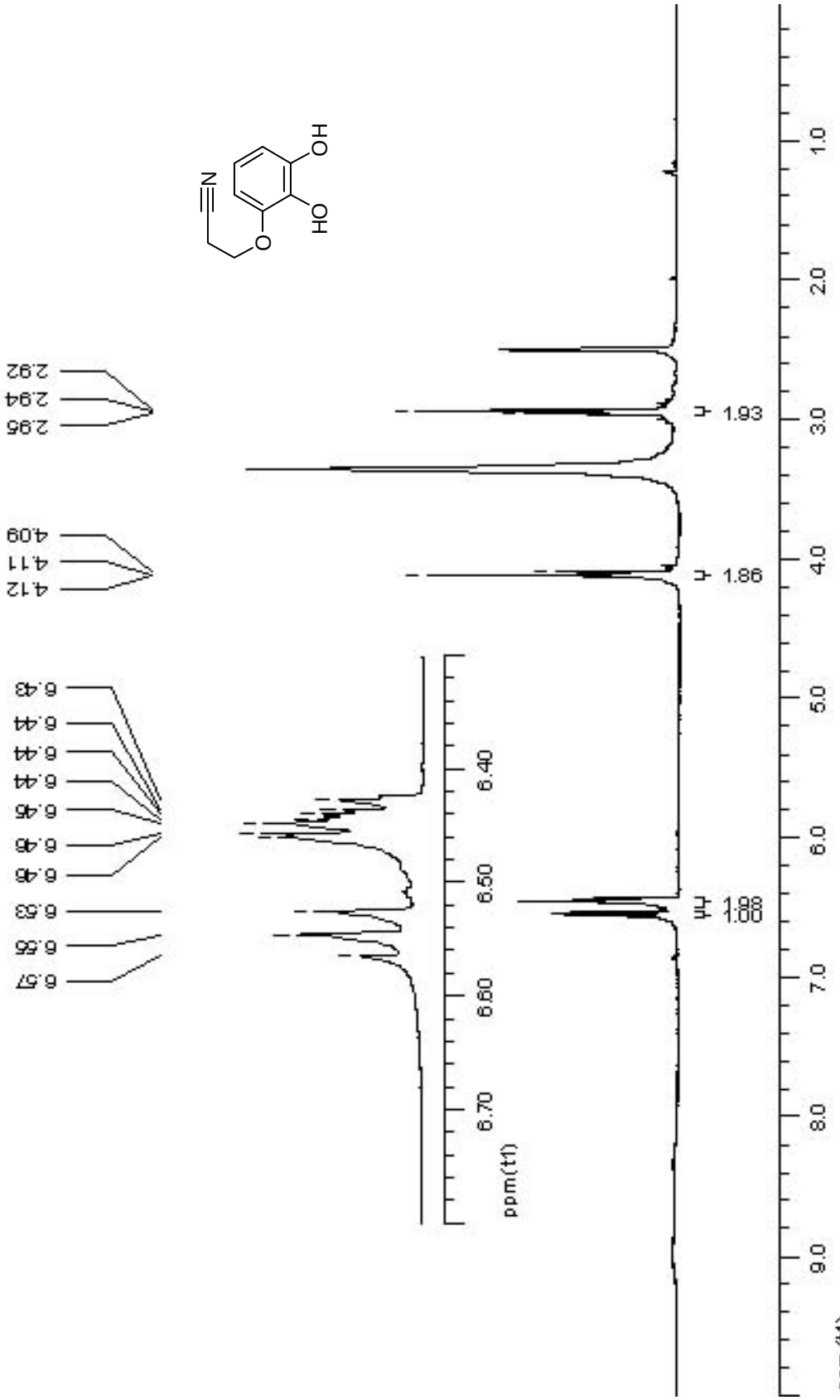

Spectrum 27: ^{1}H NMR (DMSO-d6, 400 MHz) of compound 22.

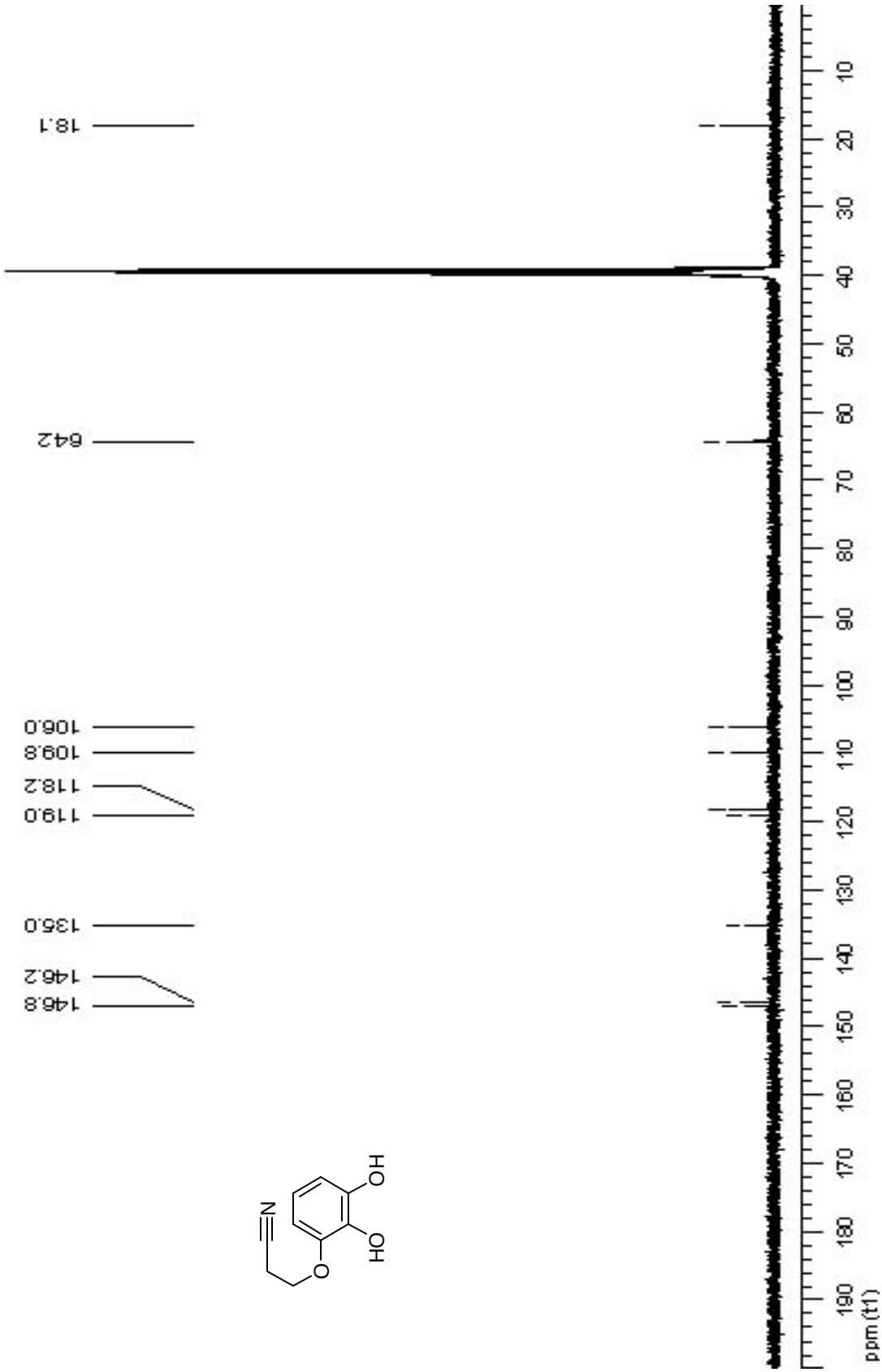

Spectrum 28: ^{13}C NMR (DMSO-d6, 100 MHz) of compound 22.

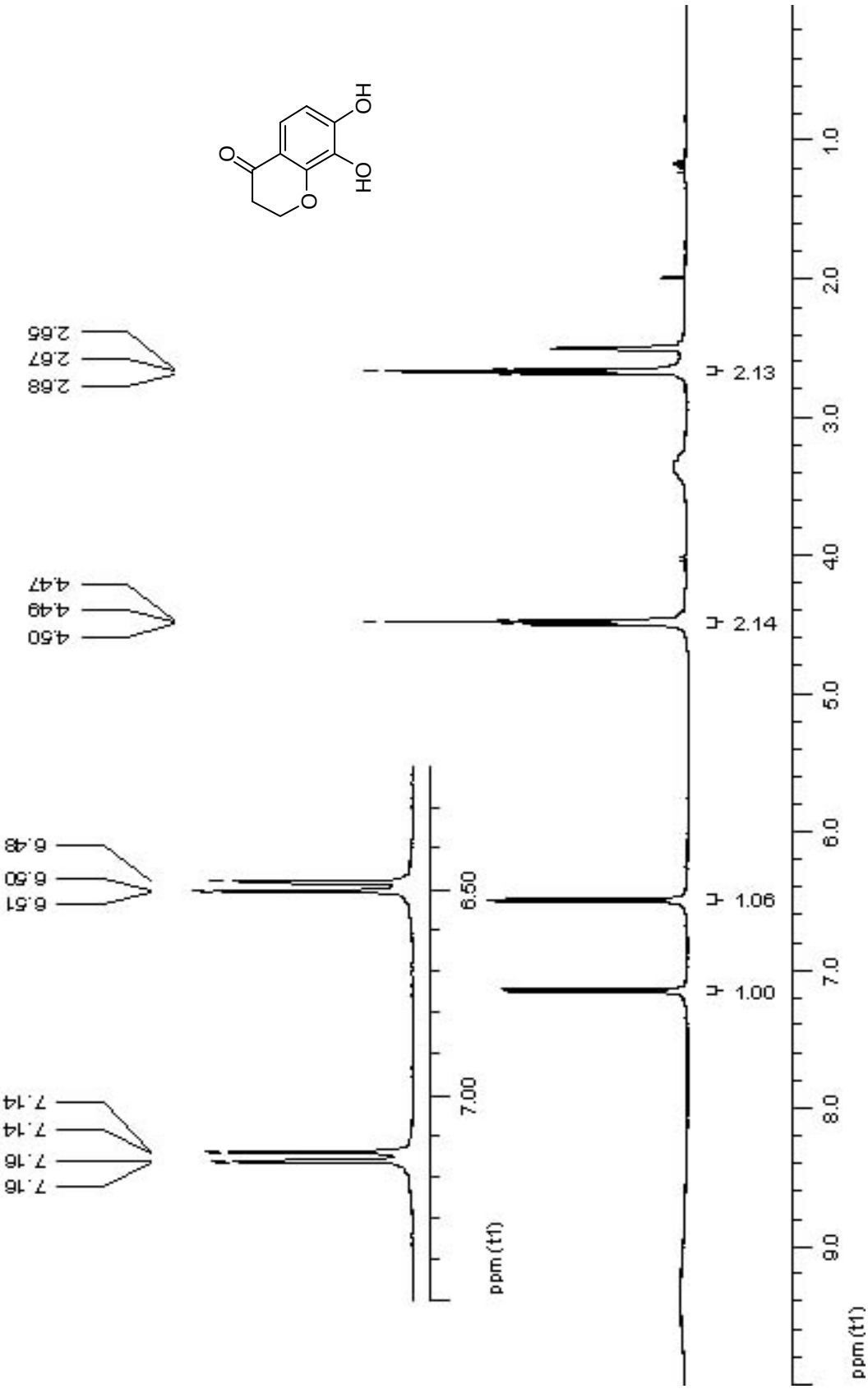

Spectrum 29: ^{1}H NMR (DMSO-d6, 400 MHz) of compound 23.

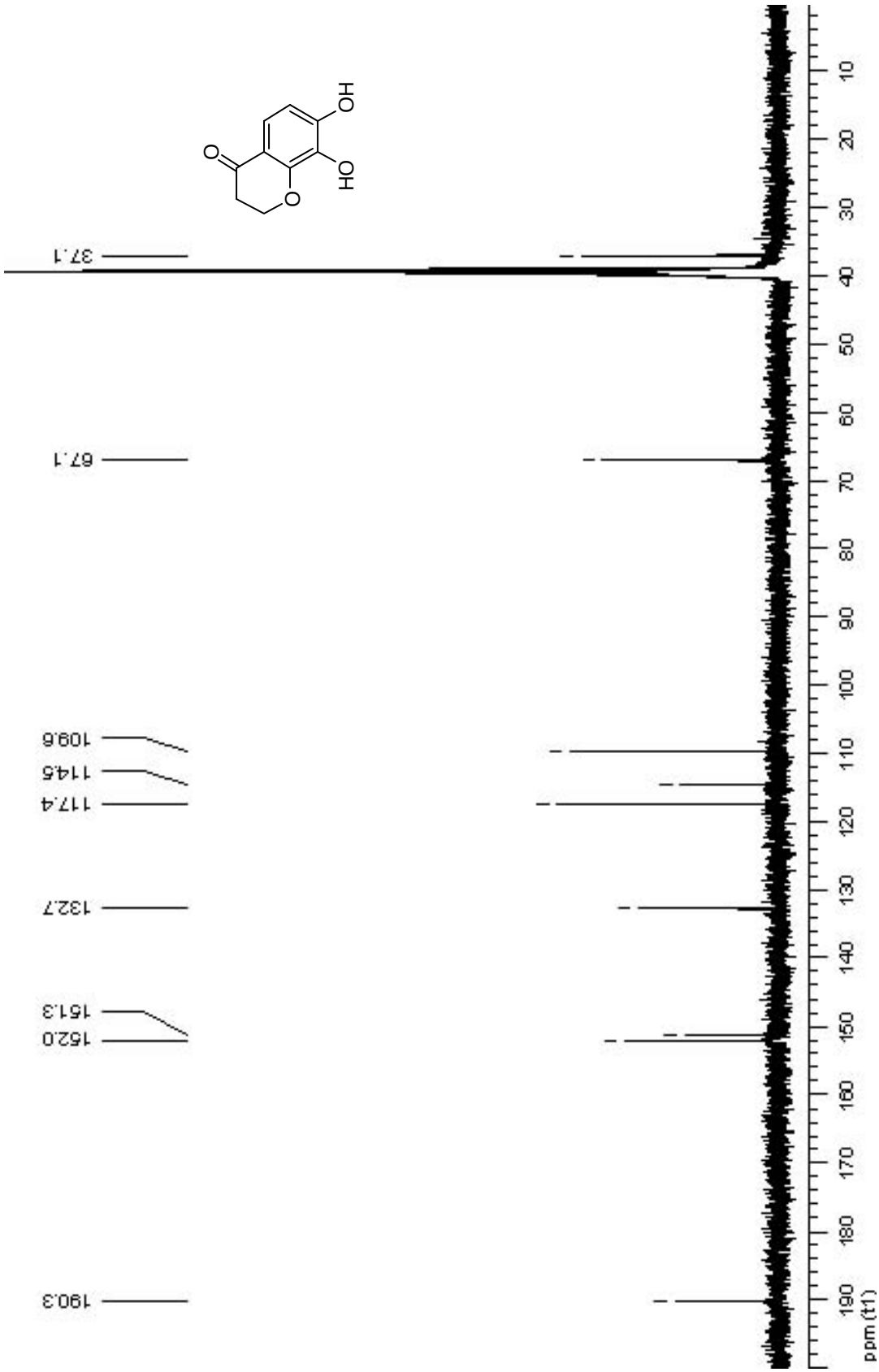

Spectrum 30: ^{13}C NMR (DMSO-d6, 100 MHz) of compound 23.

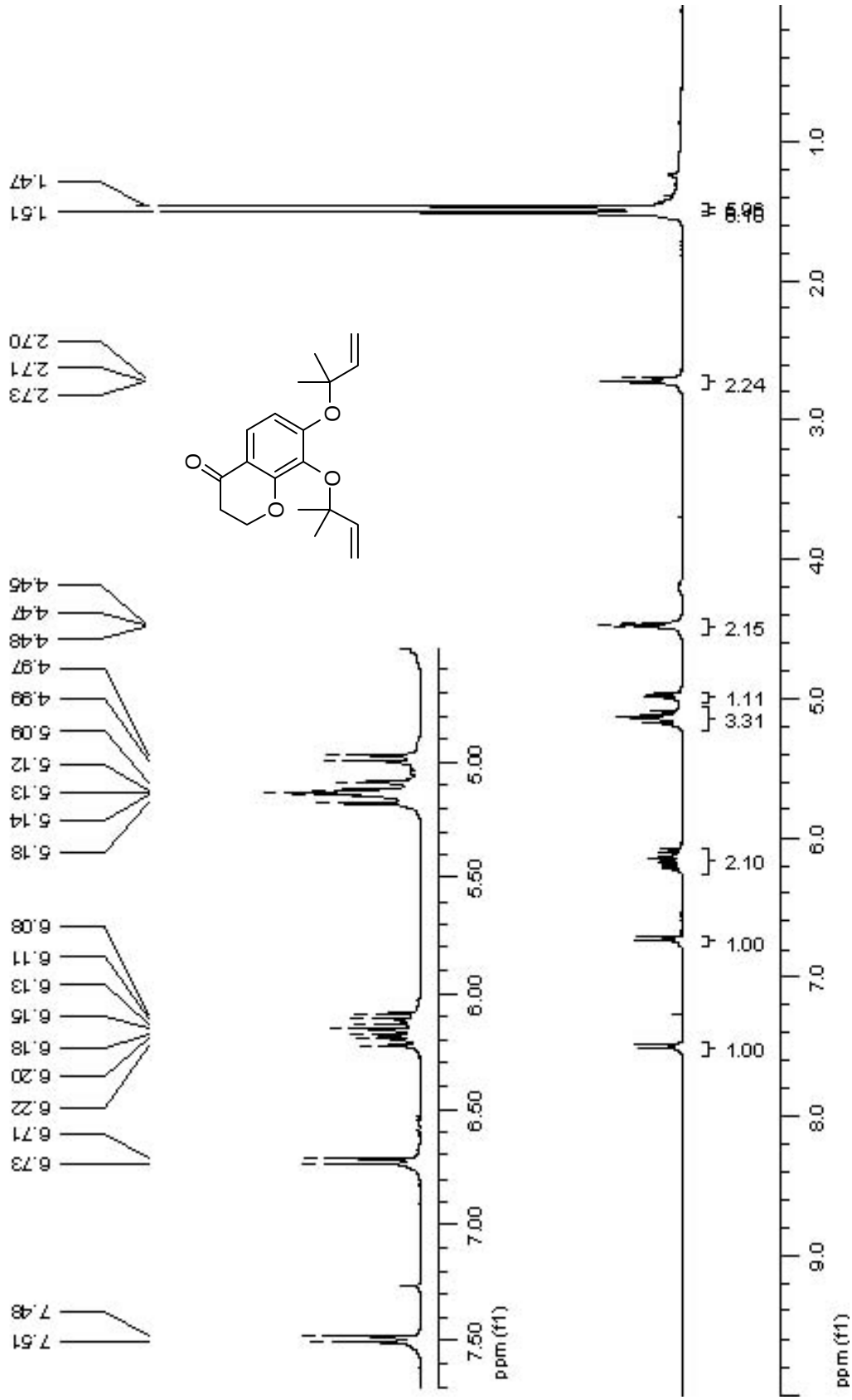

Spectrum 31: ^{1}H NMR ($CDCl_3$, 400 MHz) of compound 24.

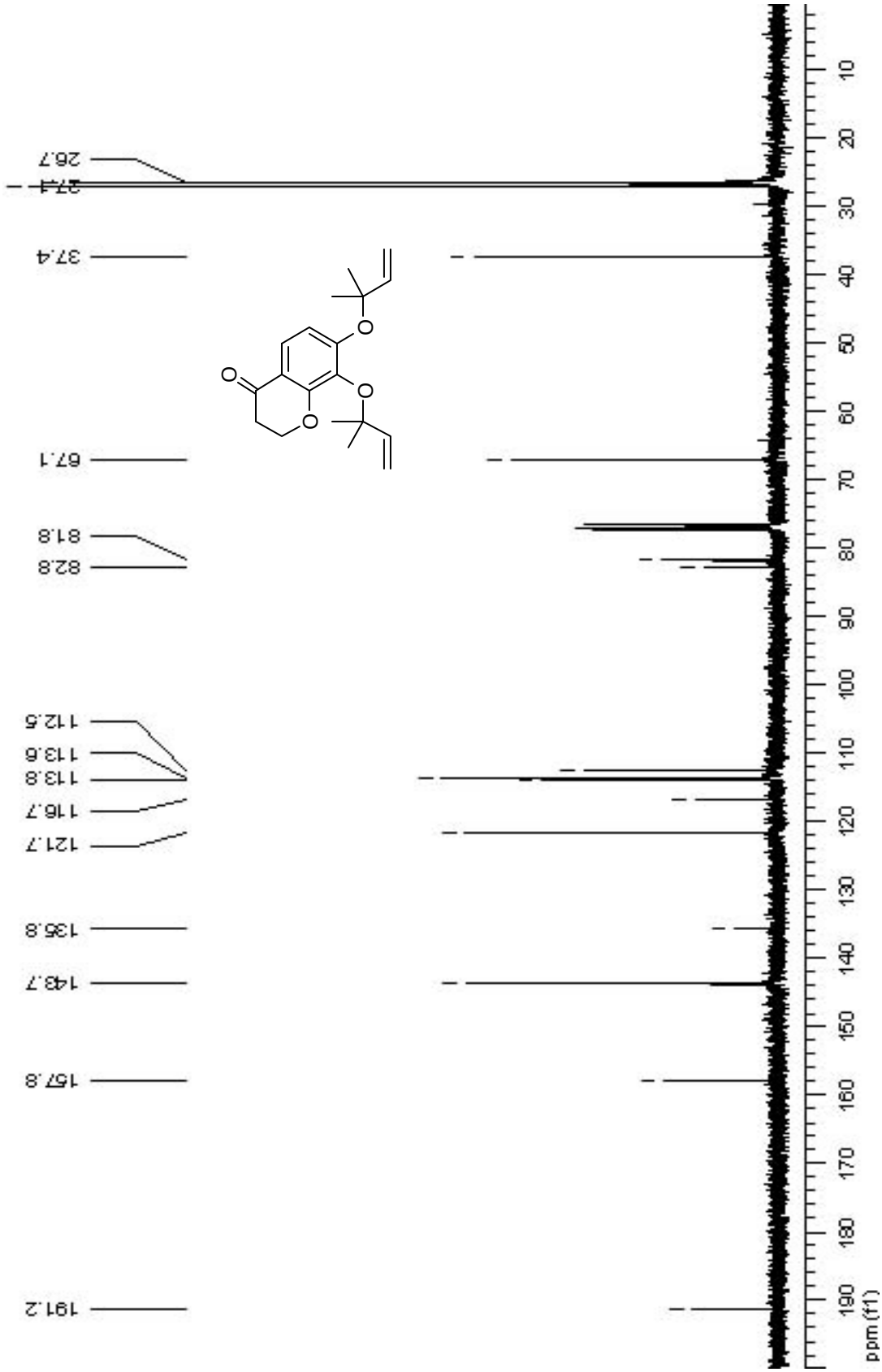

Spectrum 32: ^{13}C NMR ($CDCl_3$, 100 MHz) of compound 24.

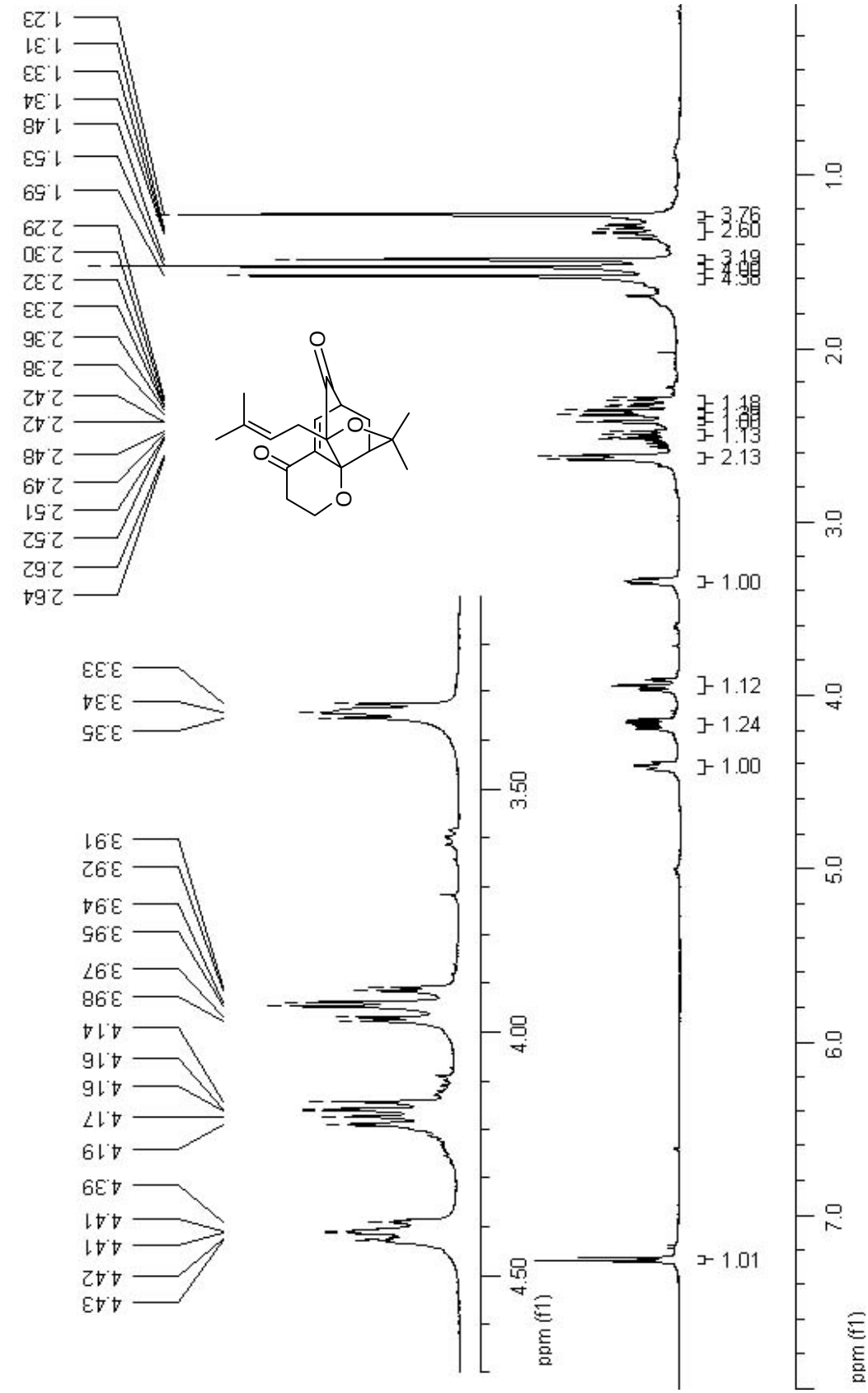

Spectrum 33: ^{1}H NMR ($CDCl_3$, 400 MHz) of compound 26.

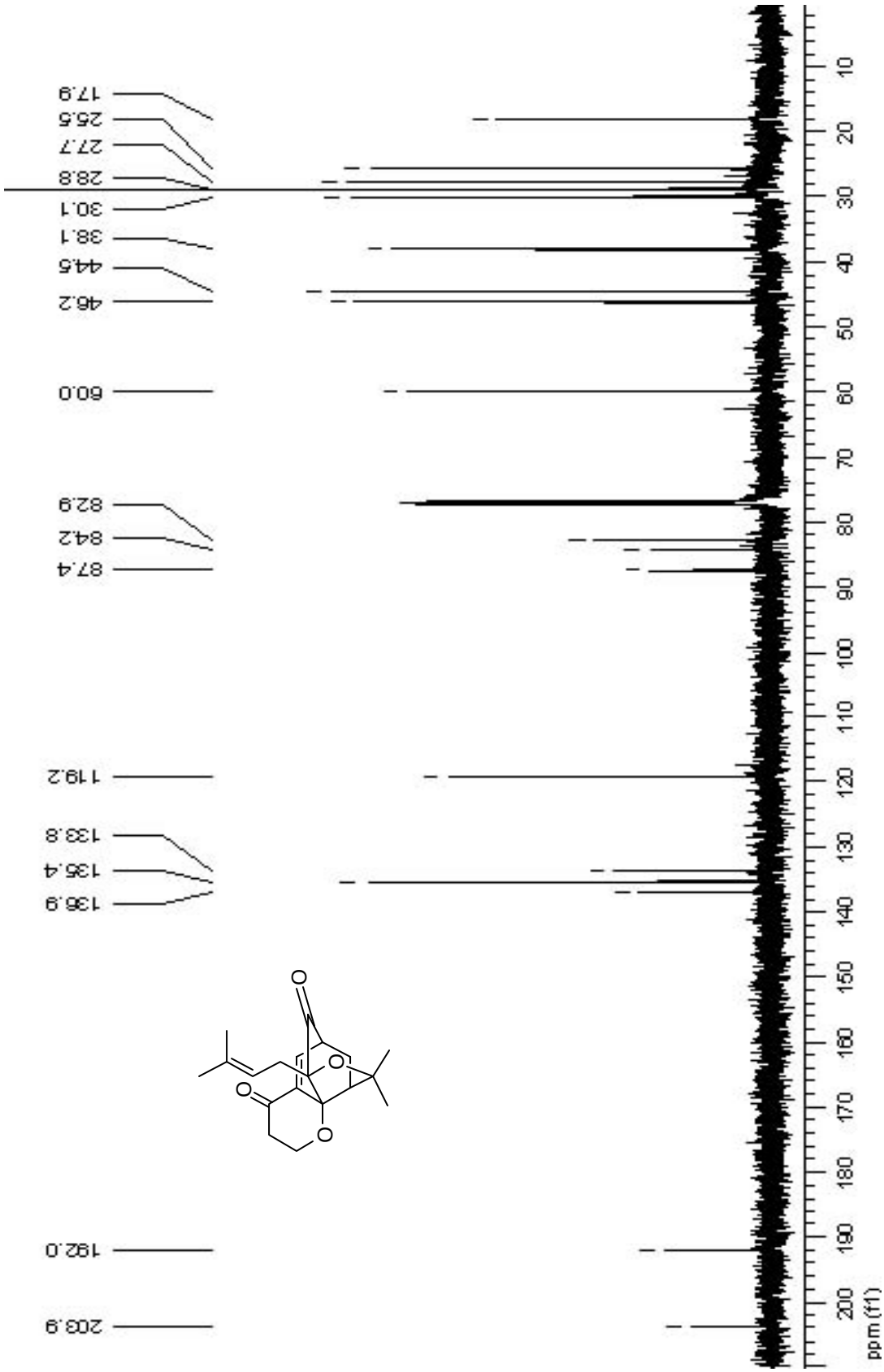

Spectrum 34: ^{13}C NMR ($CDCl_3$, 100 MHz) of compound 26.

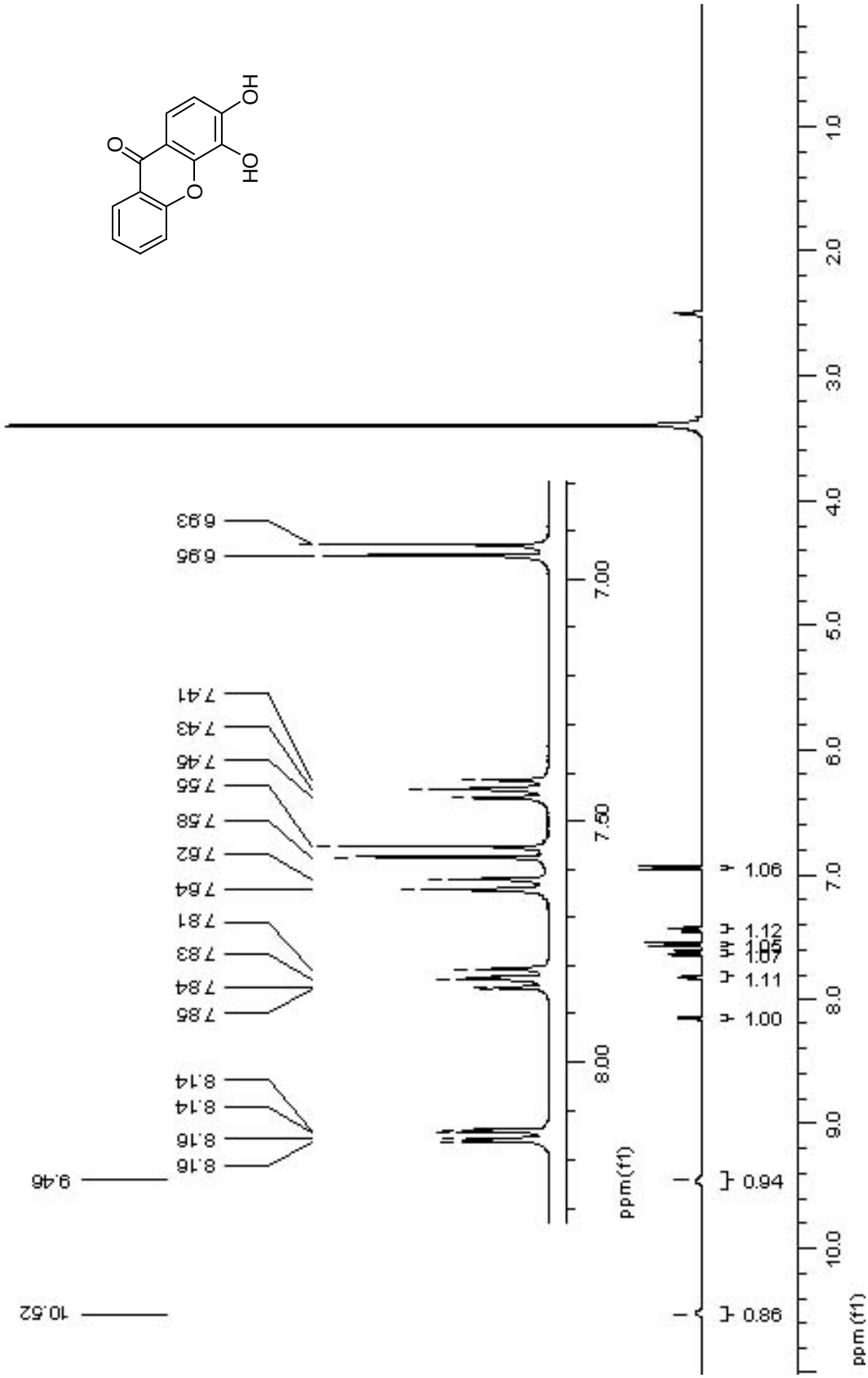

Spectrum 35: ^{1}H NMR (DMSO-d6, 400 MHz) of compound 31.

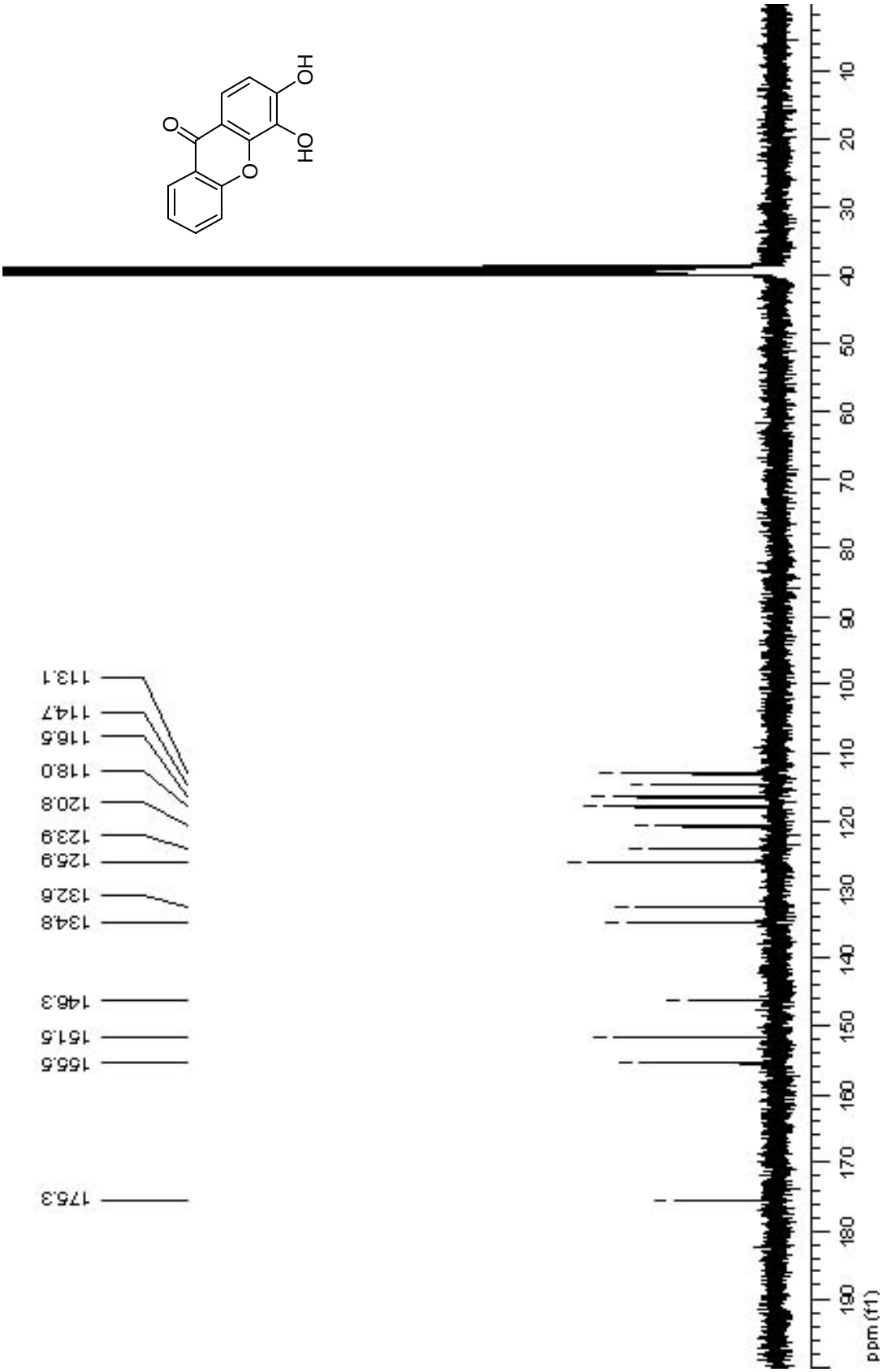

Spectrum 36: ^{13}C NMR (DMSO-d6, 100 MHz) of compound 31.

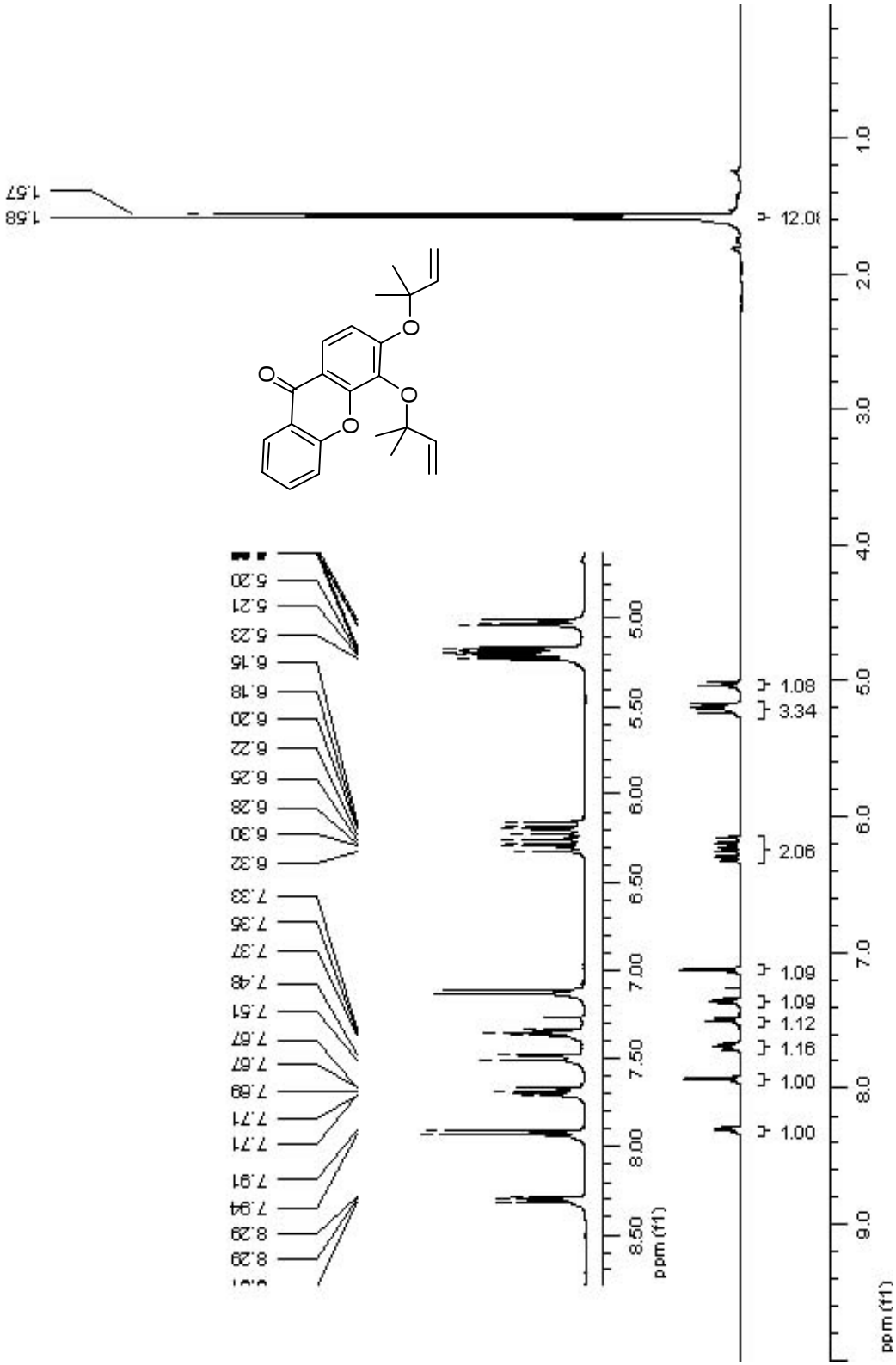

Spectrum 37: ^{1}H NMR ($CDCl_3$, 400 MHz) of compound 32.

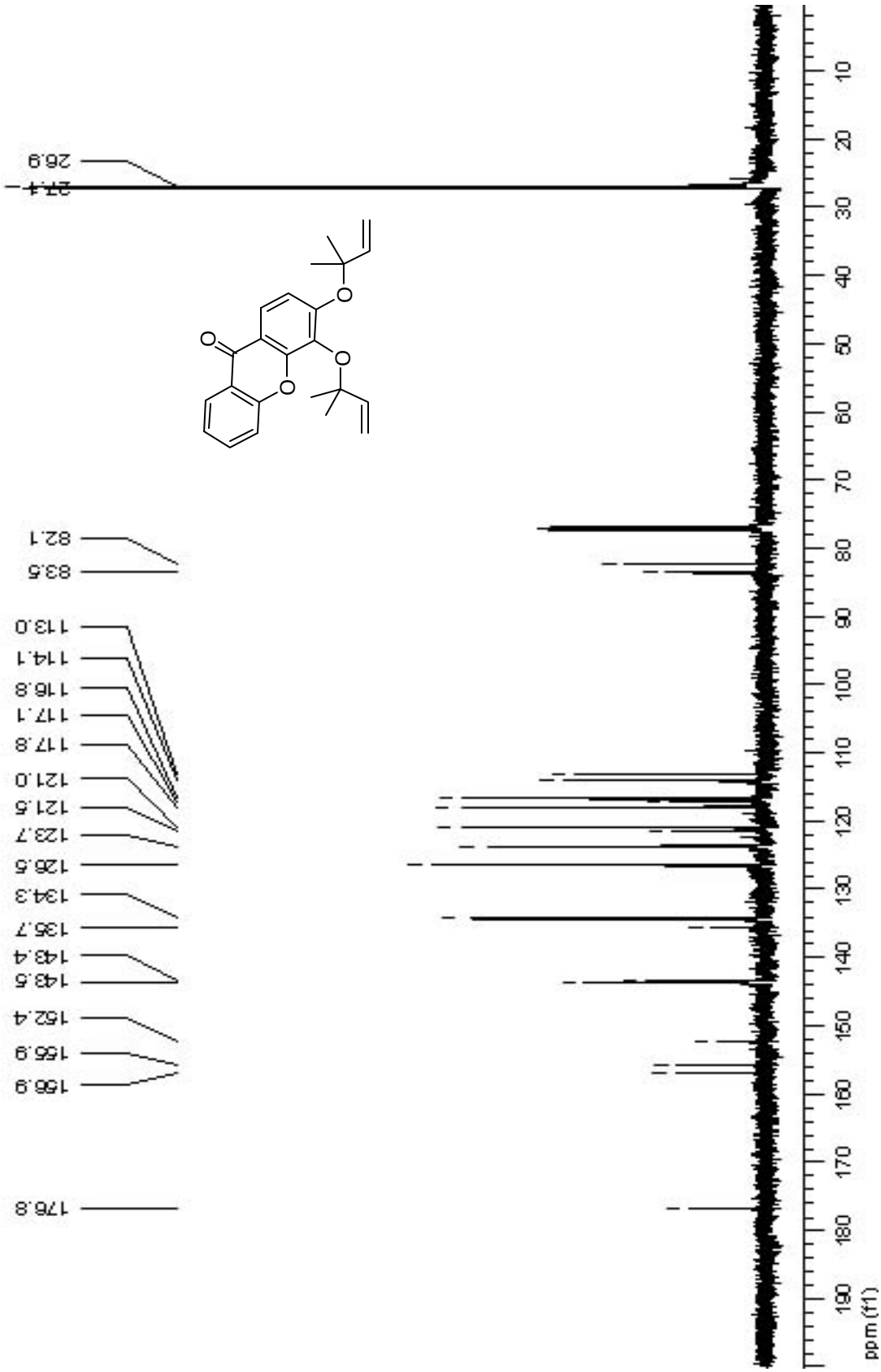

Spectrum 38: ^{13}C NMR ($CDCl_3$, 100 MHz) of compound 32.

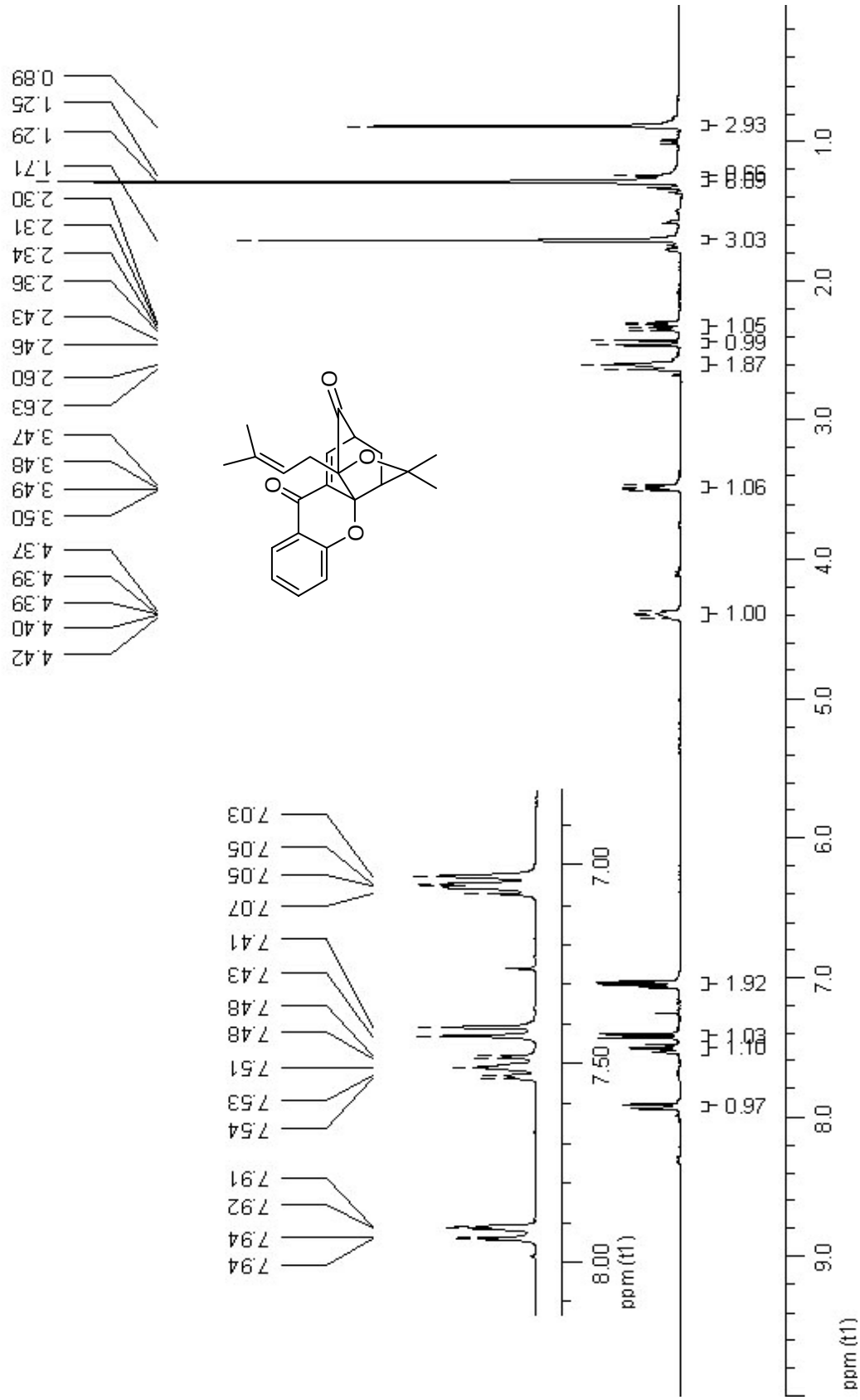

Spectrum 39: ^{1}H NMR ($CDCl_3$, 400 MHz) of compound 7.

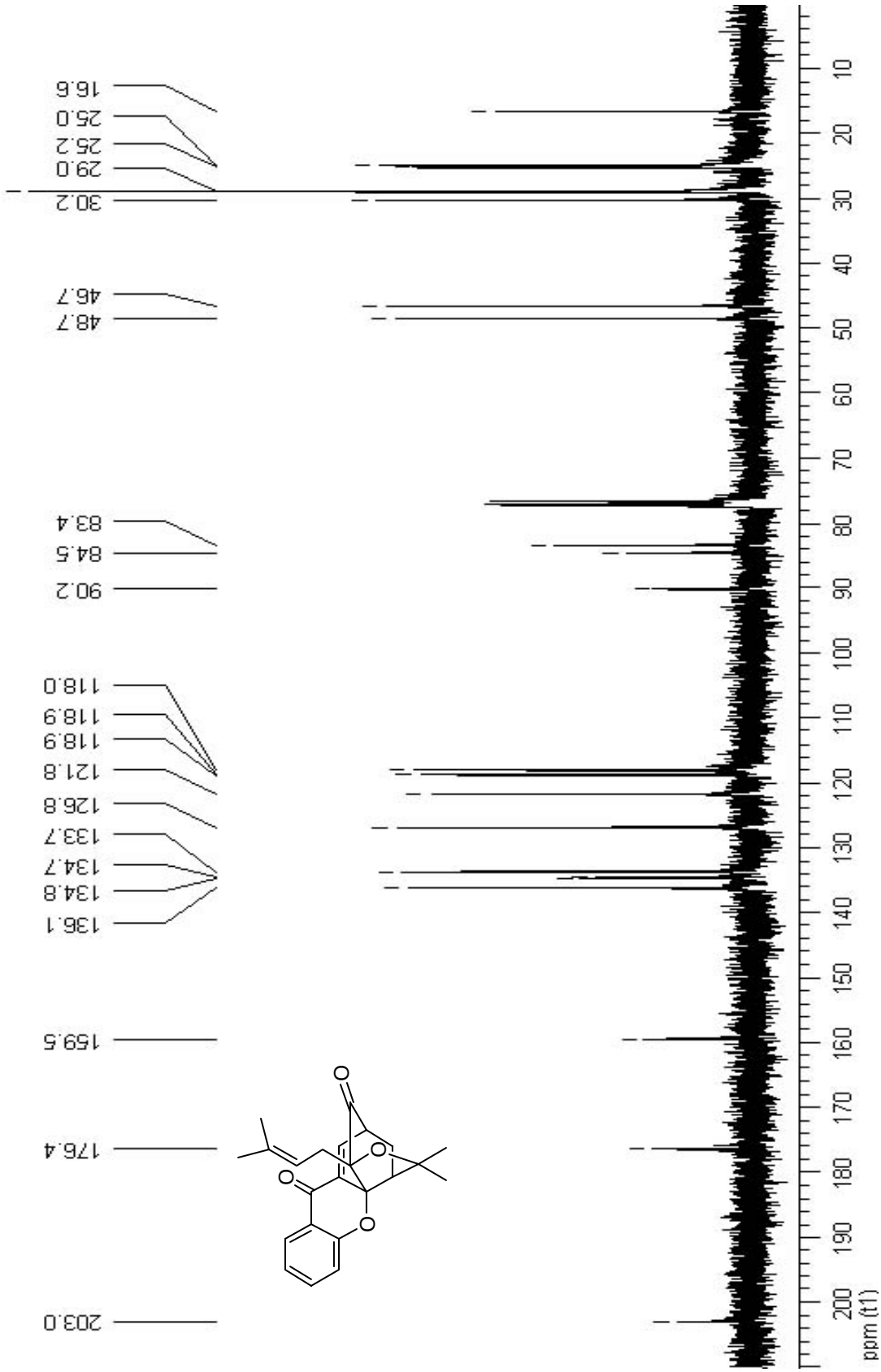

Spectrum 40: ^{13}C NMR ($CDCl_3$, 100 MHz) of compound 7.

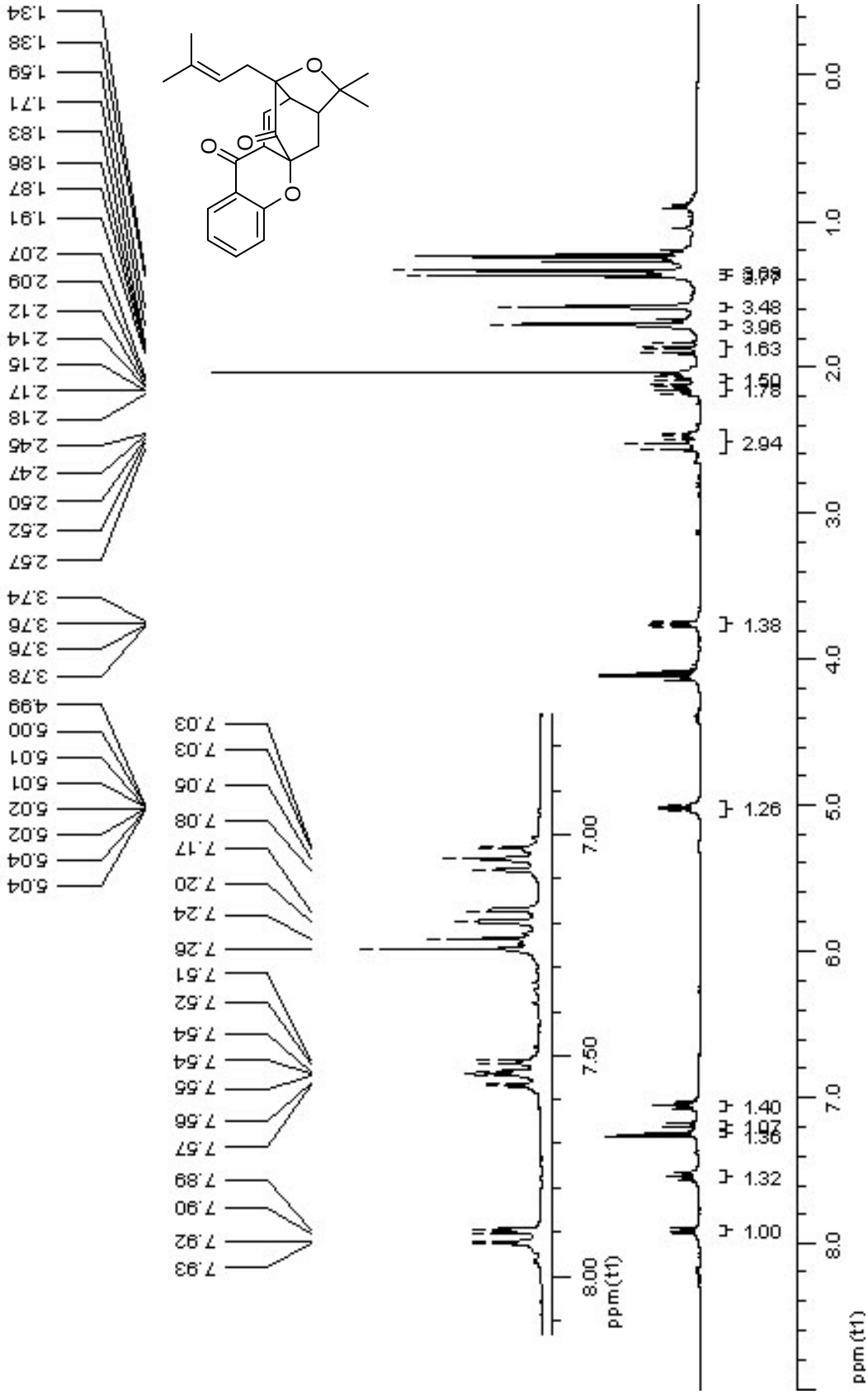

Spectrum 41: ^{1}H NMR ($CDCl_3$, 400 MHz) of compound 33.

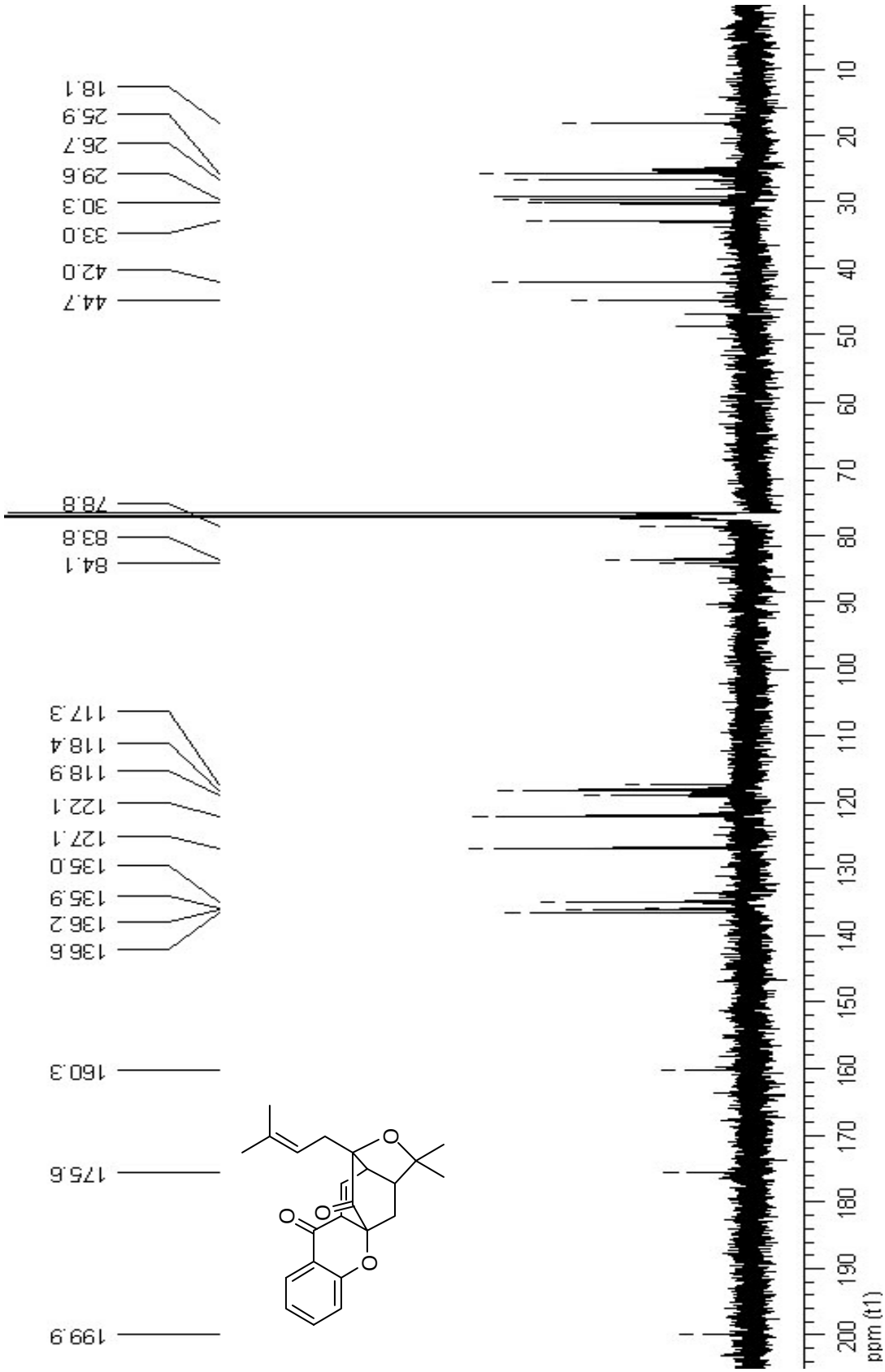

Spectrum 42: ^{13}C NMR ($CDCl_3$, 100 MHz) of compound 33.

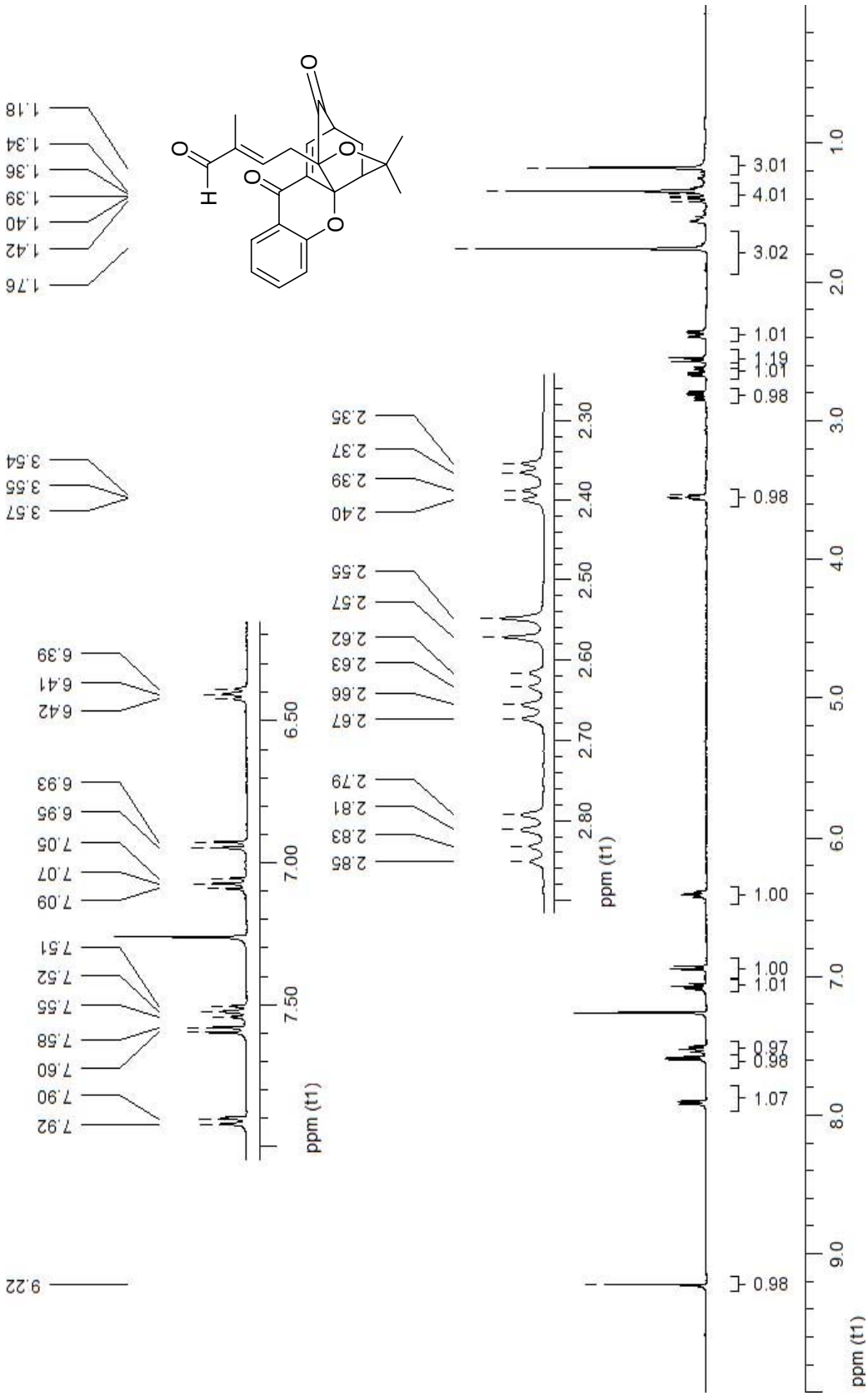

Spectrum 43: ^{1}H NMR ($CDCl_3$, 400 MHz) of compound 34.

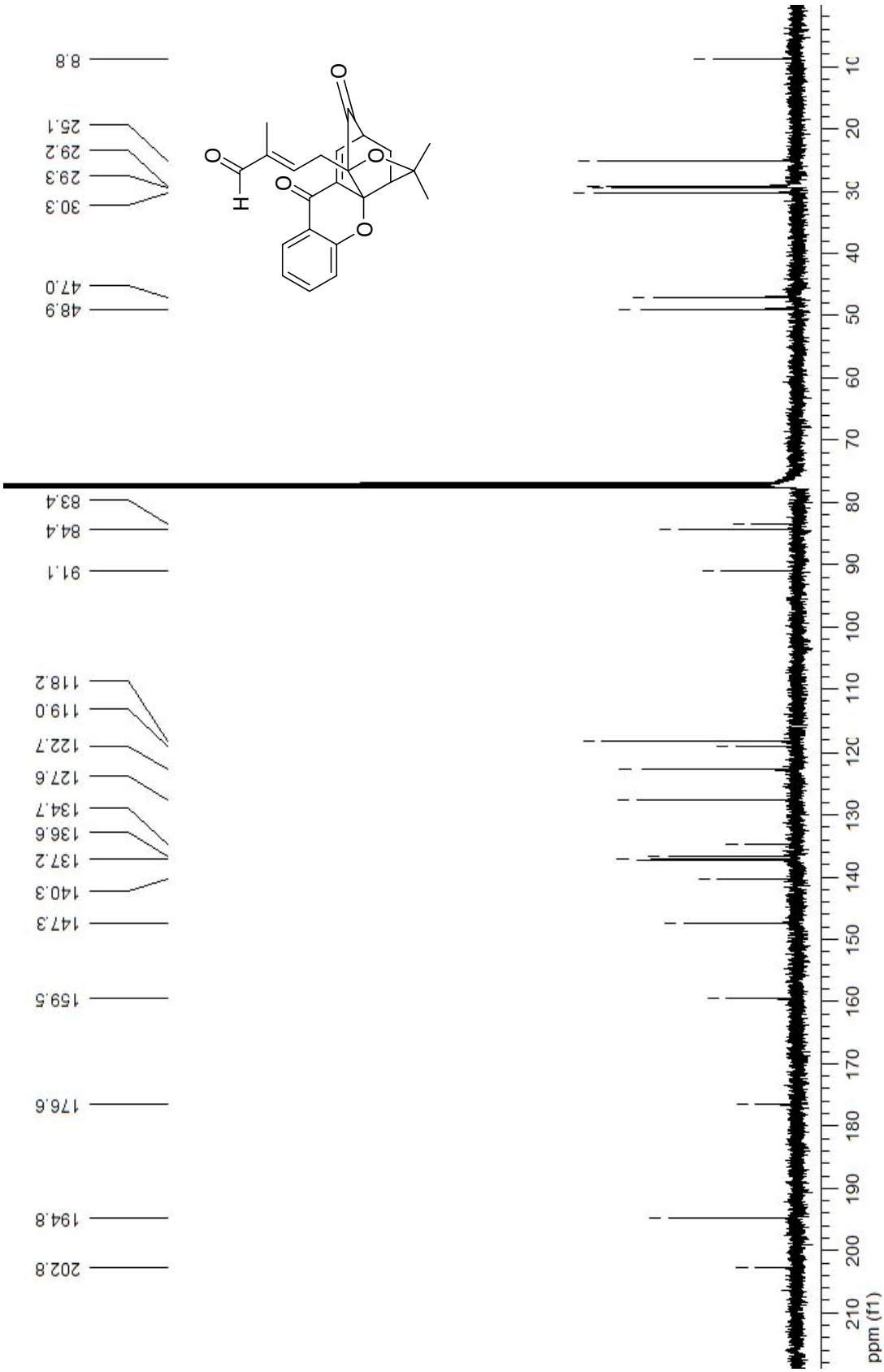

Spectrum 44: ^{13}C NMR ($CDCl_3$, 100 MHz) of compound 34.

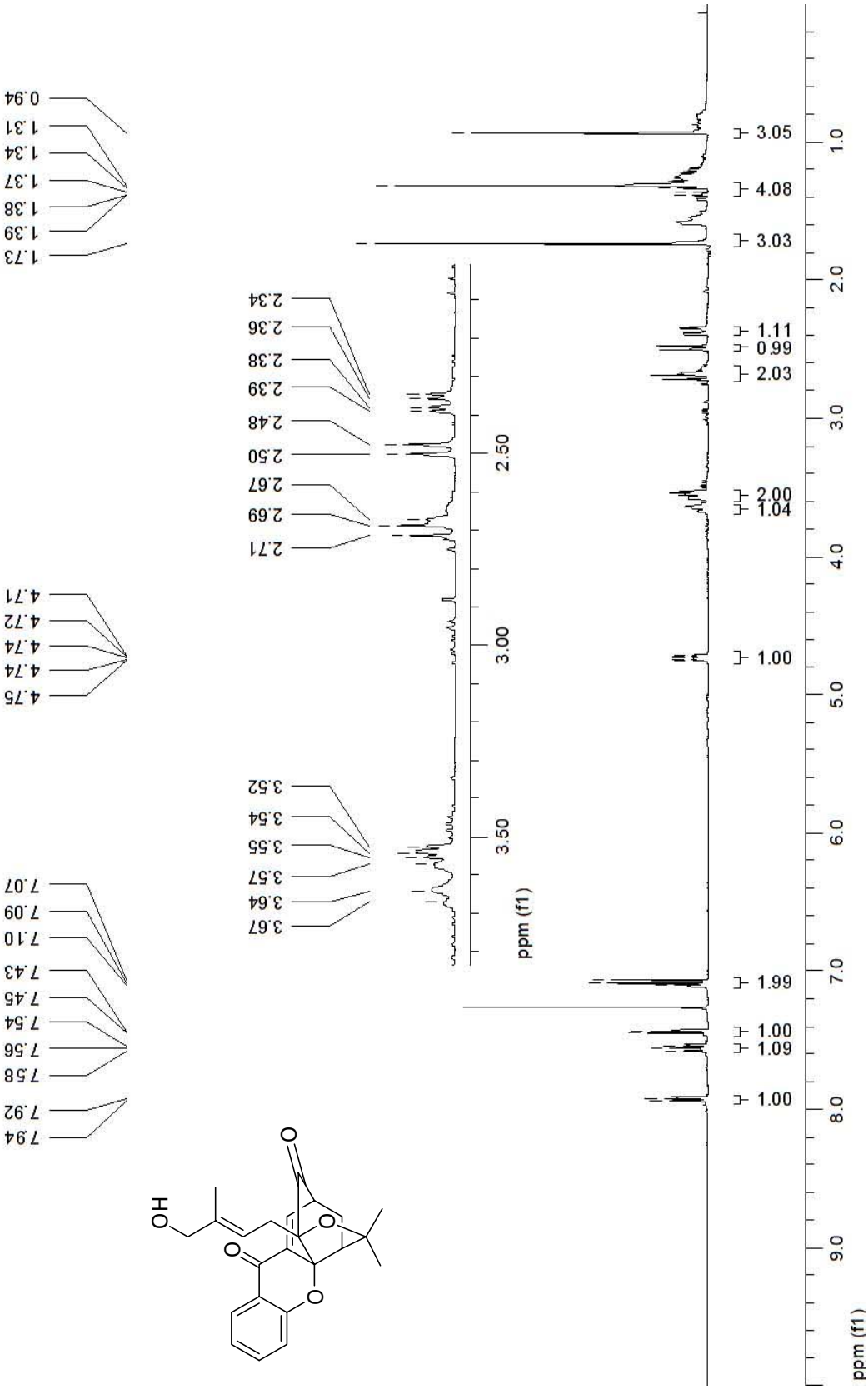

Spectrum 45: ^{1}H NMR ($CDCl_3$, 400 MHz) of compound 35.

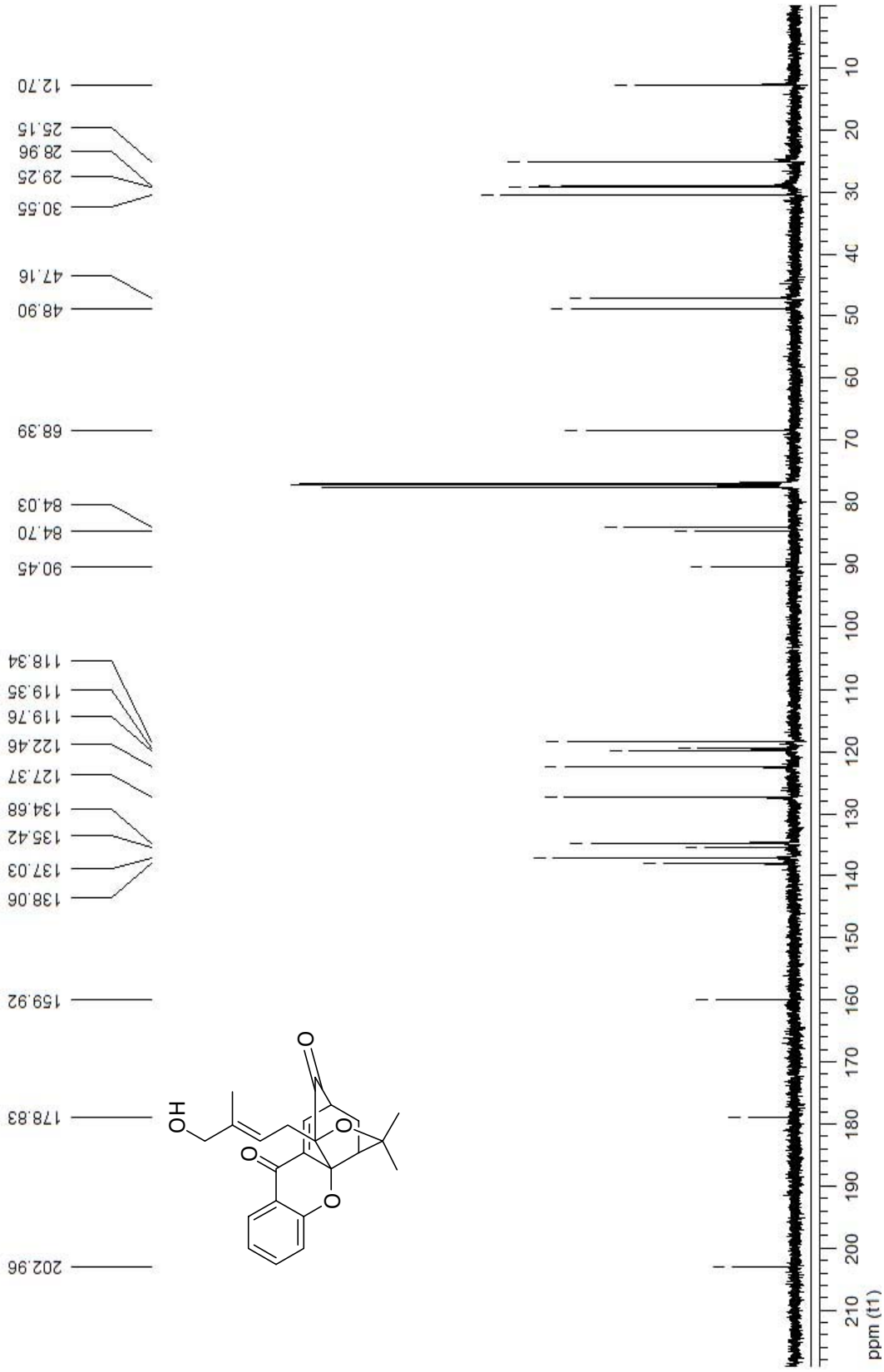

Spectrum 46: ^{13}C NMR ($CDCl_3$, 100 MHz) of compound 35.

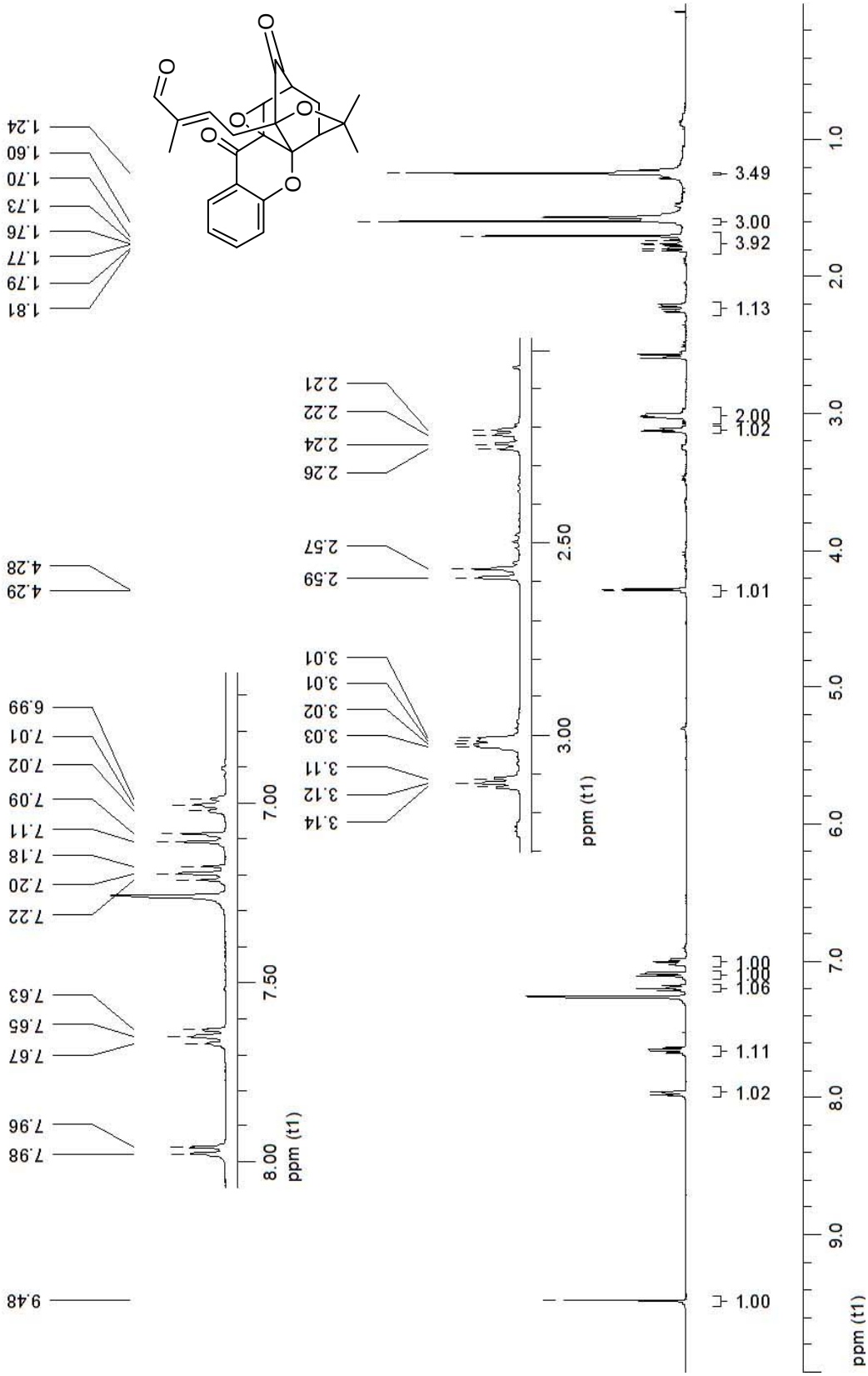

Spectrum 47: ^{1}H NMR ($CDCl_3$, 400 MHz) of compound 36.

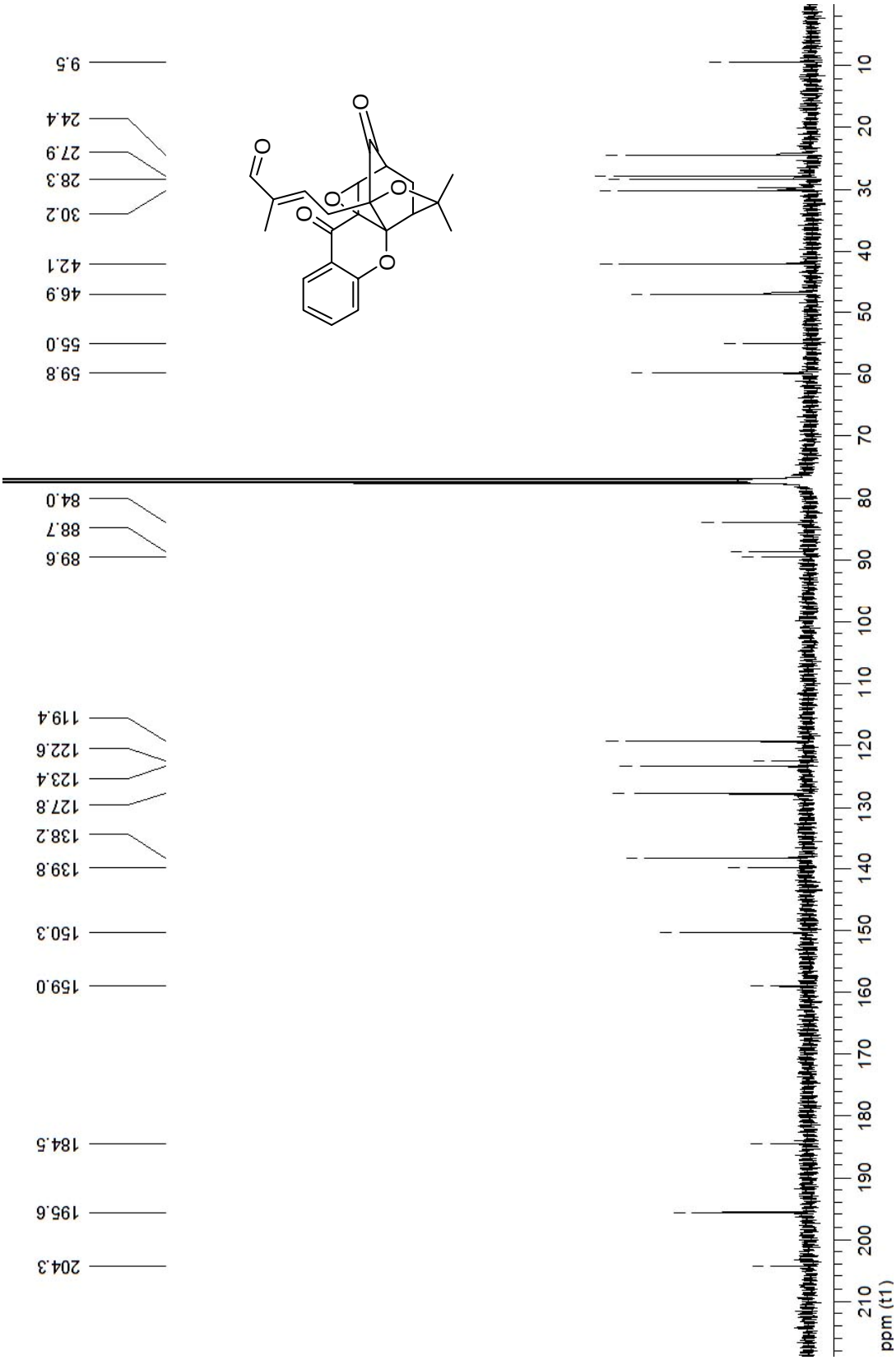

Spectrum 48: ^{13}C NMR ($CDCl_3$, 100 MHz) of compound 36.

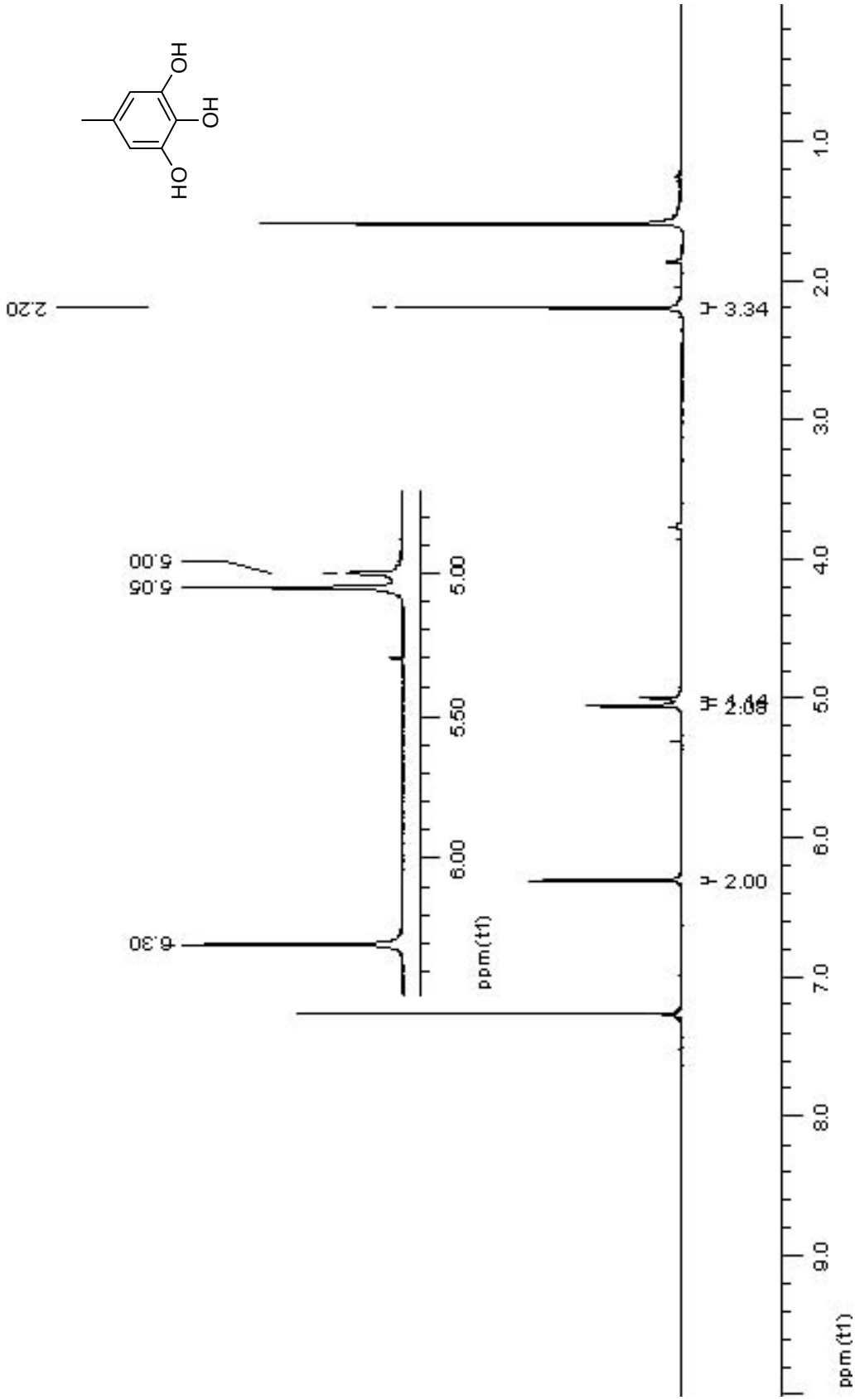

Spectrum 49: ^{1}H NMR ($CDCl_3$, 400 MHz) of compound 38.

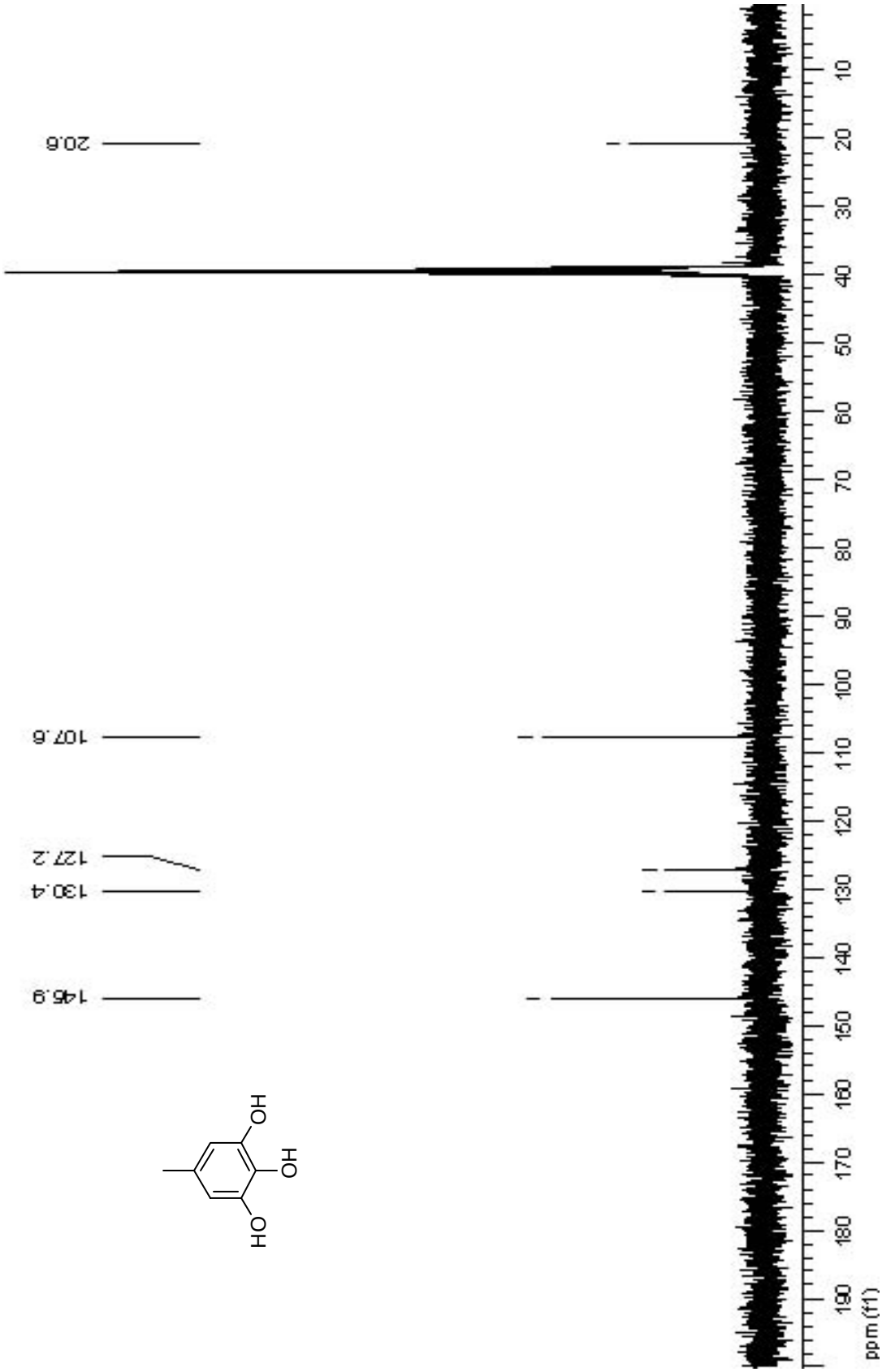

Spectrum 50: ^{13}C NMR (DMSO-d6, 100 MHz) of compound 38.

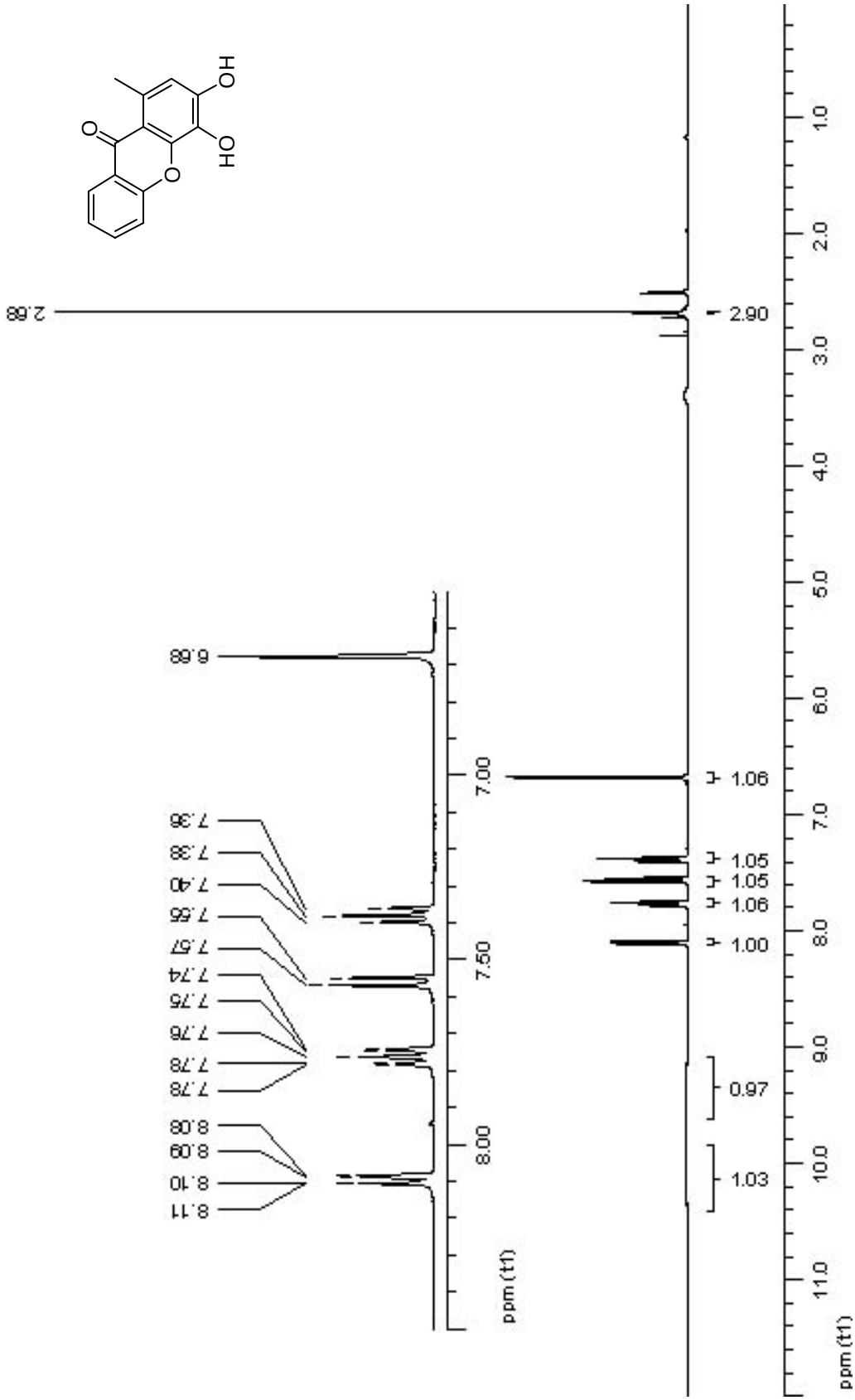

Spectrum 51: ^{1}H NMR (DMSO-d6, 400 MHz) of compound 39.

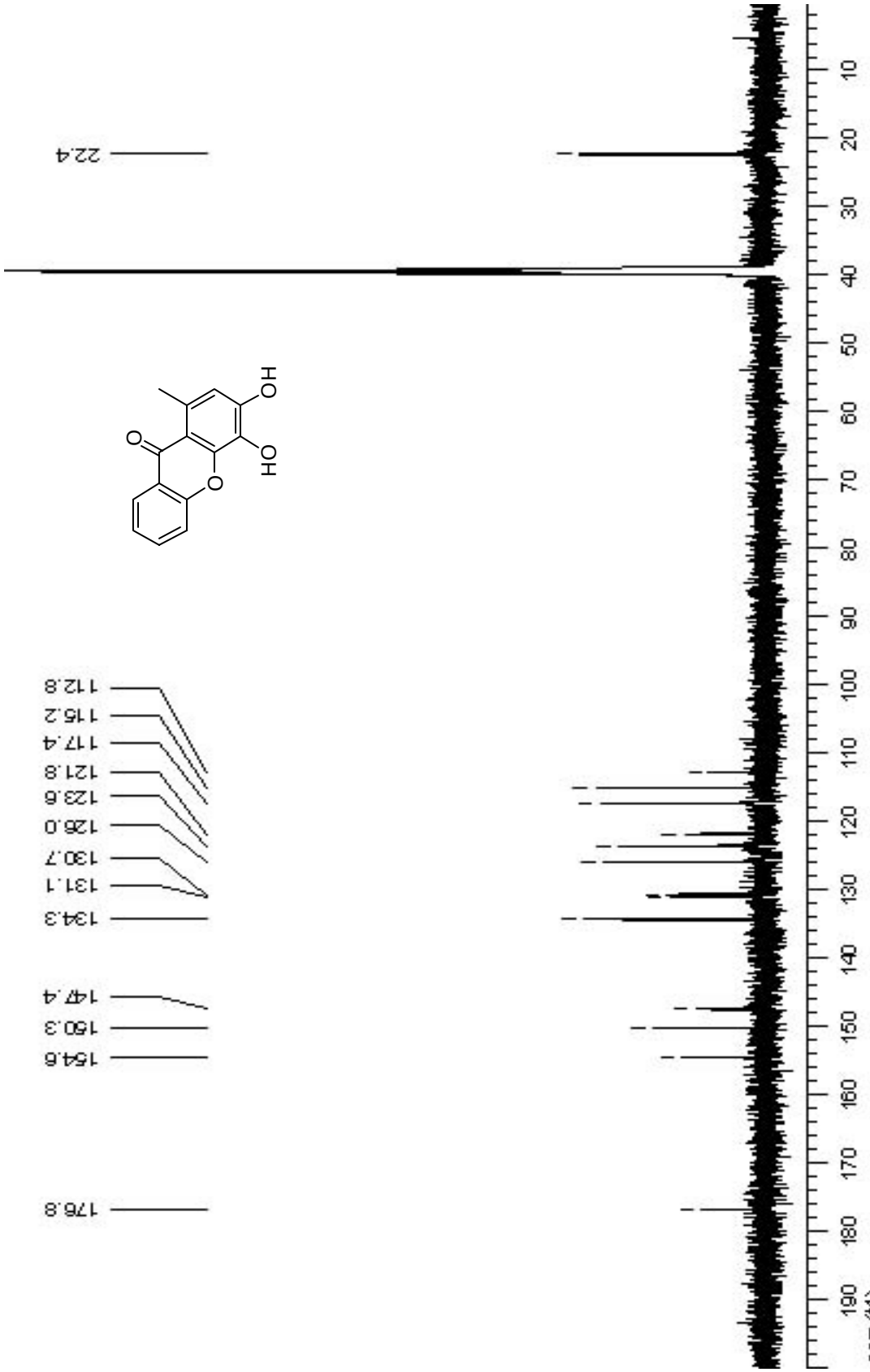

Spectrum 52: ^{13}C NMR (DMSO-d6, 100 MHz) of compound 39.

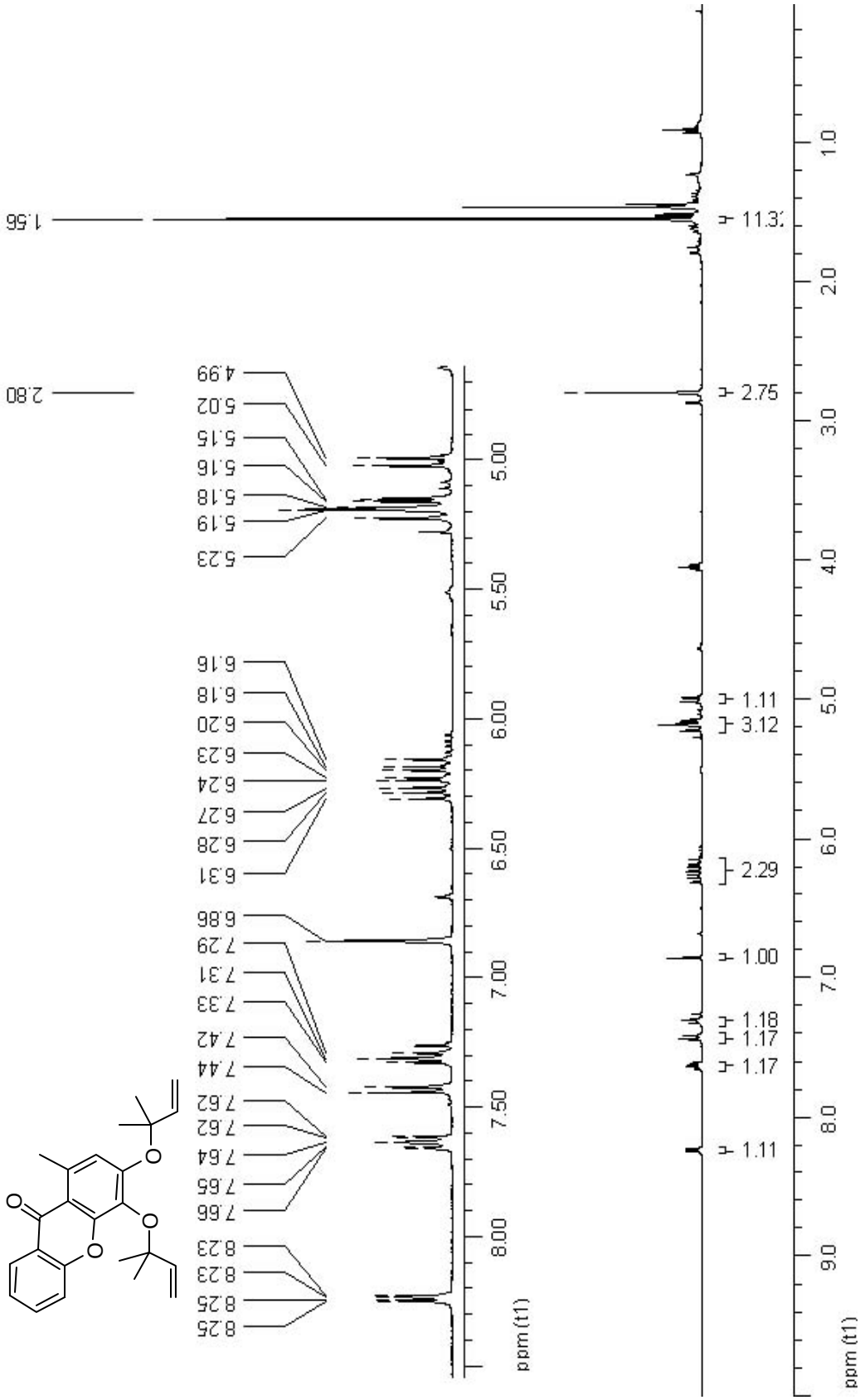

Spectrum 53: ^{1}H NMR ($CDCl_3$, 400 MHz) of compound 40.

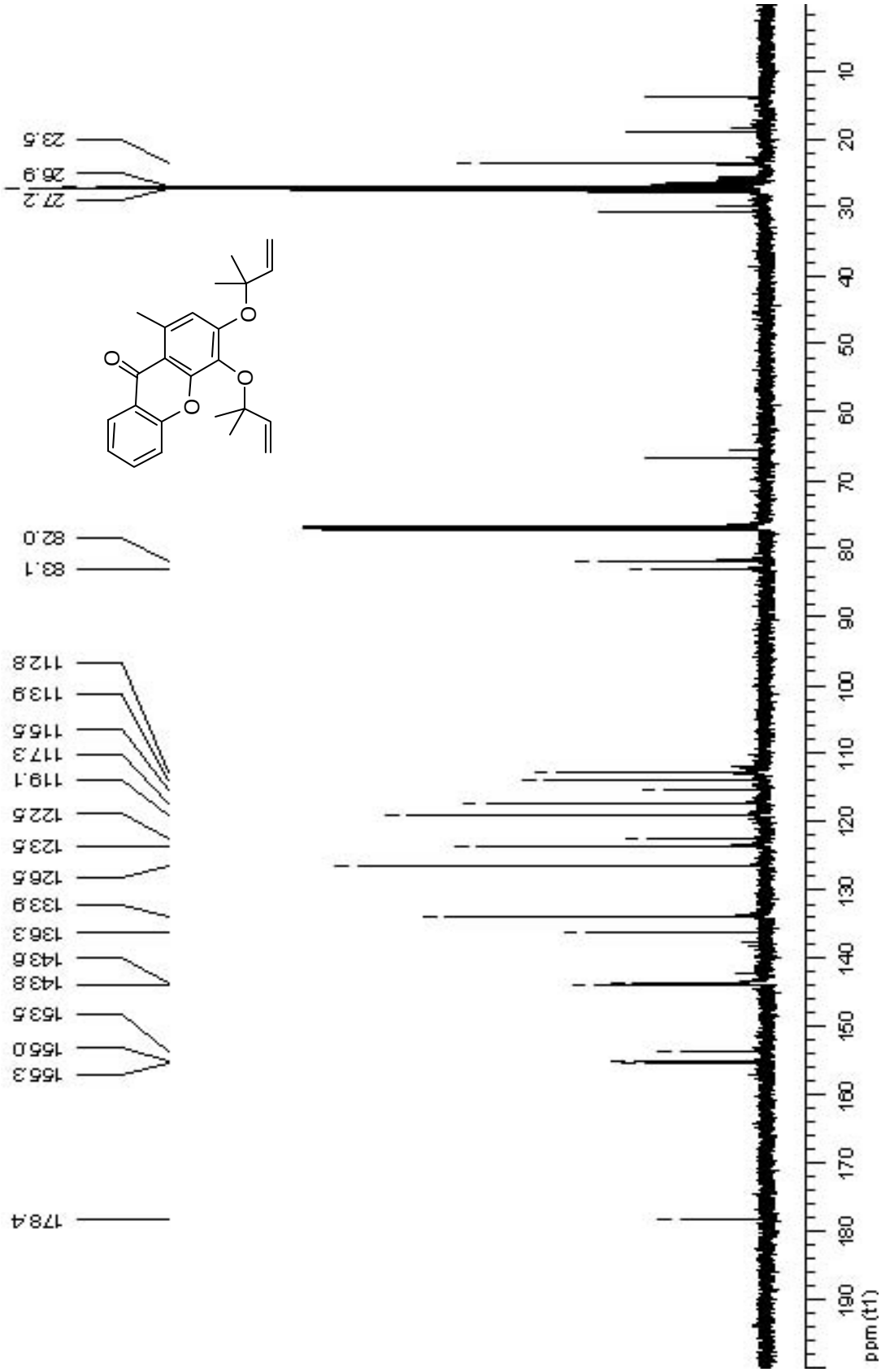

Spectrum 54: ^{13}C NMR ($CDCl_3$, 100 MHz) of compound 40.

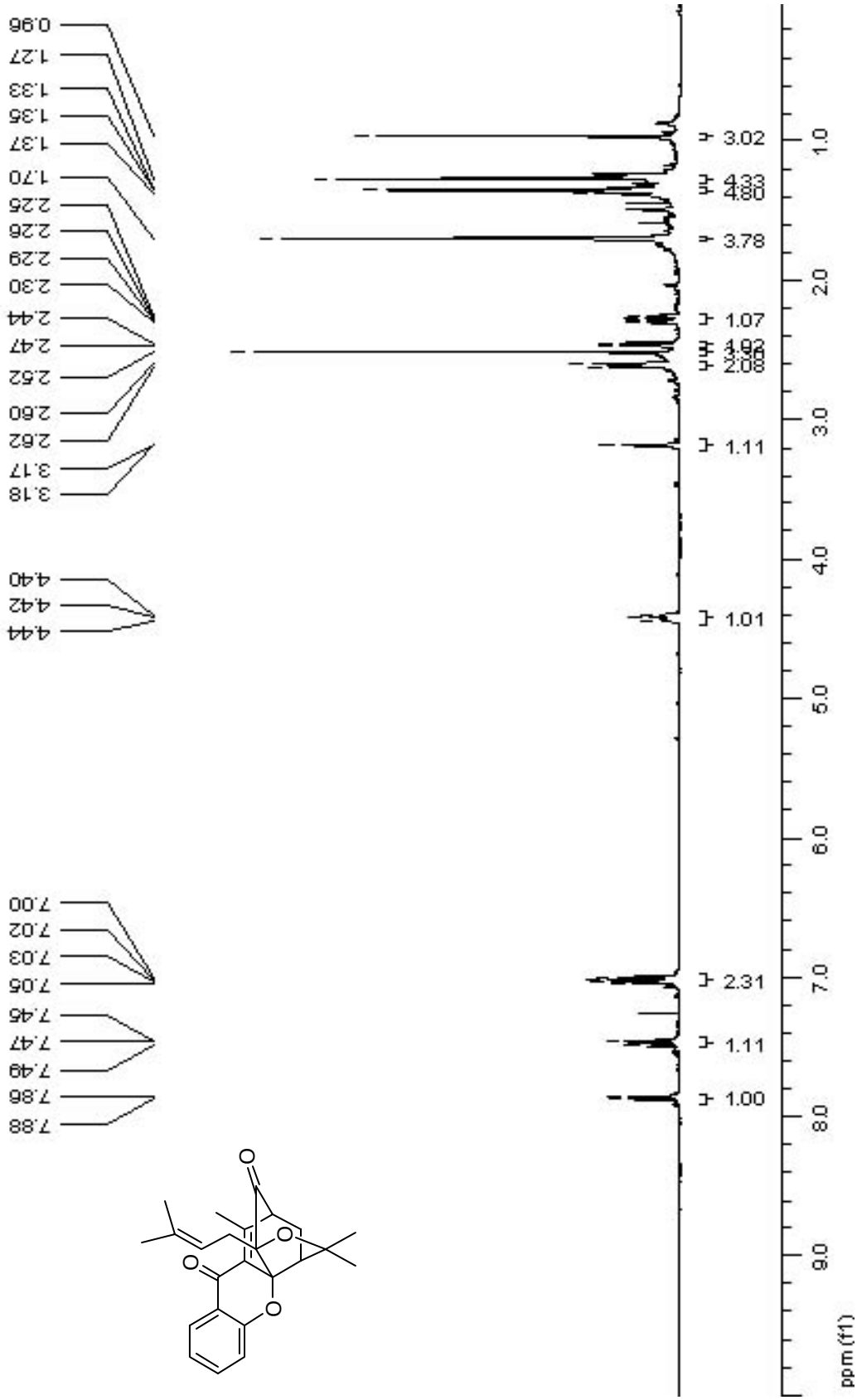

Spectrum 55: ^{1}H NMR ($CDCl_3$, 400 MHz) of compound 41.

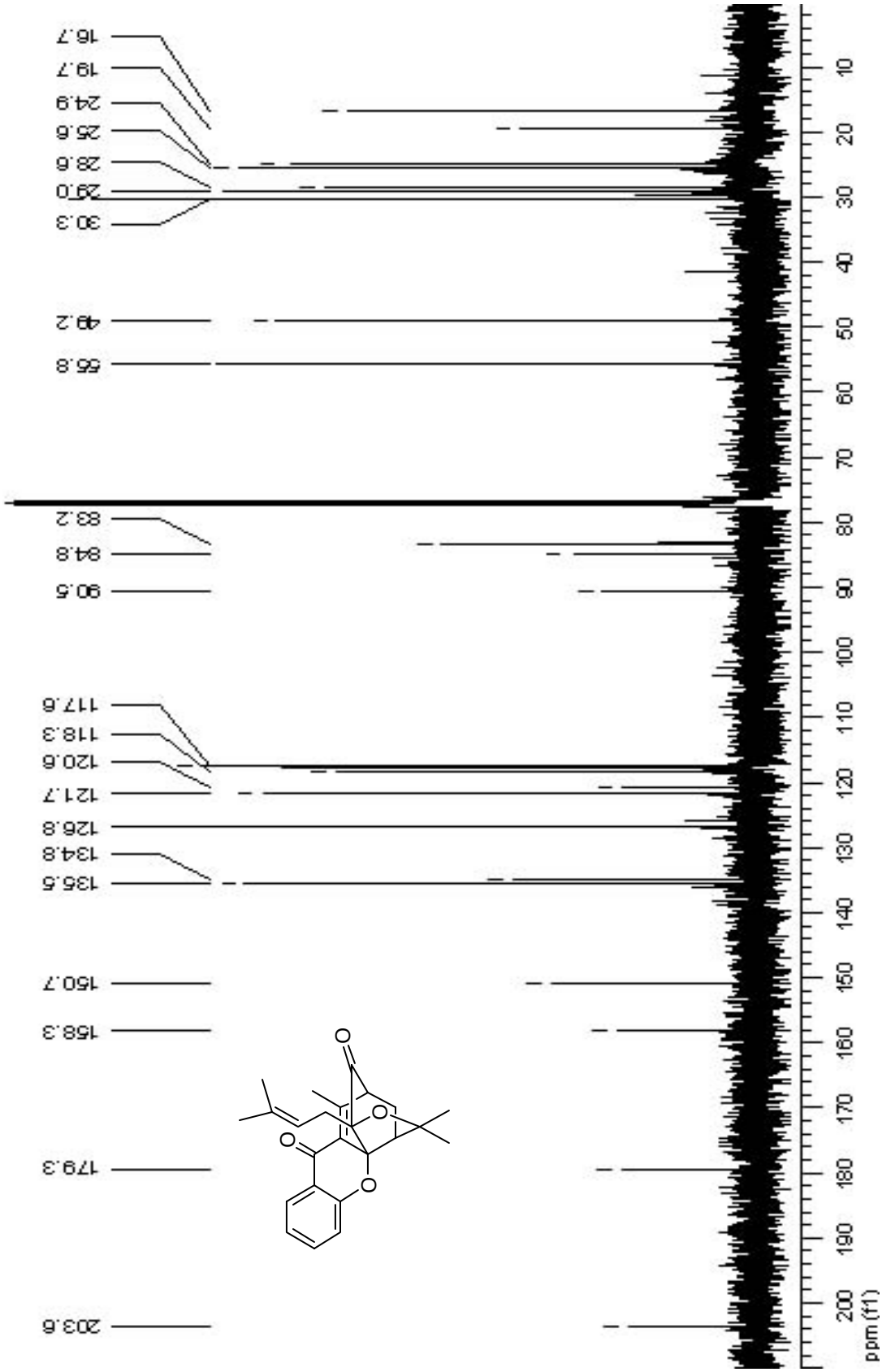

Spectrum 56: ^{13}C NMR ($CDCl_3$, 100 MHz) of compound 41.

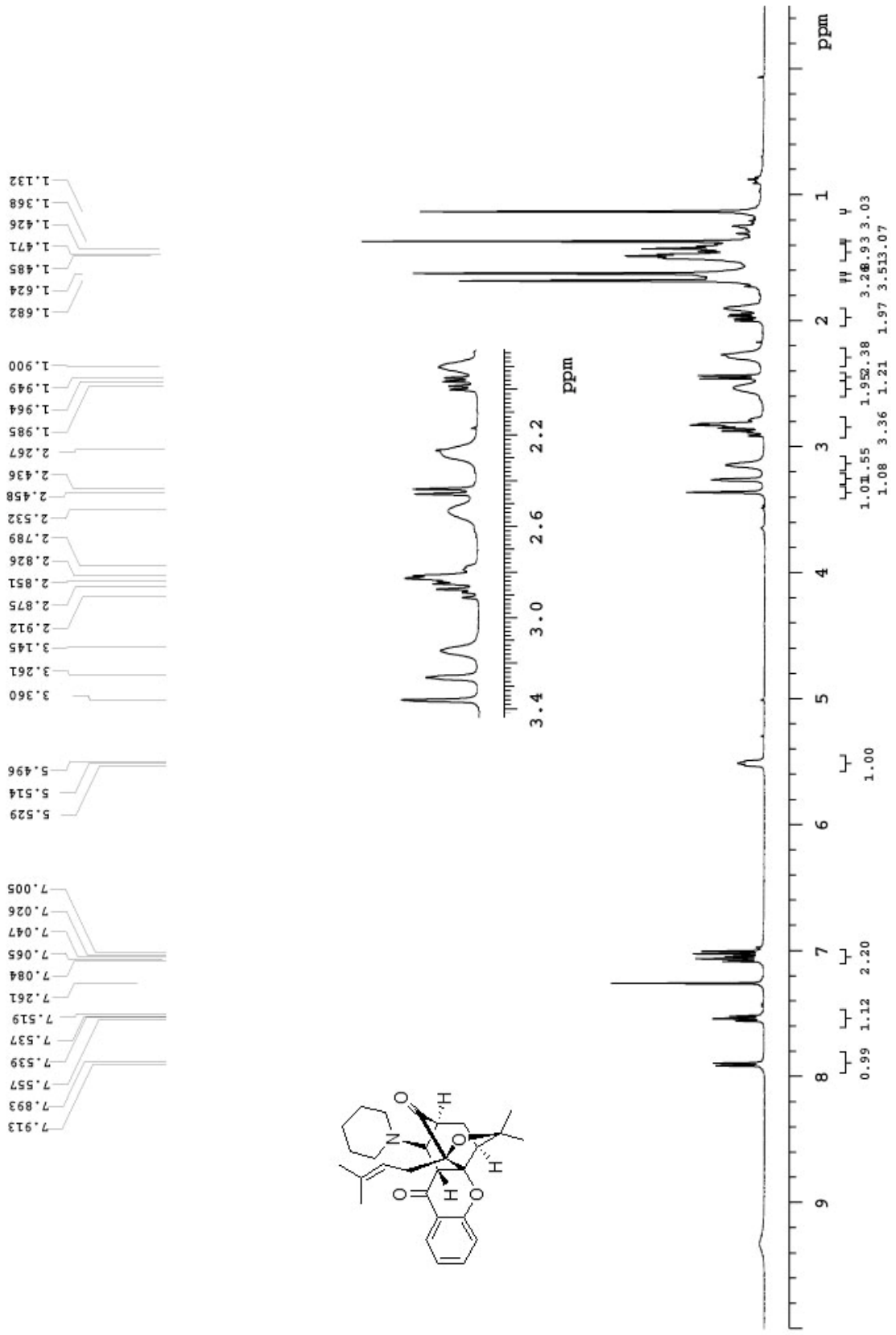

Spectrum 57: ^{1}H NMR ($CDCl_3$, 400 MHz) of compound 42.

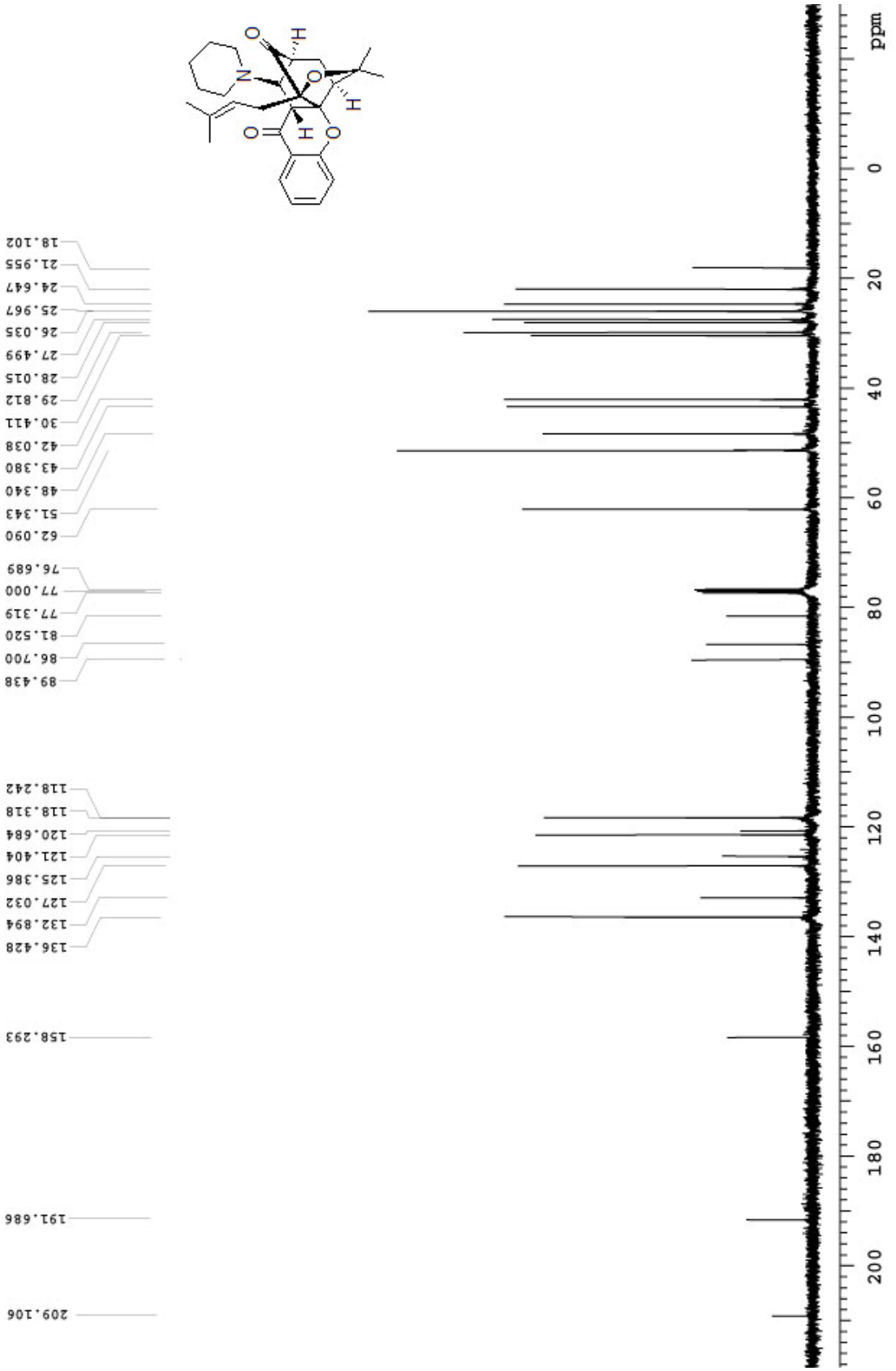

Spectrum 58: ^{13}C NMR ($CDCl_3$, 100 MHz) of compound 42.

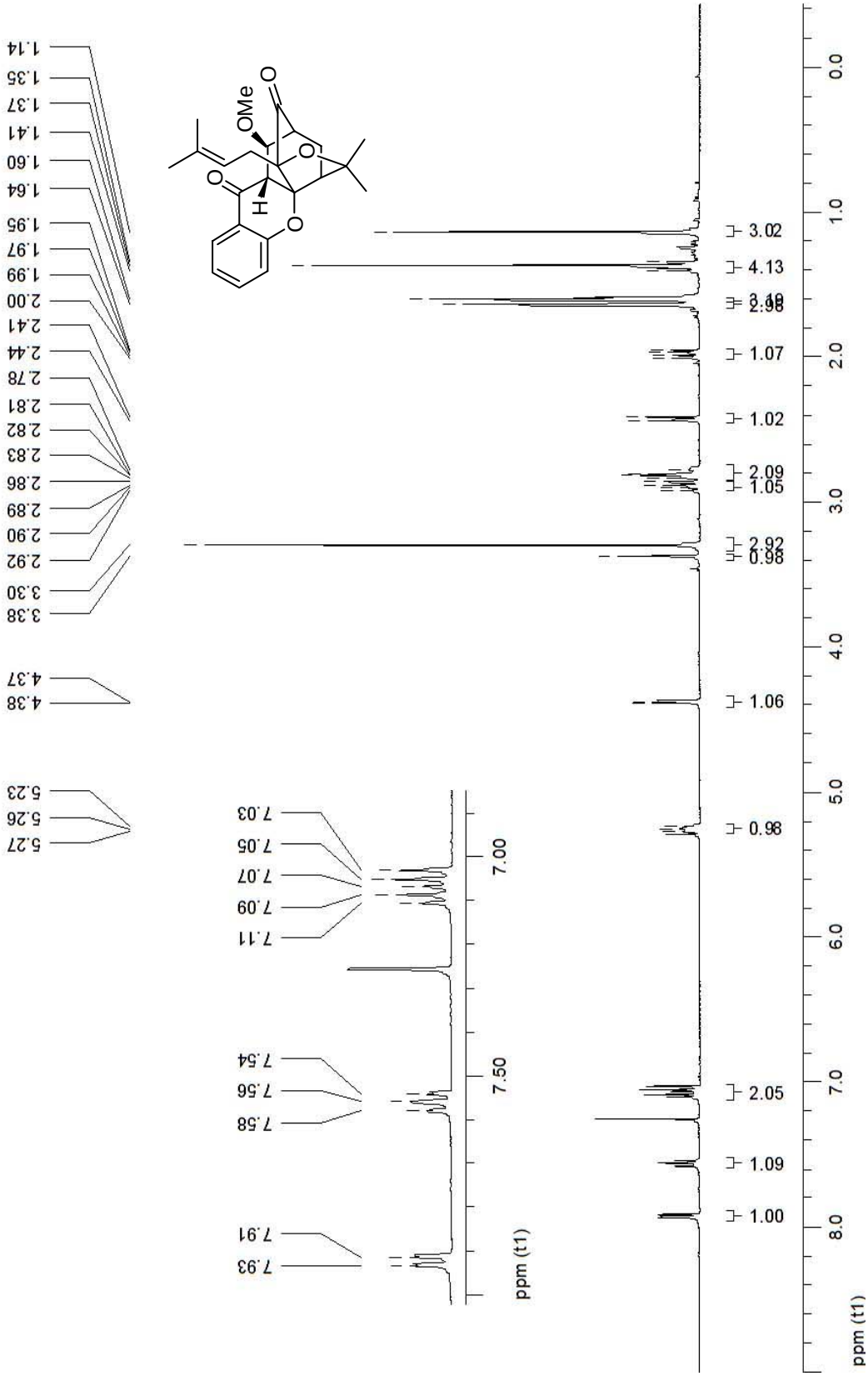

Spectrum 59: ^{1}H NMR ($CDCl_3$, 400 MHz) of compound 43.

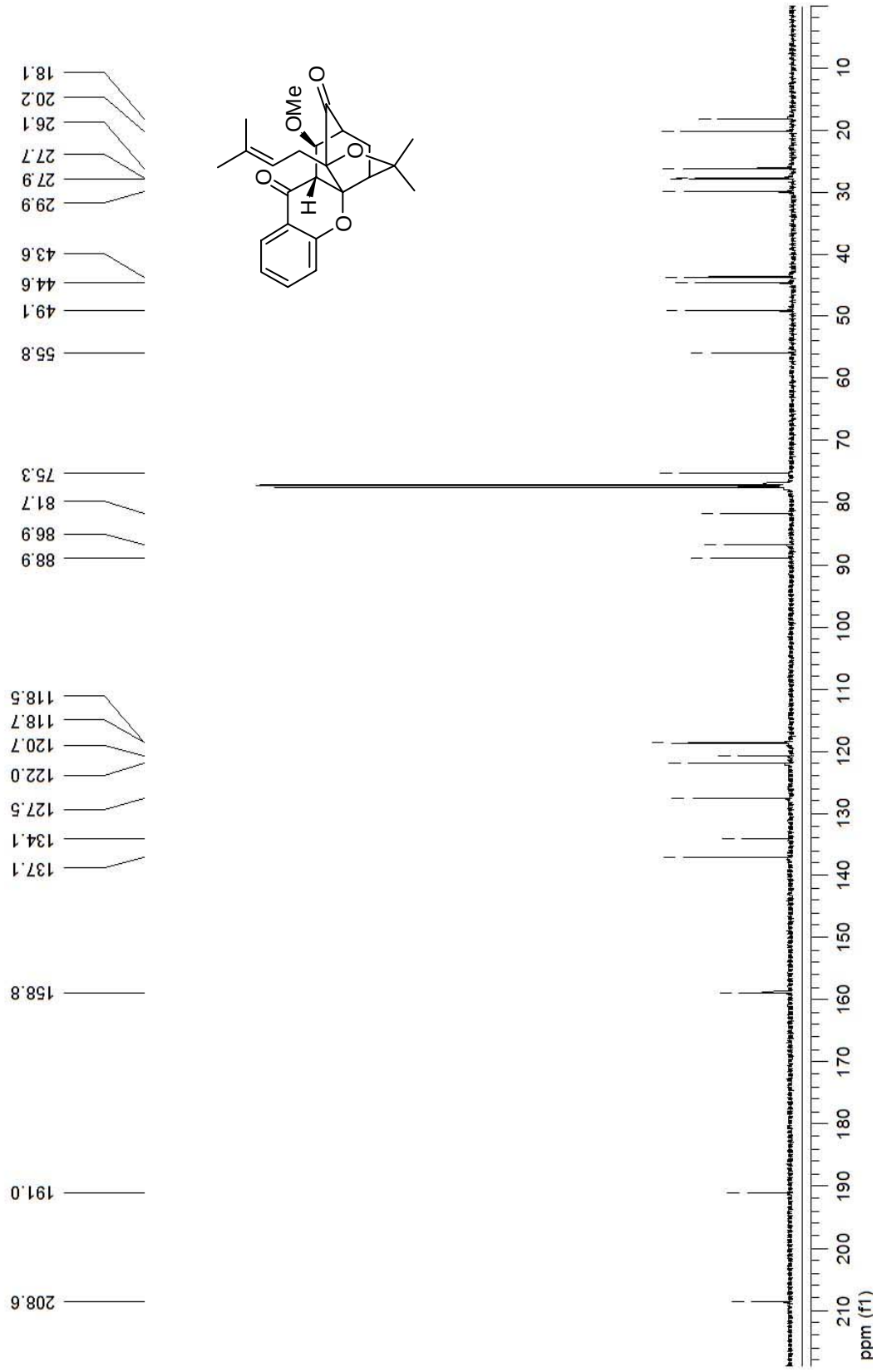

Spectrum 60: ^{13}C NMR ($CDCl_3$, 400 MHz) of compound 43.

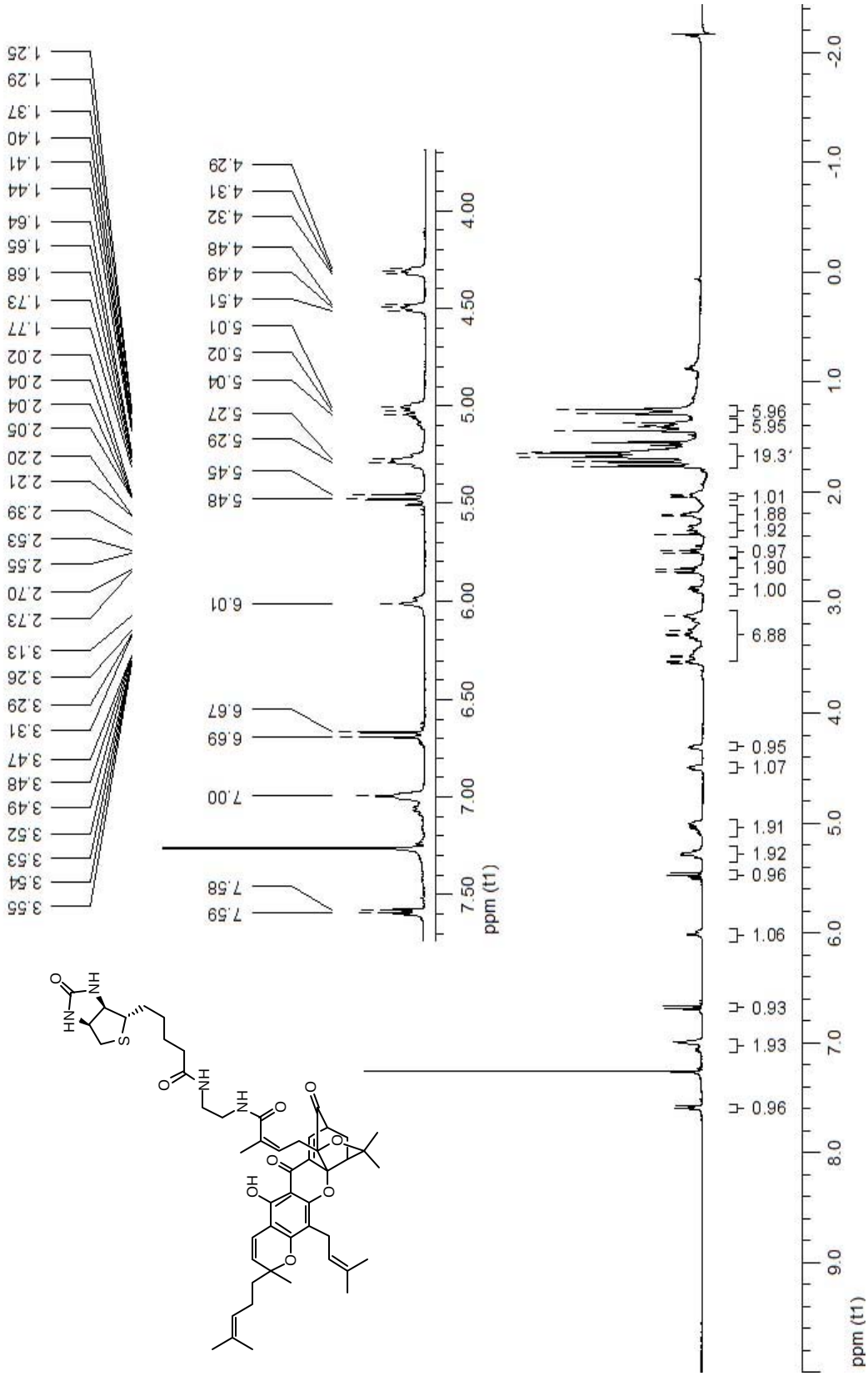

Spectrum 61: ^{1}H NMR ($CDCl_3$, 400 MHz) of compound 44.

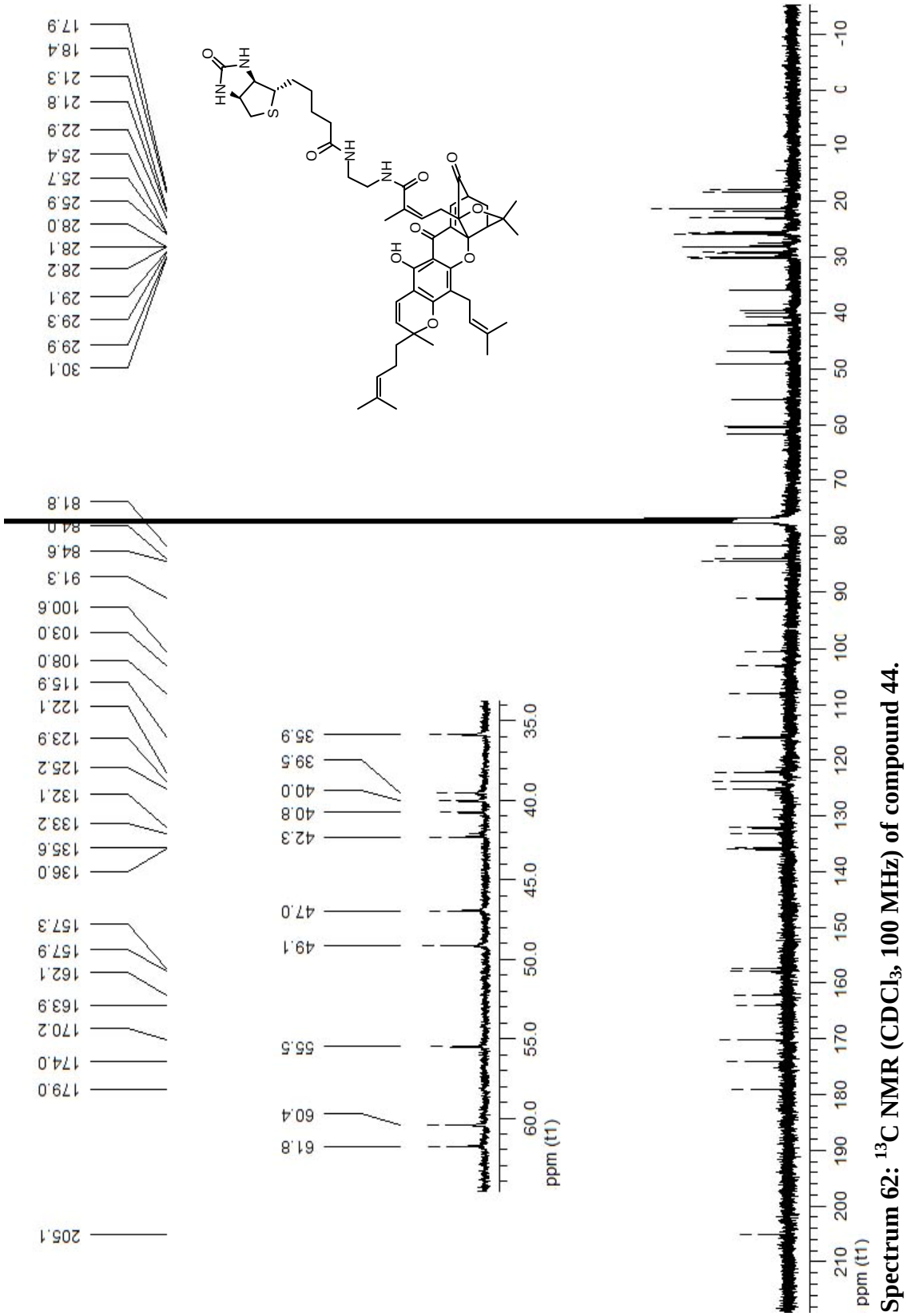

Spectrum 62: ^{13}C NMR ($CDCl_3$, 100 MHz) of compound 44.

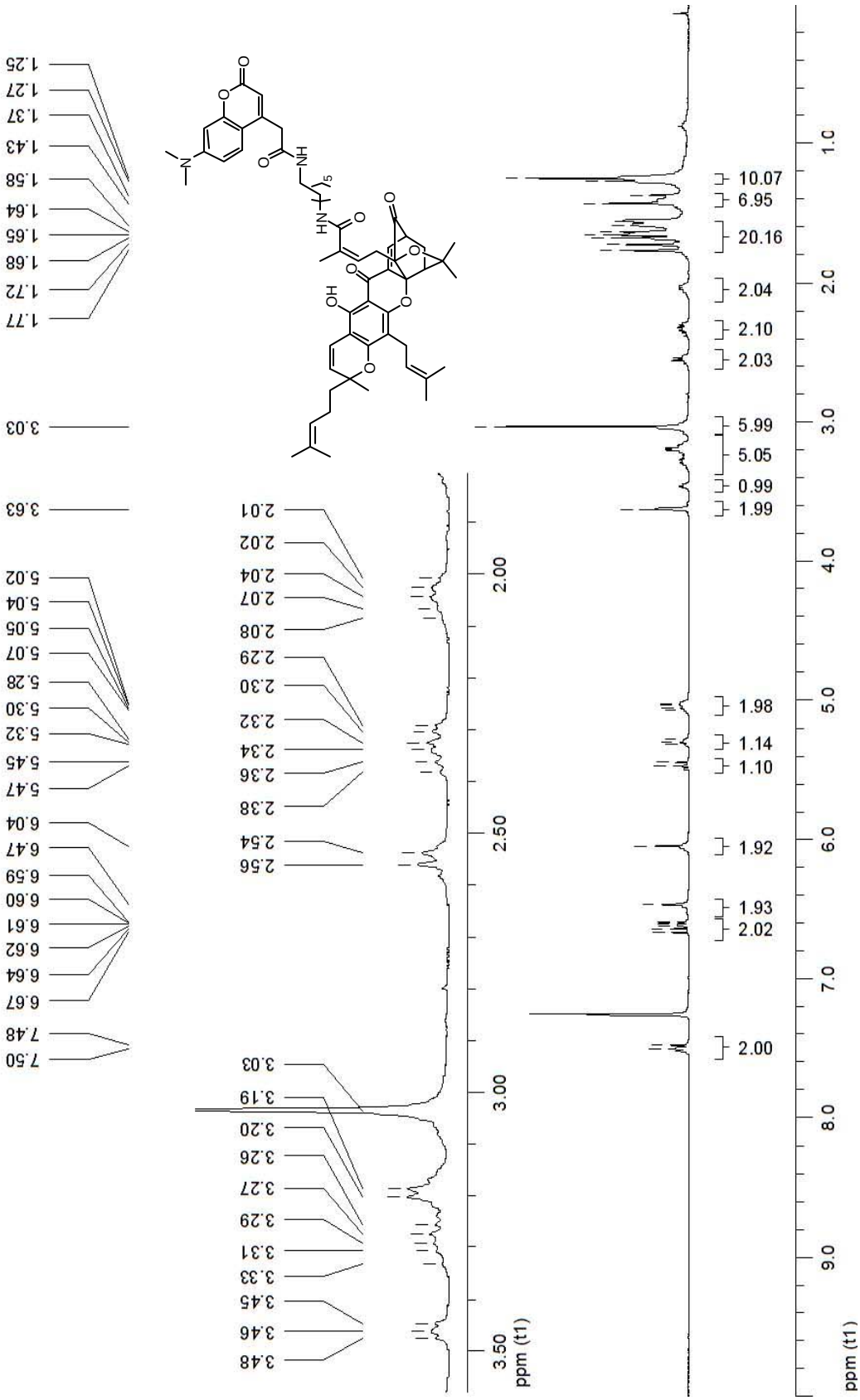

Spectrum 63: ^{1}H NMR ($CDCl_3$, 400 MHz) of compound 45.

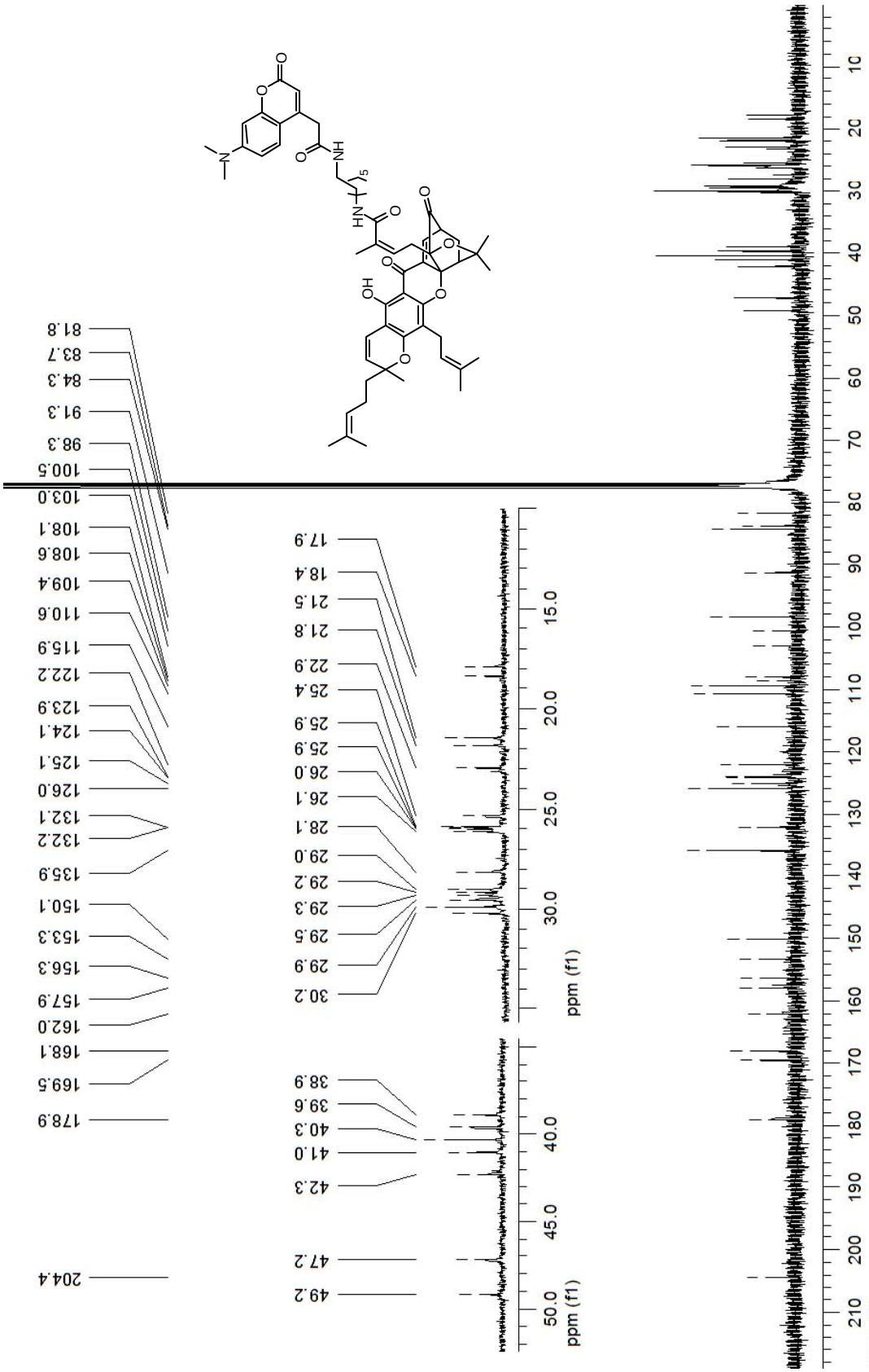

Spectrum 64: ^{13}C NMR ($CDCl_3$, 100 MHz) of compound 45.

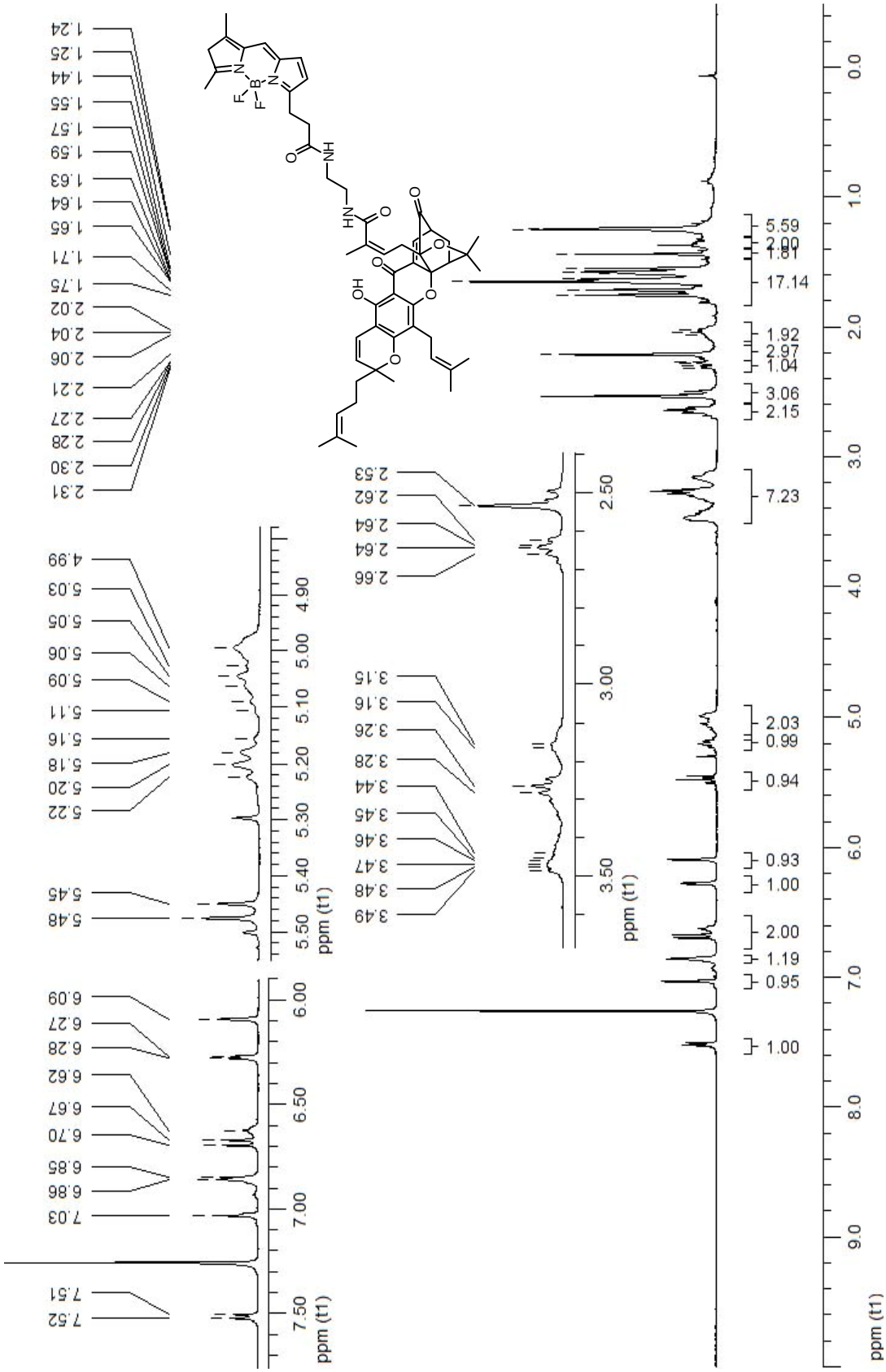

Spectrum 65: ^{1}H NMR ($CDCl_3$, 400 MHz) of compound 46.

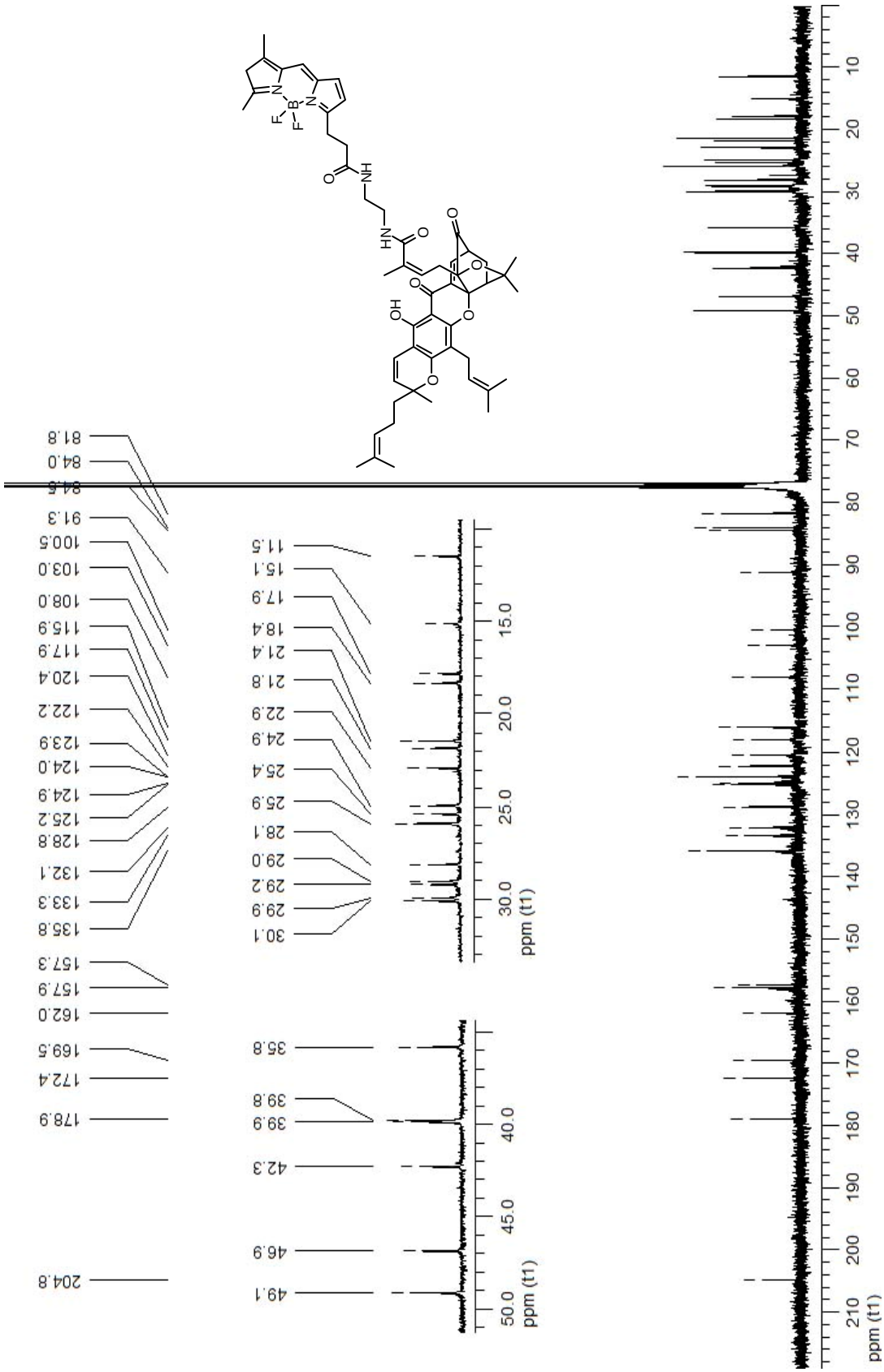

Spectrum 66: ^{13}C NMR ($CDCl_3$, 100 MHz) of compound 46.

Section 2.10 References

1. For selected general references on this topic see: (a) W. D. Ollis, B. T. Redman, I. O. Sutherland and K. Jewers, *J. Chem. Soc. Chem. Commun.,* 1969, 879-880. (b) P. Kumar and R. K. Baslas, *Herba Hungarica,* 1980, **19**, 81-91. (c) J. Gruenwald, T. Brendler, and C. Jaenicke, Eds. PDR for Herbal Medicines, 2nd Ed, Medical Economics Co. Montvale, NJ, 2000, 325-326.

2. (a) B. S. Rao, *J. Chem. Soc. (C),*1937, 853-855. (b) G. Kartha, G. N. Ramachandran, H. B. Bhat, P. M. Nair, V. K. V. Raghavan and K. Venkataraman, *Tetrahedron Lett.,* 1963, **7**, 459-462. (c) H. B. Bhat, P. M. Nair and K. Venkataraman, *Indian J. Chem.,* 1964, **2**, 405-410. (d) C. G. Karanjgaonkar, P. M. Nair and K. Venkataraman, *Tetrahedron Lett.,* 1966, 687-691.

3. (a) S.-G. Cao, X.-H. Wu, K.-Y. Sim, B. K. H. Tan, J. T. Pereira, W. H. Wong, N. F. Hew and S. H. Goh, *Tetrahedron Lett.*, 1998, **39**, 3353-3356. (b) J. Wu, Y. J.; Xu, X. F. Cheng, L. J. Harrison, K. Y. Sim and S. H. Goh, *Tetrahedron Lett.,* 2001, **42,** 727-729. (c) Y. J. Xu, S. C. Yip, S. Kosela, E. Fitri, M. Hana, S. H. Goh and K. Y. Sim, *Org. Lett.,* 2000, **2,** 3945-3948. (d) X.-H. Wu, B. K. H. Tan, S.-G. Cao, K. Y. Sim and S. H. Goh, *Nat. Prod. Lett.,* 2000, **14**, 453-458.

4. (a) W. D. Ollis, M. V. J. Ramsay, I. O. Sutherland and S. Mongkolsuk, *Tetrahedron*, 1965, **21**, 1453-1470. (b) G. Cardillo and L. Merlini, *Tetrahedron Lett.,* 1967, 2529-2530. (c) T. J. R. Weakley, S.-X. Cai, H.-Z. Zhang and J. F. W. Keana, *J. Chem. Crystallog.,* 2001, **31**, 501-505.

5. (a) W. Liu, Q.-L. Guo, Q.-D. You, L. Zhao, H.-Y. Gu, S. T. Yuan, *World J. Gastroenterol.*, 2005, **11**, 3655-3659. (b) J. Asano, K. Chiba, M. Tada, T. Yoshii, *Phytochemistry*, 1996, **41**, 815-820. (c) S.-G. Gao, V. H. L. Sng, X.-H. Wu, K.-Y. Sim, B. H. K. Tan, J. T. Pereira, S. H. Goh, *Tetrahedron*, 1998, **54**, 10915-10924. (d) O. Thoison, J. Fahy, V. Dumontet, A. Chiaroni, C. Riche, M. V. Tri, T. Sevenet, *J. Nat. Prod.*, 2000, **63**, 441-446.

6. X. Wu, S. Cao, S. Goh, A. Hsu and B. K. H. Tan, *Planta Med.*, 2002, **68,** 198-203.

7. (a) Q. Guo, Q. Qi, Q. You, H. Gu, L. Zhao, Z. Wu, *Basic & Clin. Pharmacol. & Toxicol.*, 2001, **31**, 178-184. (b) Q. Qi, Q. You, H. Gu, L. Zhao, W. Liu, N. Lu, Q. Guo, *J. Ethnopharmacol.,* 2008, **117**, 433-438. (c) H. Gu, Q. You, W. Liu, Y.

Yang, L. Zhao, Q. Qi, J. Zhao, J. Wang, N. Lu, H. Ling, Q. Guo, X. Wang *Intern. Immunopharmacol.*, 2008, **8**, 1493-1502.

8. (a) D. Zhai, C. Jin, C.-w. Shiau, S. Kitada, A. C. Satterthwait, J. C. Reed, *Mol. Cancer Ther.* 2008, **7**, 1639-1646. (b) L. Zhao, Q.-L. Guo, Q.-D. You, Z.-Q., Wu, H.-Y. Gu, *Biol. Pharm. Bull.* 2004, **27**, 998-1003.

9. (a) S. Kasibhatla, K. A. Jessen, S. Maliartchouk, J. Y. Wang, N. M. English, J. Drewe, L. Qiu, S. P. Archer, A. E. Ponce, N. Sirisoma, S. Jiang, H. Zhang, K. R. Gehisen, S. X. Cai, D. R. Green and B. Tseng, *PNAS*, 2005, **102**, 12095-12100. (b) E. Ortiz-Sanchez, T. R. Daniels, G. Helguera, O. Martinez-Maza, B. Bonavida, M. L. Penichet, *Leukemia*, 2009, **23**, 59-70.

10. (a) H.-Z. Zhang, S. Kasibhatla, Y. Wang, J. Herich, J. Guastella, B. Tseng, J. Drewe and S.-X. Cai, *Bioorg. Med. Chem.*, 2004, **12**, 309-317. (b) J. Kuemmerle, S. Jiang, B. Tseng, S. Kasibhatla, J. Drewe, S. X. Cai, *Bioorg Med. Chem.* 2008, **16**, 4233-4241. (c) N. G. Li, Q. D. You, X. F. Huang, J. X. Wang, Q. L. Guo, X. G. Chen, Y. Li, H. Y. Li, *Chin. Chem. Lett.* 2007, **18**, 659-662. (d) J. Wang, L. Zhao, Y. Hu, Q. Guo, L. Zhang, X. Wang, N. Li, Q. You, *Eur. J. Med. Chem.*, 2009, **44**, 2611-2620.

11. (a) E. J. Tisdale, C. Chowdhury, B. G. Vong, H. Li and E. A. Theodorakis, *Org. Lett.*, 2002, **4**, 909-912. (b) E. J. Tisdale, H. Li, B. G. Vong, S. H. Kim and E. A. Theodorakis, *Org. Lett.*, 2003, **5**, 1491-1494. (c) E. J. Tisdale, B. G. Vong, H. Li, S. H. Kim, C. Chowdhury and E. A. Theodorakis, *Tetrahedron*, 2003, **59**, 6873-6887. (d) E. J. Tisdale, I. Slobodov and E. A. Theodorakis, *Org. Biomol. Chem.*, 2003, **1**, 4418-4422.

12. A. Batova, T. Lam, V. Waschol owski, A. L. Yu, A. Giannis, E. A. Theodorakis, *Org. Biomol. Chem.*, 2007, **5**, 494-500.

13. E. J. Tisdale, I. Slobodov and E. A. Theodorakis, *PNAS*, 2004, **101**, 12030-12035.

14. For related synthetic studies see: (a) K. C. Nicolaou and J. Li, *Angew. Chem. Int. Ed*,. 2001, **40**, 4264-4268. (b) K. C. Nicolaou, P. K. Sasmal, H. Xu, K. Namoto and A. Ritzen, *Angew. Chem. Int. Ed.*, 2003, **42**, 4225-4229. (c) K. C. Nicolaou,

P. K. Sasmal, and H. Xu, *J. Am. Chem. Soc.*, 2004, **126**, 5493-5501. (d) K. C. Nicolaou, H. Xu and M. Wartmann, *Angew. Chem. Int. Ed.*, 2005, **44**, 756-761.

15. T. Kamei, M. Shindo, K. Shishido, *Tetrahedron Lett.*, 2003, **44**, 8505-8507.

16. N. Le Gall, D. Luart, J.-Y. Salaun, J. Talarmin, H. Des Abbayes, *Organomet.*, 2002, **21**, 1775-1781.

17. P. A. Evans, J. D. Nelson, *Tetrahedron Lett.*, 1998, **39**, 1725-1728.

18. For relevant studies on the Claisen rearrangement see: (a) F. C. Gozzo, S. A. Fernandes, D. C. Rodrigues, M. N. Eberlin and A. J. Marsaioli, *J. Org. Chem.*, 2003, **68**, 5493-5499. (b) T. R. Pettus, X.-T. Chen and S. J. Danishefsky, *J. Am. Chem. Soc.*, 1998, **120**, 12684-12685. (c) T. R. Pettus, M. Inoue, X.-T. Chen and S. J. Danishefsky, *J. Am. Chem. Soc.*, 2000, **122**, 6160-6168.

19. A. E. Hayden, H. Xu, K. C. Nicolaou and K. N. Houk, *Org. Lett.*, 2006, **8**, 2989-2992.

20. V. Siddaiah, M. Maheswara, C. V. Rao, S. Venkateswarlu, G. V. Subbaraju, *Bioorg Med. Chem. Lett.*, 2007, **17**, 1288-1290.

21. C. Paizs, U. Bartlewski-Hof, J. Petey, *Chem. Eur. J.*, 2007, **13**, 2805-2811.

22. Q.-B. Han, S. Cheung, J. Tai, C.-F. Qiao, J.-Z. Song, H.-X. Xu, *Biol. Pharm. Bull.*, 2005, **28**, 2335-2337.

23. For selected references see: (a) M. M. Gottesman and I. Pastan, *Annu. Rev. Biochem.*, 1993, **62**, 385-427. (b) S. Simon, D. Roy and M. Schindler, *PNAS*, 1994, **91**, 1128-1132. (c) A. K. Larsen, A. E. Escargeuil and A. Skladanowski, *Pharmacol. Ther.*, 2000, **85**, 217-229.

24. For selected references on this topic see: (a) Hanahan, D.; Weinberg, R. A. *Cell* **2000**, *100*, 57-70. (b) Reed, J. C.; Tomaselli, K. J. *Curr. Opin. Biotechn.* **2000**, *11*, 586-592. (c) Mckenna, S. L.; Cotter, T. G. *Apoptosis and Cancer* **1997**, 192-221. (d) Kim, R.; Tanabe, K.; Uchida, Y.; Emi, M.; Inoue, H.; Toge, T. *Cancer Chemother. Pharmacol.* **2002**, *50*, 343-352. Vermeulen, K.; Berneman, Zwi N.; Van Bockstaele, D. R. *Cell Prolifer.* **2003**, *36*, 165-175.